RSC Applied Interfaces

ROYAL SOCIETY OF CHEMISTRY

REVIEW

View Article Online
View Journal

Cite this: DOI: 10.1039/d6lf00084c

Strategic engineering of perovskite solar cells: revolutionary developments from interfacial stabilization to copper-based semiconductor innovations

Taame Abraha Berhe, *[ab] Chu-Chen Chueh, *[a] Amare Aregahegn Dubale, [c] Wei-Nien Su *[d] and Bing-Joe Hwang *[e]

Received 13th March 2026,
Accepted 14th April 2026

DOI: 10.1039/d6lf00084c

rsc.li/RSCApplInter

Perovskite solar cells (PSCs) are revolutionizing the field of optoelectronics. However, these solar devices remain difficult to scale up and suffer from surface and interface instabilities. Therefore, this review critically analyzes and discusses innovative approaches such as self-assembly monolayers, surface nanostructuring, buried interface engineering, surface redox engineering, H_2O_2-modified homogeneous NiO_2, selective template growth, and innovative scalability strategies that can overcome the limitations of surface and interface chemistry and device engineering, thereby guiding future research toward environmentally friendly, efficient, and stable PSC technologies. Beyond these relevant developments, this review aims to introduce copper–lead halide perovskites as potential alternative materials. These emerging directions also present new horizons for future applications, offering promising opportunities. Finally, we believe that the strategic engineering of PSCs has strong potential to advance practical applications.

1. Introduction

To begin with, we need to find efficient, stable and friendly PSCs at the same time for better practical energy applications in the field.

The term "energy" has a broader meaning and encompasses numerous areas, including energy generation, conversion, and storage. Consequently, energy materials combine multifunctionalities, enabling the generation, conversion, and storage of energy. Hybrid perovskites are considered multifunctional energy materials driving the next generation of optoelectronics, based on this broad energy concept. This is due to their diverse physicochemical properties and structures.[1] This enables their application in multifunctional energy-related devices.[2–4] Since their initial discovery in 2009 with a record efficiency of 3.81%,[5] halide perovskites have become a focal point of research, yielding major breakthroughs, and remain an active area of research to this day. These halide perovskites exhibit various dimensions (0D, 1D, 2D, and 3D), phase structures

[a] National Taiwan University, Department of Chemical Engineering, Soft Optoelectronic Materials and Devices Engineering Lab, P.O. Box 10617 Taipei, Taiwan. E-mail: taame.abraha@adu.edu.et, cchueh@ntu.edu.tw
[b] College of Natural and Computational Sciences, Department of Chemistry, Adigrat University, P.O. Box 50, Adigrat, Tigray, Ethiopia
[c] College of Natural and Computational Sciences, Center for Material Science and Engineering, Addis Ababa University, P.O. Box 1176, Addis Ababa, Ethiopia
[d] National Taiwan University of Science and Technology, Center for sustainable Energy Development, Graduate Institute of Applied Science and Technology, P.O. Box 106, Taipei, Taiwan. E-mail: wsu@mail.ntust.edu.tw
[e] National Taiwan University of Science and Technology, Center for sustainable Energy Development, Department of Chemical Engineering, P.O. Box 106, Taipei, Taiwan. E-mail: bjh@mail.ntust.edu.tw

Taame Abraha Berhe

Dr. Taame Abraha Berhe received his PhD from the Graduate institute of Applied Science and Technology at the National Taiwan University of Science and Technology, Taiwan. His research is focused mainly on energy harvesting, environment, and catalysis chemistry, with particular topics dealing with halide perovskite materials, solar cell devices, and other optoelectronic devices. His citation count has reached more than 2540 from reputable journals. Now, he is a Postdoctoral fellow at the National Taiwan University, Department of Chemical Engineering, and is faculty member of Adigrat University, Ethiopia, an associate member of the Royal Society of Chemistry (MRSC, 652672) and a regular member of the American Physical Society.

(orthorhombic, tetragonal, cubic, and hexagonal), compositions (single-hybrid, mixed-metal, mixed-halide, and double-layer perovskites), and electronic properties, enabling broad applications across diverse fields. Furthermore, 3D perovskites, primarily represented by $CH_3NH_3PbI_3$, have revolutionized the solar photovoltaic field with their rapid power conversion efficiency (PCE) records and remain a key focus of research and development.[6] The highest PCE of single-junction PSCs exceeds 27%,[7] with a theoretical limit of 33.7%,[8–10] while 3D/quasi-2D PSCs reach 28.99%.[11] Meanwhile, the highest PCE of tandem PSCs is 34.85%,[12] with a theoretical limit of 45%.[13] Furthermore, a perovskite/perovskite/silicon triple-junction (3-J) solar cell has achieved a PCE of 49.4%.[14,15] Not only $CH_3NH_3PbI_3$ but also $CsPbI_3$ and $FAPbI_3$ are being extensively studied due to their high power conversion efficiencies. Despite their high PCE and diverse application potential, the low stability and toxicity of perovskites are increasingly becoming major challenges for further applications. These challenges compel researchers to either seek new ways to improve unstable and toxic perovskite materials or explore alternative materials. According to current research progress, all reported halide PSCs face one of the following challenges:[16] i) high efficiency but poor stability and toxicity, ii) good stability but low

Chu-Chen Chueh

Prof. Chu-Chen Chueh received his PhD in Chemical Engineering from the National Taiwan University (NTU) (2010) and completed postdoctoral research at the University of Washington (2011–2016). He joined the Department of Chemical Engineering at NTU as an Assistant Professor in 2017 and became a Professor in 2023. His research focuses on solution-processable organic/hybrid semiconductors for memory devices, light-emitting diodes, transistors, and solar cells. He has coauthored over 280 papers in the field of organic/hybrid optoelectronics with >26 300 citations and an h-index of 83 (by Google scholar). Dr. Chueh has been recognized by Clarivate Analytics as a 2018 and 2019 Highly Cited Researcher.

Amare Aregahegn Dubale

Dr. Amare Aregahegn Dubale earned his PhD from the National Taiwan University of Science and Technology (NTUST) in 2015. He is an Associate Professor of Chemistry at the Center for Materials Science and Engineering, Addis Ababa University. His research focuses on the synthesis and characterization of nanomaterials, including metallic aerogels, semiconductors, metal oxides, carbon-based materials, and nanocomposites. His work also covers photoelectrochemical water splitting, hydrogen production, and photocatalytic degradation of organic pollutants. Additionally, he studies electrochemical energy devices: fuel cells, CO_2 reduction, hydrogen and oxygen evolution reactions, solar cells and solar-to-fuel conversion, and sensor development with >5617 citations.

Wei-Nien Su

Professor Wei-Nien Su received his Master of Engineering (Dipl.-Ing) from the University of Stuttgart, Germany, and later received his PhD from Loughborough University in the UK. Now, he is a professor at the Institute of Applied Science and Technology of the Taiwan University of Science and Technology and currently serves as the Director of the Technology Transfer Center of the R&D Department. His research interests include energy nanomaterials and electrochemical systems, including electrocatalysts, energy storage materials, and perovskite solar cells. His citation has already reached >18 993 with an h-index of 69.

Bing-Joe Hwang

Professor Bing-Joe Hwang received his PhD degree in Chemical Engineering from the National Cheng Kung University. He is a Chair Professor in the Department of Chemical Engineering and the Director of Sustainable Electrochemical Development Center at the National Taiwan University of Science and Technology. His research has spanned from electrochemistry to spectroscopy, interfacial phenomena, materials science, and chemistry. He shows excellence in research activities with >700 peer-reviewed publications, 50 patents, >48 940 citations, and an h-index of 107. He is also an Adjunct Researcher of the National Synchrotron Radiation Research Center, and the Associate Editor of ACS Sustainable Chemistry & Engineering.

efficiency and reduced toxicity, and iii) environmental friendliness and stability but low efficiency. This leads to the concluding question that "Will its inherent weaknesses cancel out its strengths, or will its strengths overcome its weaknesses?!" Therefore, the current challenge is: "Can we rediscover the existing halide perovskites or discover new halide perovskite light-absorbing materials capable of achieving high efficiency, high stability, and environmental compatibility?" The battle between the weaknesses and strengths of PSCs is evenly matched. Specifically, the weaknesses are instability, toxicity, inherent degradation, and manufacturing challenges, while the strengths are promising efficiency, tunable optoelectronic properties, low cost, and flexibility. This four-way battle of titans will likely conclude with the strengths prevailing, igniting the inherent potential of PSCs and contributing to the future energy, environmental, and economic transformation of global society.

The time has come for all researchers to seriously consider and tackle this dynamic challenge. For this, researchers must consider four critical aspects: 1) substituting stable cations into the A site within the ABX_3 halide perovskite structure; 2) replacing toxic lead atoms in the $APbX_3$ structure with other stable cations; 3) achieving simultaneous substitution of both the A site and lead atoms; and 4) understanding the key causes of interfacial chemistry and energy loss, and establishing strategies to overcome these root causes, thereby achieving robust fabrications and energy conversion in solar cells. While the first two requirements have been attempted and reported in numerous studies, the third and fourth requirements remain the most challenging tasks, indicating why halide PSCs have not succeeded in practical applications.

Therefore, the ultimate objectives of this comprehensive review are threefold. First, to explore and understand the key requirements for an ideal solar cell, the current state of efficiency and stability in PSCs, the major functional molecular bridges, modifier and stabilizer development trends compulsory to address performance bottlenecks including the roles of additives, linkers, capping agents, and ionic liquids, and their future new developments, systematically organizing the information to screen current progress and research. Second, this review aims to stimulate further exploration on how universities, research centers, industry, and companies can achieve large-scale and horizontal implementation of the following surface and interface modification approaches and technologies for further applications: i) flawless and surface nanostructured perovskite thin films, ii) buried interface engineering, iii) surface redox engineering, iv) hydroxylation of metal oxide transport layers, and iv) selective templating perovskite layer growth engineering. These studies contribute to building fabrication platforms suitable for improving the following major issues: i) passivation and wetting processes to achieve proper perovskite thin-film stacking; ii) optimization of interfacial tension to facilitate large-area manufacturing; iii) energy-level alignment and conductivity enhancement to form stable surface states; and iv) slot die coating for full-coverage high-quality perovskite film deposition, enabling scalable film deposition over large areas. Third, this review focuses on the bonding chemistry, orbital mixing control, role-sharing orbitals, copper duality, and other potential properties of copper halide perovskites and their derivatives. It explores new research and development breakthroughs based on $CuPbX_3$ and its derivatives, providing reference material and inspiration for researchers seeking new alternatives and opportunities beyond $CH_3NH_3PbX_3$ and $CsPbX_3$. Much remains to be explored regarding the relationship between photoelectronic structure and performance, spin–orbit interactions, and the control of orbital interactions. Finally, we discuss in detail the perovskite family ($ACuX_3$ (A = +1 cation) and $CuBX_3$ (B = +2 cation)), derivatives of $CuPbX_3$, and potential research directions for controlling their optoelectronic properties. This aims to promote future multifunctional energy applications, strengthen research on copper halide PSCs, advance the field, stimulate interest in this direction across academic, industrial, and commercial sectors, and drive new initiatives in these research discoveries.

2. Analysis of key requirements for an ideal solar cell

This review begins by examining the key requirements for ideal solar cell materials to further advance new discoveries, inventions, and innovations in perovskite solar cells. Without understanding these key requirements for ideal solar cell materials, achieving novel and original breakthroughs is difficult. Therefore, focusing on these key characteristics is significant from the perspective of improving the current research status and limitations faced by perovskite solar cells. Therefore, solar materials must meet the following requirements: 1) semiconductor properties with a bandgap between 1.1 and 1.7 eV; 2) direct bandgap properties enabling direct electron transitions during charge carrier transport; 3) non-toxicity and stability; 4) wavelengths of light that can penetrate the material before absorption; 5) large unit cell area and suitability for repeatable solution deposition processes. For instance, perovskites, cadmium telluride (CdTe), and copper indium gallium selenide (CIGS) are characterized by high absorption capacity.[17] High-performance solar cell materials exhibit superior light absorption capacity.[18] As shown in Table 1, the summarized parameters such as efficiency, bandgap, and absorption coefficient are closely related. Moreover, solar cell materials with a small bandgap and high absorption coefficient enhance the device efficiency. This parameter indicates the amount of light absorbed per unit thickness of the material, or the extent to which light transmits through the material before being absorbed. The absorption coefficient for single-element semiconductors is given by eqn (1).[19]

Table 1 Types of solar cell devices reported with their important parameters

Type of solar materials	Efficiency (%)	Band gap (eV)	Absorption coefficient (cm^{-1})	Diffusion length/μm	Mobility ($cm^2\ V^{-1}\ S^{-1}$)	Bottlenecks	Ref.
Single-junction perovskite	Exceeds 27.3	1.45	0.5×10^4	175 (ref. 28)	Hole = 1187 and electron = 414 (ref. 29)	Instability, toxicity, device deterioration, hysteresis, and film quality	7, 30–32
Cadmium telluride (CdTe)	22.6	1.44	1.1148×10^6	100 (ref. 33)	Electron = 1100 and hole = 100 (ref. 34)	Toxicity of cadmium and the limited global supply of tellurium	35
Copper indium gallium selenide (CIGS)	23.6	1.0 to 1.6	$>1 \times 10^5$ for 1.5 eV	2–9 (ref. 36)	Electron = 100 and hole = 25 (ref. 37)	Concerns about the scarcity and cost of indium and gallium limited production capacity, and lower efficiency compared to silicon-based cells	38
Silicon-based crystalline solar cells	**27.3**	1.1	Below 10^4 for wavelengths larger than 500 nm	250 (ref. 39)	Electron = 1000 and hole = 450 (ref. 40)	High installation costs, production costs, and material usage; a rigid structure and susceptibility to weather conditions	16
Amorphous silicon (a-Si)	**14**	**1.75**	1.7442×10^6	23.4 nm (ref. 41)	Sum of electron mobility and hole mobility of 2.9 (ref. 41)	Staebler–Wronski effect	42
Perovskite/silicon tandem solar cells (4terminal)	Exceeds 37	—	—	—	Recent efficiency is 33.62% and 1700 h (ref. 43)		44
GaAs	29.1	1.43	22 000	L_{De^-} = 20 μm for lightly doped diodes to 2 μm for heavily doped diodes[45] L_{Dh^+} = 200 μm (ref. 46)	Electron = ≤8500 and hole = ≤400 (ref. 47)	The thickness of the thin film and the surface light reflection effects,[48] brittleness, lower thermal conductivity, lack of a natural oxide layer for insulation, and higher cost	31
CZTSSe	15.1	1.0–1.5	p-type GaAs records α of 225 and n-doped GaAs varied from 3×10^{17} to 9.6×10^{17} (ref. 19)	2.5 μm (ref. 49)	39.7 (ref. 50)	The formation of secondary phases and defects, high temperature instability, and difficulty in forming a phase-pure material	51
CIGS	23.6	1.0–1.7	$3–6 \times 10^5$	3 to 22 (ref. 52)	2 to 9 (ref. 36)		53
CIGSSe	20.3	1.0–1.7	10^4	3–22 (ref. 52)	3.7 (ref. 54)	Poor energy level alignment, challenges in achieving high-efficiency solution-processed devices and deep-level defects	55, 56
CZTS	12.1	1.4–1.6	$>1.5 \times 10^4$	0.75 to 1.5 μm (ref. 57)	7.8 to 2750 (ref. 58)	Interfacial recombination; low charge carrier mobility and lifetime; defect formation and secondary phase formation	59
InGaP	22.0	1.14–2.17	100	0.6–1.1 (ref. 60)	μ_n = 3225, μ_p = 150 (ref. 61)	Limited current matching, light extraction and cracking during growth	62
InGaP/GaAs//CIGS	31.2	—	—	—	—	Potential for degradation, especially in harsh environments; complex-fabrication, and limitations in material costs	63
InGaP/GaAs/Si	33.7	—	—	—	—	Current mismatch between the Si bottom cell and the InGaP/GaAs top cell	63
InGaP/GaAs/InGaAs	32.65	—	—	—	—	Radiation damage	64
Perovskite/perovskite	Exceeds 30.1	—	—	—	—	Toxicity, scalability, and stability issues	65

Table 1 *(continued)*

Type of solar materials	Efficiency (%)	Band gap (eV)	Absorption coefficient (cm^{-1})	Diffusion length/μm	Mobility ($cm^2\ V^{-1}\ S^{-1}$)	Bottlenecks	Ref.
GaInP/AlGaAs/CIGS	28.1	—	—	—	—	Complex fabrication, tunnel junction induced deterioration, current limitation *i.e.* the short circuit current J_{SC} of whole structure is equal to smaller J_{SC} of both subcells[66]	67
$CuPbI_3$	—	1.42	1.63×10^5			Not well discovered but Pb is toxic	68
Perovskite/CuIn(Ga)Se_2 tandem solar cells	24.6	—	—	—	—	Difficulties in achieving high efficiency and stable performance, material instability, toxicity concerns with lead in perovskite	69
Perovskite/organic tandem solar cells	26.05–26.07	—	—	—	—	Challenging interconnecting layers and device engineering, toxicity concerns, material instability	70–72

$$\alpha = \frac{A\left(E - E_g - E_p\right)^2}{1 - \exp\left(\frac{-E_p}{kT}\right)} \quad (1)$$

where E is the photon energy, E_g is the band gap energy, E_p is the energy of the absorbed photons, T is the temperature in Kelvin, and k is Boltzmann's constant. The absorption coefficient of binary semiconductors is given by eqn (2).[19]

$$\alpha = A_{direct} \times \sqrt{\frac{1.24}{\lambda} - \frac{1.24}{\lambda_c}} = A_{direct} \times \sqrt{h\nu - E_g} \quad (2)$$

where λ_c is the cutoff wavelength of the material, λ is the photon wavelength, and A_{direct} is a constant value measured in $cm^{-1}\ eV^{-1/2}$. For example, the A_{direct} value of InGaAsSb, InGaAsP, InGaAs and GaSb is 26 000 $cm^{-1}\ eV^{-1/2}$, 36 600 $cm^{-1}\ eV^{-1/2}$, 22 900 $cm^{-1}\ eV^{-1/2}$, and 22 600 $cm^{-1}\ eV^{-1/2}$, respectively.[19–21] In addition to the absorption coefficient, other factors include a band gap of 1–2 eV, nearly equal refractive index of different layers, carrier concentration, diffusion length, and monolithic single-junction and tandem structures.

The main performance loss mechanisms of these solar cells include the charge transport layer (*e.g.* spiro-OMeTAD) absorption, light reflection at the air–glass interface or at the front electrode entrance, and absorption by the front electrode (F:SnO_2).[17,22,23] Other loss mechanisms include intrinsic loss, degradation, emission loss, shunt resistance, thermalization loss (heat generation), depletion region, Carnot losses, grain boundary recombination, shading and spectral mismatch.[17,24–27] The photon efficiency (η_{photon}) represents the loss mechanisms such as transmission, reflection or absorption by the front electrodes but not absorbed by the solar materials, calculated as the external collection efficiency (η_C^{ext}) divided by the internal collection efficiency (η_C^{int}) as shown in eqn (3):

$$\eta_{photon} = \frac{I_{gen}}{I_{inc}} = \frac{\eta_C^{ext}}{\eta_C^{int}} \quad (3)$$

$$\eta_C^{ext} = \frac{I_{SC}}{I_{inc}} \quad (4)$$

$$\eta_C^{int} = \frac{I_{SC}}{I_{gen}} \quad (5)$$

where I_{gen} is the light-generated current and I_{inc} is the incident spectrum incident. When $I_{inc} = I_{gen}$, the solar cell has infinite optical thickness, no reflective loss, and no grid shadowing. If $\eta_{photon} \rightarrow 1$, then $\eta_C^{ext} \rightarrow \eta_C^{int}$ or $I_{gen} \rightarrow I_{inc}$, indicating that the solar cell design should achieve minimum reflectance $r(\lambda)$ and a minimum grid shadow, with nearly all photons $E > E_g$ absorbed and sufficient optical thickness. The efficiency of solar cell is given by eqn (6)–(9):

$$\eta = \frac{P_{max}}{P_{in}} = \eta_{ideal}\eta_{photon}FF\eta_V\eta_C^{int} \quad (6)$$

where,

$$\eta_{ideal}\left(E_g\right) = \frac{\frac{1}{q}E_g I_{inc}}{P_{in}} \quad (7)$$

and,

$$V_{OC} = \frac{1}{q}E_g \text{ and } FF = 1 \quad (8)$$

$$\eta_V = \frac{V_{OC}}{\frac{1}{q}E_g} \quad (9)$$

where η_V is the voltage efficiency and $\frac{1}{q}E_g$ is the bandgap voltage. The best solar cell achieves a V_{OC} value of 0.4 V lower than the band gap voltage. The challenge facing the development of next-

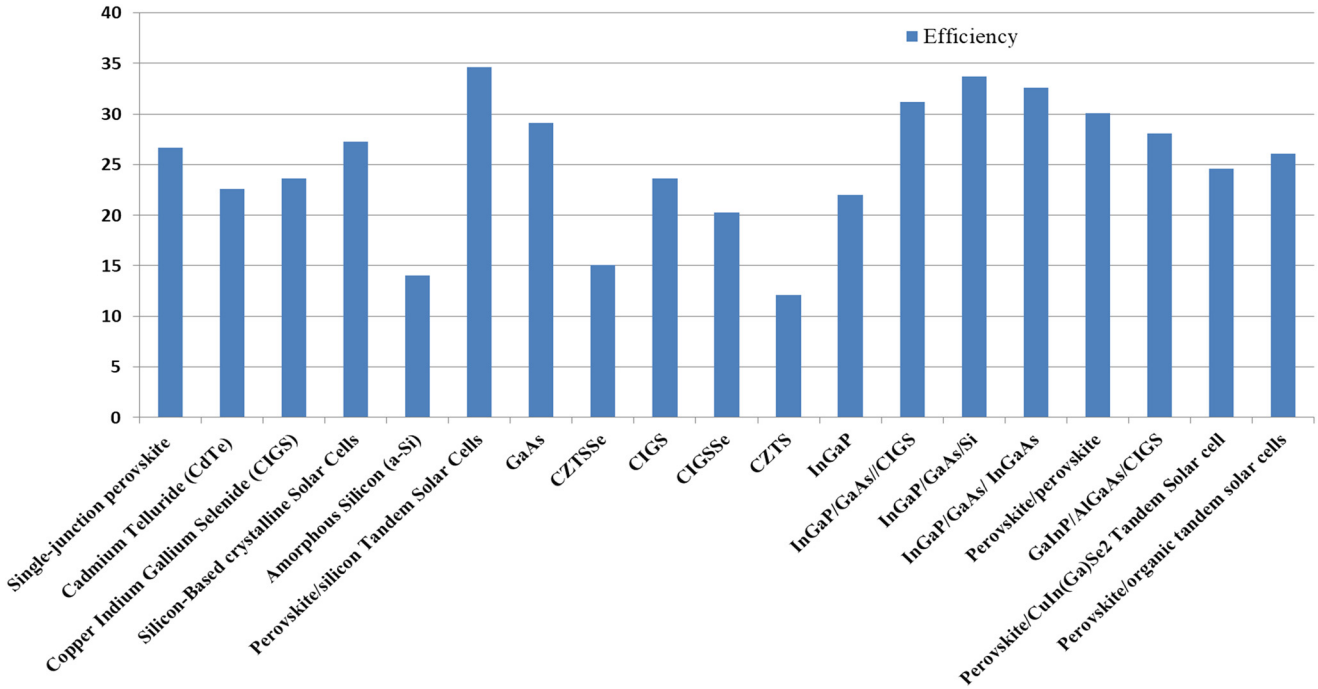

Fig. 1 Comparison of the efficiency of various solar cell devices presented in Table 1.

generation solar cells is the need for a V_{OC} value close to the band gap voltage. As shown in Fig. 1, the efficiencies of various solar cell materials are quite different due to different bad gaps, absorption ability, and other thermalization and semiconducting properties. The depletion region is an area where the number of flow charge carrier decreases, hence blocking the efficient transport of electrons between layers in a solar cell device. The total depletion width depends on the acceptor concentration and donor concentration. For instance, decreasing either acceptor concentration or donor concentration will increase the depletion width. The total depletion width is given by eqn (10):

$$w = \sqrt{\frac{2\varepsilon_1 V_b}{q}\left(\frac{1}{N_A}+\frac{1}{N_D}\right)} \quad (10)$$

where w is the depletion width, ε is the dielectric constant, V_b is the built-in potential, N_A is the acceptor concentration, q is the electric charge, and N_D is the donor concentration. The net recombination rate in this depletion region is given by eqn (11):

$$\text{Net recombination rate per unit volume} = \frac{n_i}{\tau_{dep}}\left(e^{\frac{qV}{2kT}}-1\right) \quad (11)$$

where n_i is the intrinsic concentration and τ_{dep} is the depletion layer lifetime.

Moreover, the diffusion length (L) is given in eqn (12):

$$L = \sqrt{D\tau} \quad (12)$$

where τ is the lifetime of the excited carrier and D is the diffusion coefficient. Based on this point of view, the selection of suitable materials is a very important step for high-performance solar cells.

If the recombination is negligible, all photon fluxes are absorbed with no reflection, and the efficiency of an ideal semiconductor is given by eqn (13):

$$\eta = \frac{\lambda q}{hc}\left[\frac{E_g}{q}-\frac{kT}{q}\ln\left(1+\frac{E_g}{kT}\right)\right] \quad \text{or} \quad \eta = \frac{FF\cdot I_{SC}\cdot V_{OC}}{P_{in}} \quad (13)$$

where η is the efficiency, λ is the wavelength, κ is Boltzmann's constant, T is the temperature, FF is the fill factor, I_{SC} is the short-circuit current, V_{OC} is the open-circuit voltage and P_{in} is the incident power of light. For such ideal semiconductors to perform efficiently, it is necessary to have a perovskite layer with high crystallinity, phase homogeneity, no defects, and high-quality interfaces (Fig. 2).[73]

Not only the active material of the absorber, but also all component materials of the solar cell devices shall not act as sources of performance loss mechanisms. Another strategy is to mitigate the types of loss mechanisms such as optical, thermal and electrical losses.[75–77] Based on the review analysis, the design of an efficient solar cell considers the following factors:[73,78]

1. The band gap of semiconductors shall be between 1 and 1.6 eV to achieve the optimal cell efficiency.

2. Improving η_{photon} by reducing optical losses such as absorption, reflectance, and grid shadowing in optical components and maximizing the optical thickness of solar cells.

3. Improving FF by reducing shunt and series resistances in the cell and its connections.

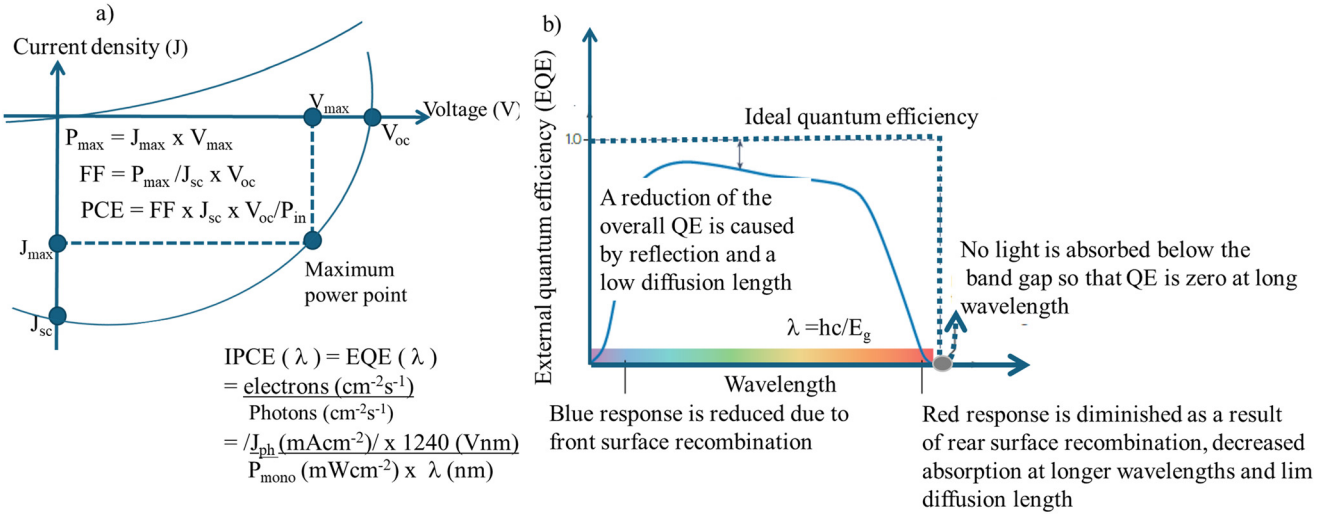

Fig. 2 A typical current density–voltage (*J*–*V*) curve (a) and quantum efficiency spectrum as a function of wavelength (b), reproduced from ref. 74 with permission from Nature Publishing Group, Copyright 2025.

4. Improving η_{ideal} by selecting a suitable band-gap semiconductor.

5. By reducing surface and bulk recombination rates, respectively, improving η_C^{int} and η_V, thereby enhancing I_{SC} and V_{OC}.

6. For sustainability considerations, selecting environmentally friendly, air-stable and non-toxic semiconductors is crucial.

The very important challenge here is whether it is possible to optimize all four requirements for the development of the best solar cells. Researchers may be able to fulfill one of these requirements, but this does not mean that their devices will achieve optimal cell efficiency. Therefore, it is expected that the simultaneous fulfillment of all these requirements will lead to highly efficient solar cells. From this perspective, what are the advantages of perovskite solar cells? Can PSCs simultaneously exhibit the excellent properties required for the best solar cells? Will they be among the most efficient solar cells in the future? How about copper halide perovskite solar cells? Research will answer these crucial questions. To investigate these research questions and move forward in this field, it is imperative to analyze current efficiency and stability state of art in the journey of PSC trends followed by nexus development new trends in the field.

3. Analysis of current stability and efficiency trends in perovskite solar cells

Without thoroughly analyzing and understanding the research status, key challenges, and bottlenecks hindering the practical application of PSCs, it is impossible to improve the efficiency, stability, and scalability in the market. Therefore, crystal structure, material properties, and device structural characteristics are the core focus areas for understanding and resolving the shortcomings faced by PSCs.

3.1. Analysis of the perovskite crystal structure

What does structural instability in $CH_3NH_3PbX_3$ semiconductor solar cell materials signify? This issue indicates that the crystal structure and phases of $CH_3NH_3PbX_3$ cannot withstand conditions such as air, humidity, and temperature. Furthermore, PCE devices made from $CH_3NH_3PbX_3$ readily degrade when exposed to these conditions. What is the root cause of this degradation in these materials and devices? The primary cause of instability lies in the organic cage, particularly the $CH_3NH_3^+$ group, while the origin of toxicity is the Pb metal atom. This is because the $CH_3NH_3^+$ group exhibits high basicity and strong solubility in humid environments, attributable to the highly polar, hydrophilic NH_3^+ group forming hydrogen bonds. When exposed to singlet oxygen, the reaction yields various reaction products depending on thermodynamic energy. For example: $CH_2NH_2 + HOO \rightarrow CH_2NH^+H_2O$, $CH_2NH^+H_2O \rightarrow H_2O$, $CH_2NH^+H_2O \rightarrow NH_2CHO + H_2O$, $CH_2NHO + H_2O \rightarrow CH_2NH^+H_2O$, $CH_2NH^+H_2O + O_2 \rightarrow CH_2NH^+H_2O_2HCHO + NH_2OH$, and CH_3NH^+OOH is formed.[79] However, upon reacting with oxygen, the following products are formed: $4CH_3NH_2(g) + 13O_2(g) \rightarrow 4CO_2(g) + 10H_2O(g) + 2N_2(g)$, ultimately yielding CO_2, H_2O, and N_2. Furthermore, the photooxidation of methylamine refers to the reaction that generates radicals, amides, and imines upon light irradiation in the presence of oxygen.[80] Moreover, addressing this issue may enable the identification of novel strategies to overcome the crystal structural instability and the development of alternative stable materials such as $MPbX_3$ (M = Cs^+, Cu^+, Ag^+, *etc.*), potentially contributing to the achievement of desirable PCE and stability. Currently, materials identified as alternatives to $CH_3NH_3PbI_3$ are primarily classified into two types:[81] fully inorganic perovskites (*e.g.*, $CsPbI_3$) and organic–inorganic hybrid halide perovskites with various structural organizations.

3.2. Analysis of device stability and efficiency

PSCs exhibit various device structures, such as mesoporous, planar, and tandem structures (*e.g.*, n-i-p type, p-i-n type).[82] While one structure may demonstrate superior performance to another, all structures remain unstable unless encapsulated. To achieve practical application and commercialisation, it is necessary to ensure at least 20 years of stability through various strategies to stabilise halide perovskites.[83] The highest stability record reported to date was achieved under continuous solar irradiation at 35 °C using a $Cs_2PbI_2Cl_2$ encapsulation layer, demonstrating five years of stability.[84,85] $Cs_2PbI_2Cl_2$ is a wide bandgap semiconductor with a relatively low effective carrier mass and photoconductivity.[86] This is insufficient to enable the practical deployment and application of PSCs. The stability of PSCs depends not only on the perovskite absorber layer but also on the quality of the hole and electron transport layers, metal electrodes, and device structure. Devices exhibiting the highest performance feature an n-i-p structure.[87] In this structure, the hole transport layer should function as a stabilizer for the device.[88] Another device structure is the p-i-n configuration, known for its compatibility with multi-junction devices and operational stability.[89] Compared to the n-i-p structure, p-i-n structure devices exhibit lower efficiency.[87] In addition to these mesoporous structures, planar structures exhibiting stability dependent on the bonding angle also exist.

Square and triangular structures in planar devices exhibit lower stability than the corresponding linear structures. This arises from the increased bonding angle (namely 180°) in linear structures. Consequently, mesoporous structure devices demonstrate higher stability than the planar devices.[90,91] This is because they exhibit superior electron extraction capability and high resistance to performance degradation due to ion-void migration.[90,92] Numerous other factors contribute to the superior stability of mesoporous structures compared to planar structures, including nucleation sites, uniform growth, and oxygen/water adsorption capacities.[88,93] Meanwhile, another device structure exhibiting higher stability than other bare perovskite devices is the tandem device with an a-Si/perovskite structure, where the a-Si functions as a UV filter.[94] Despite these factors and mechanisms being enumerated, the fundamental causes of degradation and performance decline remain unclear. Continued efforts to identify new causes are therefore crucial and have not yet been fully elucidated.[95] Addressing stability issues and lifecycle management in PSCs represent key research directions for the coming decade.[96,97] Based on our comprehensive analysis, stability and efficiency enhancements mainly depend on three big strategies: i) innovative functional modifiers and molecular bridges, ii) formulation and design of perovskite materials and iii) innovative interfacial modification approaches.

3.2.1. Analysis of the effect of functional modifiers and molecular bridges. Currently, ionic liquids, spacer ions, additives, and capping layers are major research themes for enhancing the performance of PSCs. However, the precise nature of the remarkable properties exhibited by these materials remains unclear. Stability and efficiency performance is highly dependent on the type, property and nature of spacer ion, additive, ionic liquid, or capping layer. In recent years, various types of functional modifiers and molecular bridges have been employed to simultaneously enhance both stability and efficiency, as shown in Fig. 3A and B. These ionic liquids, spacer ions, additives and capping layers include thiourea,[98] PVP,[99] Sm^{3+},[100] Eu,[101] KI,[102] NaF,[103] $ZnCl_2$,[104] caffeine,[105] bis-PCBM + BrPh-ThR,[106] ZnP,[107] SP3,[108] alkylamine ligads,[109] 2-hydroxyethylmetacraylate,[110] 1-propionate-4-amino-1,2,4-triazolium tetrafluoroborate,[111] Zn-TFSI,[112] BQ and F4TCNQ,[113] butyl ammonium,[114] phenethylammonium iodide (PEAI),[115] bromo benzyl ammonium,[116] MTEAC,[117] FABAX,[118] aminovaleric acid iodide,[119] PEA^+ and SCN^-,[120] $BMIMBF_4$,[121] BA,[122] $(NpMA)_2PbI_4$,[123] FIM,[124] RATZ,[125] [bvbim]Cl,[126] poly-1-vinyl benzyltriethylammonium chloride [PILAm],[127] and $Cs_2PbI_2Cl_2$ capping layer.[128] From this analysis of the highest stability, it can be seen that higher stability is associated with lower efficiency, and *vice versa* (Fig. 3A and B). Therefore, there is a strong trade-off between stability and efficiency. Thus, optimizing stability and efficiency to at least achieve an acceptable range is highly demanding. The highest measured stability (51 000 ± 7000 hours, equivalent to 5 years) was achieved with $CsPbI_3$.[85] This active interlayer also achieved a shorter stability range of 720 hours.[129] Therefore, ionic liquids, spacer ions, additives and interlayers were observed in achieving different stability records. If the key lies in the type and nature of these functional modifiers and bridges, which ionic liquids, spacer ions, additives and top layers could be potential materials for the long-term stability of PSCs?

3.2.2. Analysis of the effect of formulation design of perovskites. The stability and efficiency of PSCs are affected not only by the ionic liquids, spacer ions, additives and capping layers, but also by the type, properties, and chemical formulation of perovskite semiconductors. Fig. 4 shows stability *versus* perovskite formulation and design. Thus, studies have reported various potential perovskites for stability testing, such as $CH_3NH_3PbI_3$,[119,125] $CsPbI_3$,[117,128] $MACu_xI_3$,[130] $CsPb_{0.97}Sm_{0.03}Br_3$,[100] $CsPb_{1-x}Eu_xI_2Br$,[101] $(CsFAMA)Pb(I_{0.85}Br_{0.15})_3$,[102] $Cs_{0.05}FA_{0.54}MA_{0.41})Pb(I_{0.98}Br_{0.02})_3$,[103] $MAI(PbI_2)_{1-x}(ZnCl_2)_x$,[104] $(BA)_2(MA)_3Pb_4I_{13}$,[114] $Cs_{0.05}(FA_0.85MA_{0.15})_{0.95}Pb(I_{0.85}Br_{0.15})$,[111] $(FAPbI_3)_{0.85}(MAPbBr_3)_{0.15}$,[116] $PEA_2MA_{n-1}Pb_nI_{3n}$,[131] $FAPBI_3$,[118] $(FA_{0.65}MA_{0.20}Cs_{0.15})Pb(I_{0.8}Br_{0.2})_3$,[120] $MAPbI_3$,[132] FAMACs,[133] $(FA_{0.83}MA_{0.17})_{0.95}Cs_{0.05}Pb(I_{0.9}Br_{0.1})_3$,[134] $MAPbI_3$,[126] $FA_{0.83}Cs_{0.17}Pb(I_{0.6}Br_{0.4})_3$,[122] $(FA_{0.85}MA_{0.15})_{0.95}Cs_{0.05}Pb(I_{0.9}Br_{0.15})_3$,[124] and $Cs_{0.17}FA_{0.83}Pb(I_{0.9}Br_{0.1})_3$.[127]

As shown in Fig. 4, various active perovskite absorbers with various formulations and designs were proposed to improve the stability of PSCs. Based on this in-depth analysis of efficiency and stability trends, this review aims to provide a comprehensive overview of the related development trends that reflect the promising prospects put forward by renowned researchers. These related developments will provide

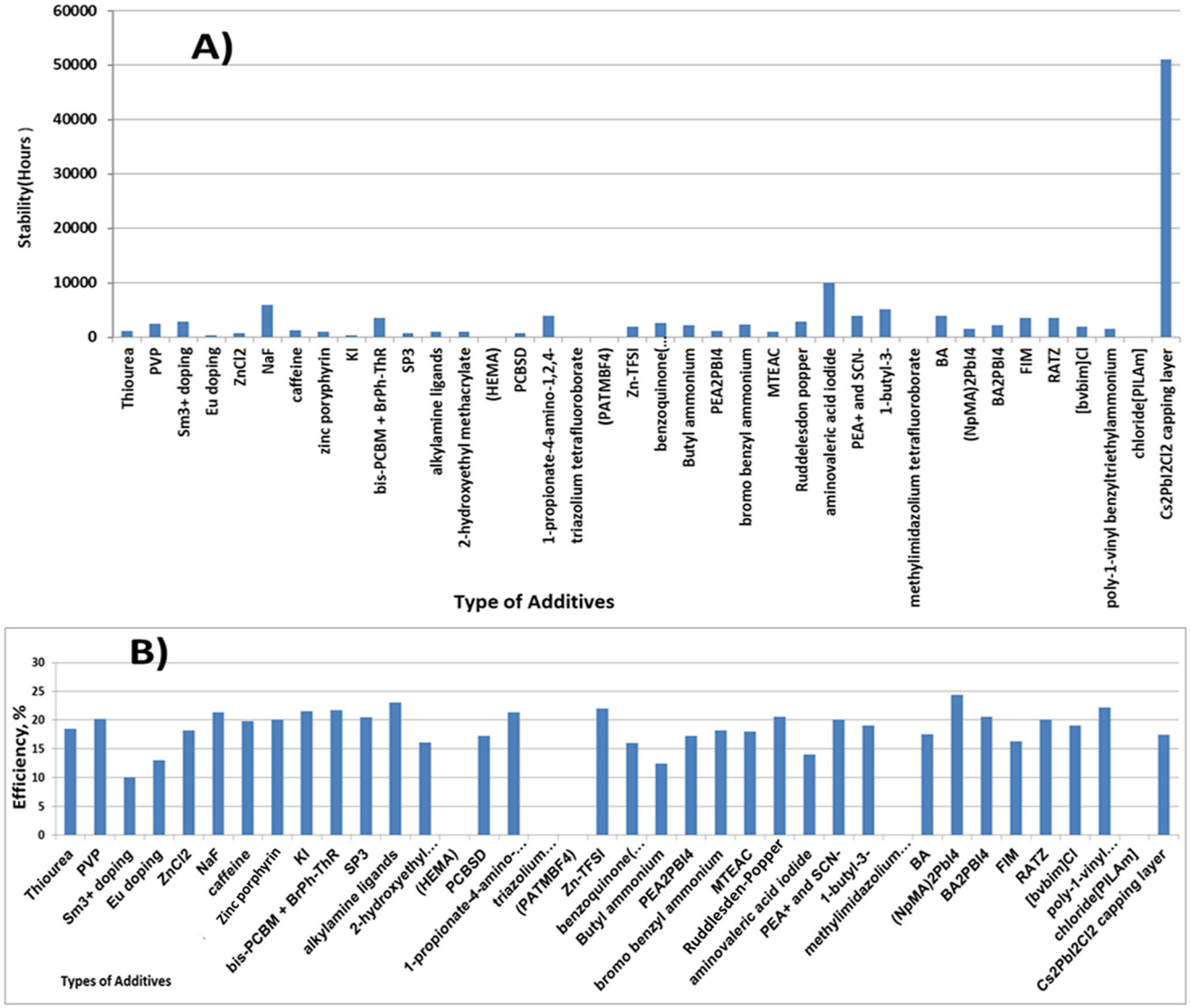

Fig. 3 Effect of additives on the stability (A) and efficiency (B) of PSCs.

researchers with important reference points to reorganize their new ideas according to future research needs for new breakthroughs.

Not only stability and efficiency but also scalability and durability are critical factors for advancing PSCs toward commercialization, where the innovative interfacial modification approaches are considered as the third strategy to drive the market commercialization. Based on the understanding from the in-depth analysis, this review was organized to present key development trends required to overcome the performance bottlenecks focusing on the innovative interfacial chemical engineering of PSCs followed by new materials engineering such as copper-based semiconductor innovations as ways of forward looking the future breakthrough developments and advancements of the field. In addition, awakening points of discussion and multifunctional energy applications of copper halide perovskites are reflected to attract the scientific community towards this new development.

4. Key development trends required to address performance bottlenecks

What are some better solutions to ensure the commercialization and field installation of PSCs to enhance operational efficiency?

The next steps in the development of PSCs are clearly centered on the following eight key areas: 1) stability, 2) efficiency, 3) environmental impact reduction, 4) recyclability, 5) scalability, 6) durability, 7) overcoming performance bottlenecks such as limitations in interfacial chemistry and surface redox control, and 8) the development of novel semiconductors and devices such as new copper halide perovskite semiconductors and their device structures. This nexus development trend aims toward the ultimate goal of achieving cost-effectiveness and sustainability in manufacturing and commercialization while addressing challenges like stability, efficiency, environmental impact, recyclability, scalability, and durability. Meanwhile, the next step

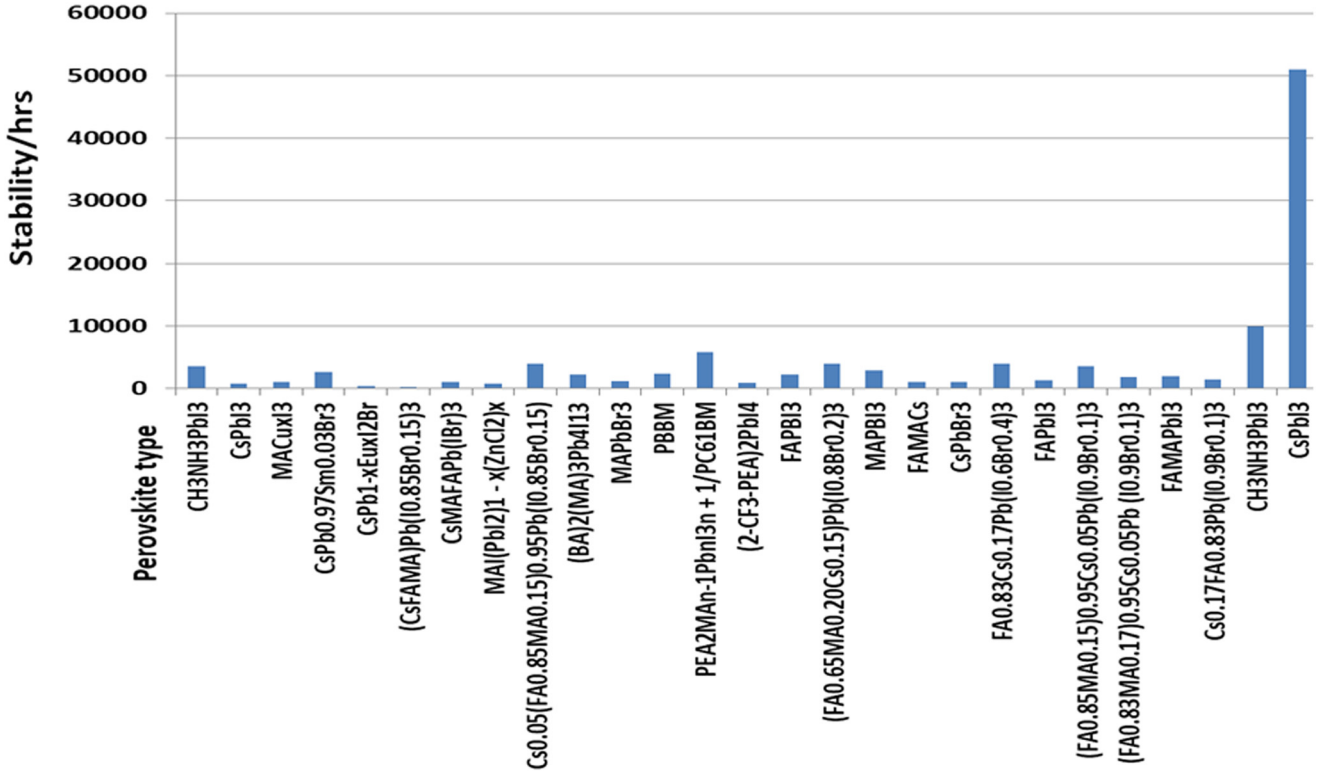

Fig. 4 Effect of different perovskite absorbers on the stability of perovskite solar cells.

in this development addressing PSC performance challenges, as shown in Fig. 5, is to focus on surface and interface chemistry—the limiting factors for stabilizing interfaces, active perovskites, device structures, charge transport layers, and electrodes—or to identify new stable perovskite materials capable of withstanding various material and device degradation conditions. Therefore, $CuBX_3$ and $ACuX_3$ are positioned as "next-generation PSC energy materials" in the upcoming paradigm shift in solar photovoltaic research.

For this purpose, researchers have been exploring various strategies, among which additive engineering,[110,120,135–137] interface engineering,[138–143] electron and hole transporting layer engineering,[144] defect engineering,[145,146] perovskite absorber composition engineering,[147–150] solvent engineering,[151–154] coordination engineering[3,154,155] and device architecture engineering[14,90,91,146,156–165] are the most common approaches. Under these potential research directions, 5 years of stability have been reported.[84] The winning strategy for achieving this performance is the engineering of inorganic capping layers. In general, PSCs are experiencing a glimmering phase of rapid advancement in 2026, transitioning from high-efficiency laboratory curiosities to commercial-ready, durable photovoltaics. Key breakthroughs include PCEs surpassing 27% for single-junction cells, greater than 33% for flexible tandem solar cells and over 34% for perovskite–silicon tandem cells. These advancements are the result of improved stability, flexible form factors, and eco-friendly manufacturing, positioning PSCs to revolutionize urban energy generation, wearables, and space applications.

While understanding the opportunities in the development of PSCs, it is highly necessary to understand the key issues, challenges and obstacles in improving the stability of PSCs. This understanding shall focus not only on PSCs but also on perovskite tandem solar cells. Based on this need, the following bottlenecks, challenges, obstacles, and issues exist:

The first stability challenge faced by tandem solar cells lies in their device structures. Specific challenges include the charge transport layers, operation conditions and encapsulation methods suitable for tandem structures.[166–169] The second bottleneck is the lack of a stable testing protocol, which is of critical importance.[95,170–173] While such protocols are essential, they alone cannot resolve the instability issues inherent in PSCs.[174,175] Some reports have mentioned stability testing protocols from other regions.[95,175] These consensus points are based on consensus stability testing protocols for organic photovoltaic materials and devices.[176] However, in our view, such testing protocols may not be suitable for PSCs due to the unique characteristics of perovskite materials, device architectures, interface configurations, and intrinsic chemical composition and structure. These factors result in significantly different sensitivities to external environmental stress conditions such as light, temperature, electric bias, moisture, and air compared to organic photovoltaic materials and devices.[177,178] This needs further validation and testing of these protocols. Additionally, there are testing categories such as damp heat, thermal cycling, light socking and dark

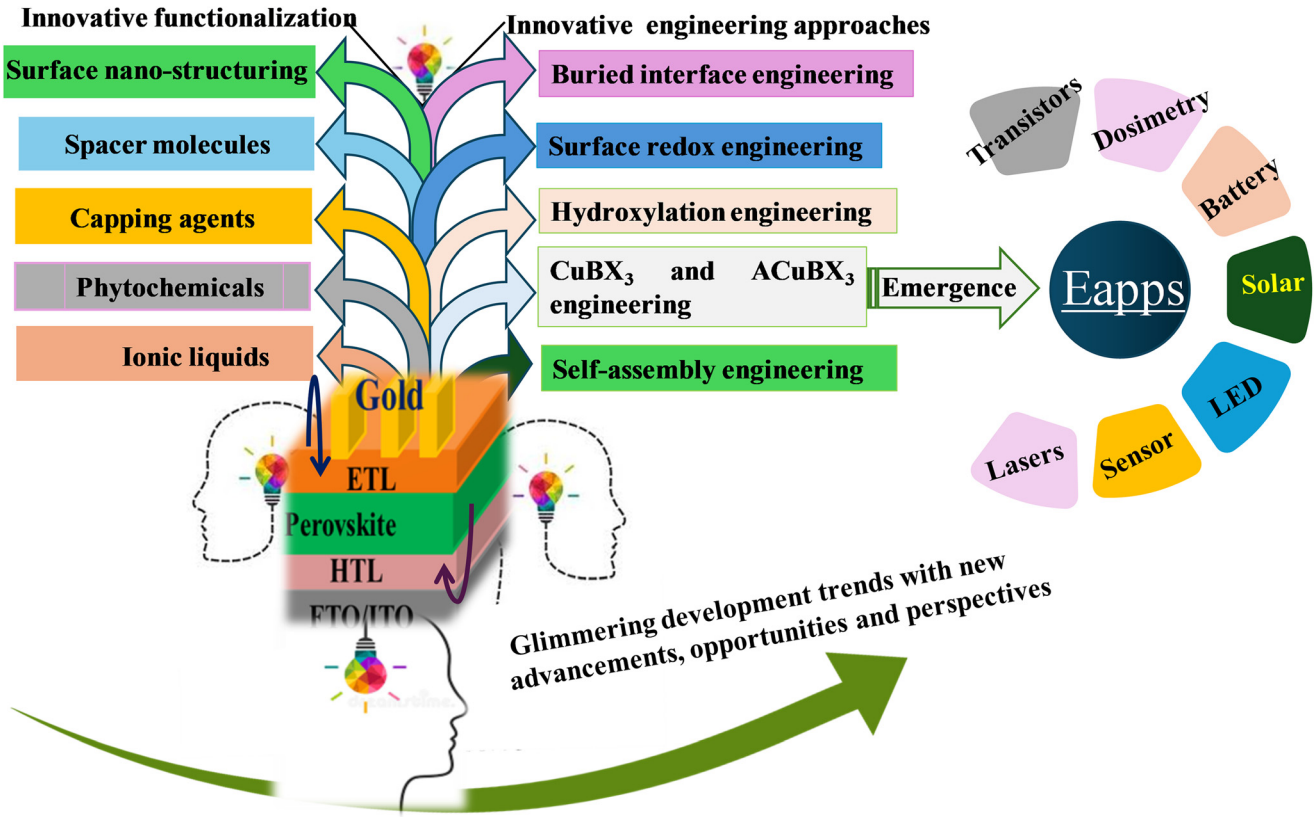

Fig. 5 Key development trends in PSCs and the emergence of new copper halide perovskites for future multifunctional energy applications.

storage. In these stability tests, factors such as testing duration, T80 lifetime, and encapsulation must be considered.[95] Therefore, the stability testing protocols for organic photovoltaics may not be well suitable to PSCs and tandem solar cells. According to the key standard ISOS stability protocols, there are several critical variables that must be met under general test conditions: these variables include negative or positive fixed voltage, ambient conditions (such as controlled humidity), room temperature (such as 65 °C and/or 85 °C), inert gas and vacuum, dark conditions, or one-sun illumination.[179–183]

The third bottleneck is the active perovskite absorber semiconducting layer. The key factor is the influence of moisture. $CH_3NH_3PbI_3$, due to its organic cage structure, cannot tolerate moisture, air exposure, light exposure, and higher temperatures, and is prone to dissolution, oxidation, and combustion. The stability and efficiency of perovskite materials, in general, vary with dimension. Two-dimensional materials are more stable than 3D perovskites but have lower efficiency.[184]

The fourth bottleneck comprises interface-induced instability and low efficiency. The interface is also another factor causing device instability and low efficiency. Recent studies have shown that supramolecular engineering can overcome this challenge. The results indicate that the initial efficiency remains at 96% after 1050 hours, demonstrating the great promise of supramolecular engineering-based double host-guest (DHG) complexation strategies.[185] Moreover, interface misalignment and defect states are key factors in device degradation and require optimization through interface engineering and defect passivation.[142,186–190] The fifth bottleneck is that there are some factors that affect the stability of both PSCs and tandem solar cells, such as:

UV/visible light: UV/visible light may induce the photo-oxidation of component materials of perovskite solar cells, leading to degradation and device failure.[82,191] To overcome this challenge, photoprotective phytochemical molecules in a very thin layer shall be composited to the perovskite device together with the other layers.

Moisture and oxygen: moisture causes perovskite dissolution, while oxygen causes methylamine oxidation and acts as a trap site.[82,192,193] Recently, CuSCN@P3HT as an interface hole transporting layer with additional water splitting ability has been introduced to split the water-rich moisture coming in to attack the perovskite light-absorbing active material.[144] Solar cell device made of CuSCN@P3HT hole transporting material achieved a PCE of 7.91% under a humid atmosphere greater than 80% measured after 28 days. As shown in Fig. 6a, the insertion of a CuSCN@P3HT layer lowers the energy of the HTL to create suitable alignment of the energy levels with the perovskite layer to better extract and transport holes in the device across the interfacial layers (Fig. 6b). Furthermore, while the main work process is the working principle of the PSC, the additional parasitic process occurs due to the water splitting activity of the perovskite/CuSCN@P3HT interface, responsible for the *in situ* oxygen evolution assured by the Fermi level of CuSCN and the

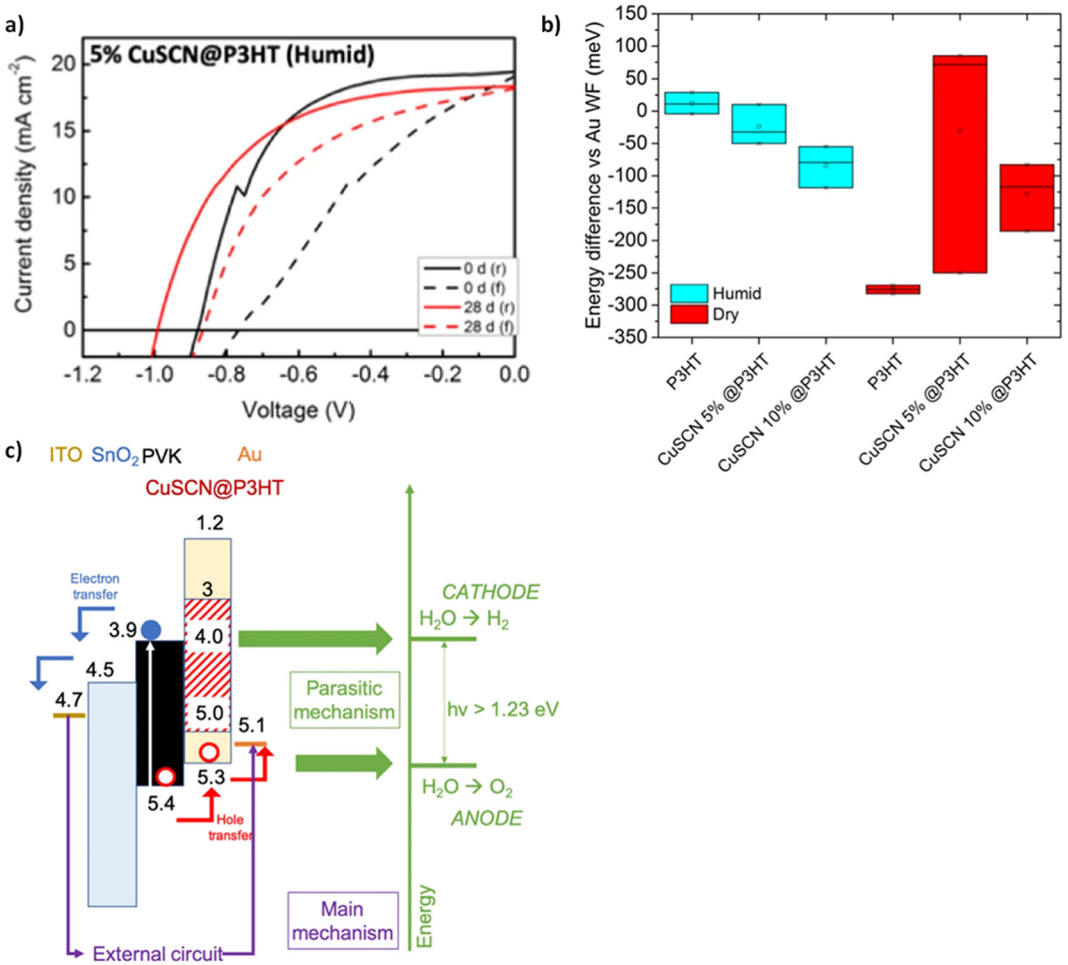

Fig. 6 PSCs configured with CuSCN@P3HT as a hole transport material for water splitting. a) Energy alignment and b) PSC process and water splitting parasitic process configured together, c) proposed mechanisms happening within the water splitting-integrating PSC. Reproduced from ref. 144 with permission from Nature Publishing Group, Copyright 2021.

valence band of p-doped P3HT acting as the cathode and anode, where hydrogen and oxygen evolution occurs (Fig. 6c). Moreover, research shall direct towards making superhydrophobic metal oxide surface such as NiOx for the moisture proofing of inverted perovskite solar cells.[194] Surface architecture and surface chemistry to make lotus leaf and rose petal like metal oxide and perovskite surface nanostructure are suggested to overcome moisture sensitivity.[195]

Mobile ions: the presence of mobile ions triggered by instability affects the stability of PSCs.[196–199] However, conversely, the presence of mobile ions can also improve the tolerance of PSCs.[200] This indicates that there is currently no consensus on the presence of mobile ions in the PSCs. Back electrodes in perovskite solar cells (PSCs) are critical components for charge collection, replacing the expensive metals gold and silver with stable, low-cost alternatives such as carbon, alloys and copper. The aim is to enhance stability and reduce fabrication costs.[140,187,201,202]

Device structure: clearly, device structures such as planar, mesoporous and tandem architectures exhibit different levels of stability. The structure of the PSC devices significantly influences their efficiency and stability.[146,156,161,165,203–206] Perovskite materials cannot withstand high temperatures, leading to a decline in their performance.[207,208] Charge transport layer may be sensitive to photooxidation, degradation, and oxidation caused by oxygen.[209–211] To achieve this, what will be the next winning strategy in the development of these new PSCs? The winning strategy should focus on identifying non-toxic, Earth-abundant, and inexpensive elements, as well as appropriate additives, ionic liquids, ion spacers, or capping agents.[212] Most importantly, it must be stable under light, moisture, oxygen and temperature, while replacing methylamine with flexible device configurations in PSC structures to maintain the stability, efficiency and scalability of PSCs.

4.1. Innovating functional molecular bridges, modifiers and stabilizers

PSCs face four major challenges. Whilst exhibiting high power conversion efficiency, they suffer from low stability, lack of scalability, harmful toxicity, and severe recombination and contact defects that cause energy loss. Addressing these

challenges requires the introduction of functional materials and molecules such as functional molecular bridges, modifiers, and stabilizers. The objective of designing these materials is to realize superior PSCs with enhanced stability and efficiency, thereby achieving scalability. Molecular bridges enhance charge transport processes and reduce energy loss,[213–215] whilst molecular modifiers aim to improve charge extraction and passivation of defects and trap states,[216] both contributing to enhanced performance stability. Therefore, stabilizing materials function as protective layers shielding perovskite from environmental factors such as ultraviolet light, moisture, air, temperature, and other elements that accelerate perovskite degradation.[86,179,217] Their purpose is to ensure long-term device stability, thereby fostering the scalability of PSCs. The objective of this section is to extract the underlying rationale behind the application of functional molecular bridges, modifiers, and stabilizers—namely, what characteristics are required for functional materials to address the performance bottlenecks in PSCs. These rationales will likely lead to smart discoveries that advance research in this field.

4.1.1. Properties of 'additives and spacer ions' to enhance the solar cell performance. In the photovoltaic research field, additives hold significant potential for applications. To select appropriate additives, there is one question that must be answered. When selecting appropriate additives, one critical question must be addressed first: "Which properties of additives are suitable for enhancing the performance of solar cells?" This is the first question that every researcher must understand when choosing additives for photovoltaic and energy applications. The key characteristics of additives used to enhance the efficiency and stability of solar cells include: defect passivation capability, increase in crystallization in the absorber solar semiconductor, improvement of charge transport and extraction across the layers, enhancement of ion and carrier mobility, enhancement of light absorption and harvesting, resistance to stress conditions, prevention of material degradation and device deteriorations.[218–220] The mechanism is achieved *via* the formation of acid–base adducts between Pb^{2+} and the lone-pair electrons of nitrogen, oxygen and sulfur in the additives, as well as hydrogen bonding interactions between additives and formamidinium and methyl amine functional groups.[218,221–223] Spacer ions are crucial for enhancing the stability of PSCs, as they prevent interlayer oxidation.[224] While choosing spacing spacer ions, they must meet the following requirements: size, solubility, hydrogen bonding, shape and charge.[225–228] The number of benzene ring, structure flexibility, size and chain length, types of functional groups, and the combination of two or more spacer cations on reducing lattice distortions, adjusting crystallization and proper growth orientation, and stabilizing perovskite structure and morphology are important considerations in selecting organic spacer ions for solar cell applications.[229–232] The spacer ions play a role in enhancing the mobility of ionic charge transport across layers while decreasing stack resistance.[233] Furthermore, incorporating larger organic cations into 2D perovskite structures can enhance the environmental and structural stability of PSCs.[234,235] Besides, PSCs require flexible and hydrophobic organic spacer ions with shorter side chains.[236]

4.1.2. Properties of 'ionic liquid' required to enhance the solar cell performance. Ionic liquids are highly suitable for enhancing the efficiency and stability of solar cells. 'How to make ionic liquids suitable for solar cell research' is the key issue in selecting appropriate ionic liquids. Ionic liquids possess highly important properties that can enhance the performance of solar cells and general energy devices.[237–241] These properties include: the ability to interact with specific components of the solar cell devices through structural design, adjustable viscosity, excellent electrochemical stability, high ionic conductivity, higher polarity, low melting point, good thermal stability, and low volatility,[242–247] Through mechanisms such as passivation defects, trap states, and recombination centers, as well as enhancing interfacial energy level alignment to improve charge carrier transport and ion mobility between layers in the solar cells, ionic liquids can enhance stability and efficiency.[248–252]

4.1.3. Properties of 'capping layer' required to enhance the solar cell performance. Implementing capping layers to enhance the performance of PSCs has become quite common. However, the implementation of capping layers has been a trial-and-error process.[253] Considering this, a strategic selection mechanism has been proposed, such as organic molecules with small topological polar surface areas and low hydrogen-bonding donors, which are associated with active perovskite absorbers, to enhance the PSC stability.[253,254] Under this strategic approach, the use of a $Cs_2PbI_2Cl_2$ capping layer has stabilized the perovskite/hole transport layer interface and suppressed ion migration into the hole transport layer, achieving five years of stability.[128,255] The advantages of capping layers in PSCs lie particularly in changing surface chemistry to induce stable photoactive layers. Due to their larger parcel size, they prevent most incident light from directly transmitting through, thereby protecting against methylammonium loss.[253,256] The primary function of the capping layer is to suppress carrier surface recombination and protect the active perovskites from degradation. Its anti-reflective properties enhance short-wavelength spectral response and improve charge carrier collection.[257]

Cation exchange properties are vital for enhancing the performance of perovskite solar cells.[258] The primary application of cation exchange in PSC is to improve material properties, thereby enhancing the reproducibility and performance. This improves the infiltration, penetration and permeability of perovskites in the device structure's porous configuration, reducing recombination and enhancing absorption efficiency and stability.[224] Such exchange may occur at the A or B sites of the perovskite structure. However, depositing 2D perovskites can impair reproducibility and performance due to weak cation exchange capacity, poor perovskite penetrations/infiltrations, strong binding energy, limited absorption, and poor interfacial charge transport.[179] As shown in Fig. 3, a $Cs_2PbI_2Cl_2$ capping layer has been implemented to enhance the performance of PSCs, thereby achieving better stability. Fig. 7 shows the uncapped (Fig. 7A)

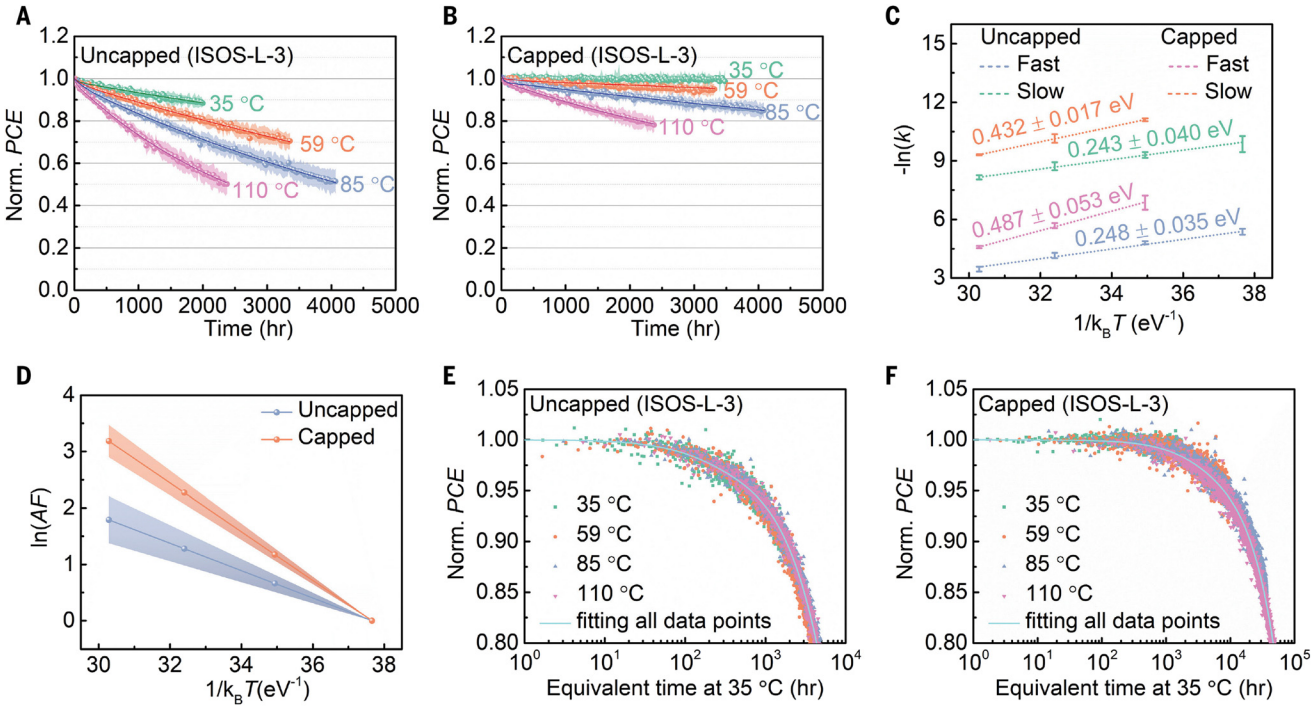

Fig. 7 Accelerated aging of PSCs under the ISOS aging standards. Reproduced from ref. 179 with permission from AAAS, Copyright, 2022. A) uncapped and B) capped PSCs operating at 35°, 59°, 85°, and 110°C, with standard deviation envelopes. C) Natural logarithm of degradation rates (k_{fast} and k_{slow}) versus $1/k_BT$ obtained from biexponential fits to PCEs for uncapped and capped PSCs, where T is the aging temperature. D) Natural logarithm of AF versus $1/k_BT$ with the standard deviation represented by the shaded area around each line. E and F) Normalized PCE of uncapped and capped PSCs plotted against the equivalent aging time at 35 °C.

and capped (Fig. 7B) perovskite solar cells, indicating that the capped device exhibited superior performance compared to the uncapped one. Furthermore, Fig. 7C shows the logarithmic relationship between the decay rate of the uncapped and capped devices, *i.e.*, $1/k_BT$, where k_B and T represent the Boltzmann constant and temperature, respectively. As a result, the decay rate of the uncapped device is faster, while that of the capped one is slower. Fig. 7D shows the logarithmic relationship between the lifetime accelerated factor (AF) of the uncapped and capped devices, *i.e.* $1/k_BT$. Fig. 7E and F show the relationship between normal PCE and aging time at 35 °C, indicating that the performance of the capped device is superior to that of the uncapped one. The device successfully demonstrated in this study achieved 10 000 h of device stability. Thus, it is believed that the ion exchange, passivation effect, and perovskite infiltration properties have been significantly improved, thereby reducing recombination effects and device instability.

4.1.4. Synergistic effects of phytochemicals in photovoltaics. Why do phytochemicals play a crucial role in enhancing the performance of solar cells? Which components are particularly vital for this application? How much of these phytochemicals are required to achieve high-performance solar cells? What mechanisms are at play? Why do phytochemicals exhibit unique applicability in the field of energy conversion? From the perspective of enhancing PSC performance, what multifunctional advantages do they offer in terms of both stability and efficiency improvements? Additives have widespread applications in fields such as batteries, solar cells, and fuel cells, enhancing safety, cycling life, efficiency, and performance through electrolyte optimization, as well as improving electrochemical properties.[259–263] Among additives, those with high phytochemical properties and compositions are highly valued in the photovoltaic field. The roles of phytochemicals include enhancing light absorption and efficiency, photosensitization, and crystallization. The composition of such essential phytochemicals include alkaloids, tannins, terpenoids, betacyanins, anthocyanins, flavonoids, and glycosides, as shown in Table 2.[264] When these compounds coexist in the same plant source, their synergistic effects play a crucial role. The origin of synergistic effects that enhance device efficiency stems from the distinct roles each compound plays within the system. For instance, flavonoids possess electron-donating and -accepting properties, which further enhance charge transport and thus improve device efficiency; glycosides provide structural support for semiconductor materials such as perovskites and other light-absorbing materials, enabling solar cell devices to exhibit long lifetimes, impact resistance, and durability, ensuring stable photoconversion efficiency during long-term safe operation.[264–266] Moreover, phytochemicals enhance the PCE by creating balanced charge mobility, reducing recombination, providing photoprotection and favorable morphology, and enhancing electron–hole transfer characteristics.[267–269] Furthermore, volatile solid additives improve the repeatability and stability of solar cell devices.[263]

Table 2 Promising phytochemical-rich plants for solar cells

No.	Type of plant	Phytochemical compounds	Efficiency achieved (%)	Ref.
1	*Aloe vera*	Chromones, anthraquinones, anthrones, steroids, tannins, flavonoids, alkaloids, and phenolic compounds	23.61%	270, 271
2	Pomegranate (*Punica granatum* L.)	Phenolic acid, flavonoids, tannins, amino acids, and alkaloids	2.0% (ref. 272)	273
3	*Ocimum gratissimum*	Flavonoids, alkaloids, saponins, phenolics, tannins and terpenoids	1.81% (ref. 274)	275
4	*Centella asiatica*	Sterols, phenolic acids, polyacetylenes, apigenin, patuletin, kaempferol, rutin, flavonoid quercetin, madecassoside, centellose, triaponosides, and triterpenoids	18.5% (ref. 276)	277
5	*Punica granatum* L.	Phenolic acid, anthocyanins, anthocyanidins, flavanols	3.63% (ref. 278)	
6	Turmeric and carotene dyes	Curcumin, beta-carotene and lycopene	9.78% and 7.81%	279

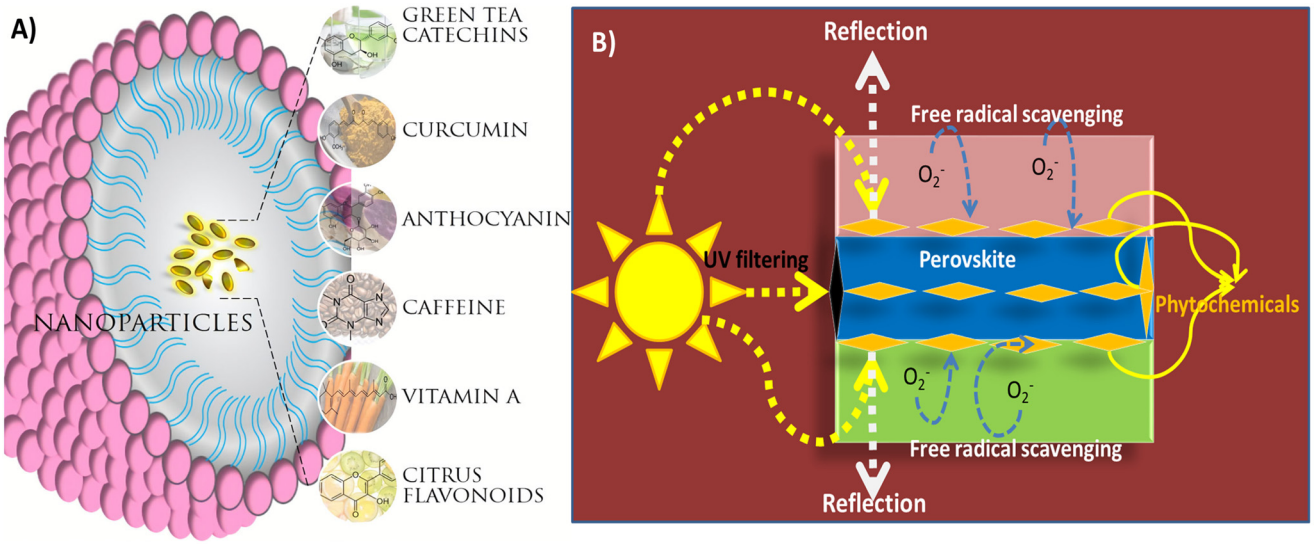

Fig. 8 Nanosized phytochemicals: A) different classes of photoprotective natural products, reproduced from ref. 280 with permission from Springer Nature, Copyright 2020. B) Proposed working mechanisms of action of phytochemicals in photoprotective and free radical scavenging of free radical oxygen species.

Phytochemicals include polyphenolic compounds produced in citrus fruits (flavanones), onions (flavonols), berries, cherries (anthocyanidins), grape seeds (proanthocyanidins), soy (isoflavones), green tea (catechins), and others; flavonols, isoflavones, anthocyanins, catechins, terpenes, resins, alkaloids, lignin, vitamins, and spirulina (spirulina maxima), as shown in Fig. 8A. Furthermore, PSC stability is affected by light intensity, such as ultraviolet (UV) light. Therefore, it is necessary to utilize nanosized phytochemicals from plant crude extracts as photoprotective agents. These components possess UV absorption capabilities, which can serve as UV filters and reduce UV-induced reactive oxygen species, as shown in Fig. 8B.[280] This represents a strategy for stabilizing solar devices through the use of phytochemicals. What mechanisms underline the advantages of phytochemicals? The primary mechanisms have been reported as reflection, absorption and anti-oxidant activity. These properties, derived from phytochemicals, provide photoprotective benefits such as absorbing and reflecting the most harmful UV light. This anti-oxidant activity has also been proposed to scavenge free radicals generated during photooxidation when exposed to light, as shown in Fig. 8B.

Moreover, the mechanisms of action of phytochemicals are particularly useful in the following areas: electrode interaction: phytochemical compounds adsorbed on the surface of solar cell electrodes overcome sedimentation that can affect chemical interactions, active surface area, and current flow within the electrodes.[281,282] Charge transport layer infiltration: phytochemicals help charge carriers easily penetrate each layer and effectively collect charges at the corresponding electrodes, thereby enhancing the charge transport layer's ability to conduct electricity by effectively separating electrons and holes.[283,284] The antioxidant performance can protect the active perovskite layer from damage caused by oxidative stress (see Fig. 9).[285–287] Electrode morphology modification: Phytochemicals are used as electrode additives to modify surface properties, shape, particle size, electro-catalytic activity, nanoparticle growth and aggregation, conductivity, physical adsorption, and

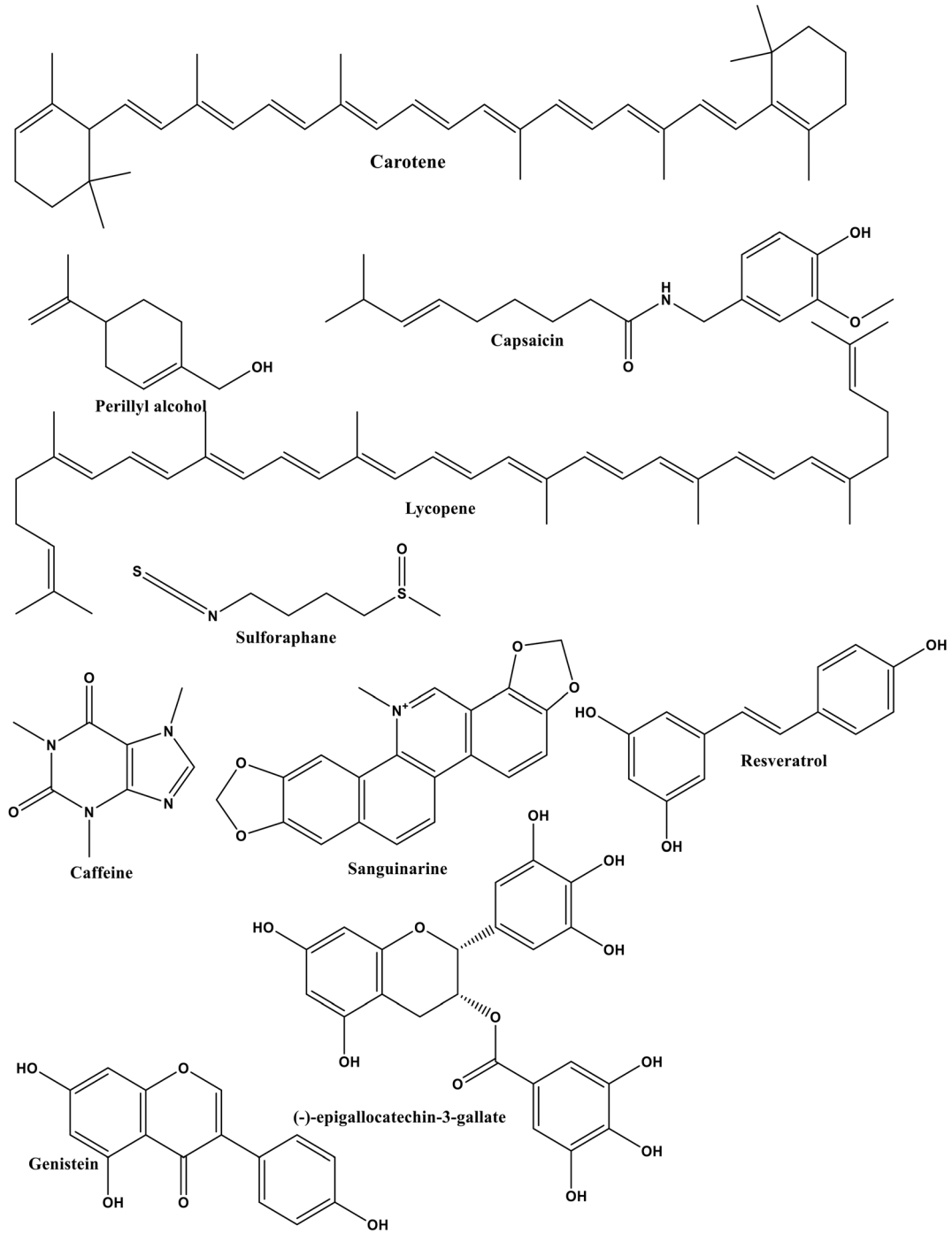

Fig. 9 Schematics of phytochemicals against UV degradation, reproduced from ref. 292 with permission from Thieme Gruppe, Copyright 2008.

charge carrier transport. Through structure–property changes, the morphology is optimized to enhance the device performance.[288–291]

4.1.5. Phytochemical crystal engineering. Although plant chemicals have made significant contributions in various applications, they also have drawbacks such as hygroscopicity, chemical instability, high melting points, and low dissolution rate and solubility.[293] To address these drawbacks, crystal engineering is a promising strategy.[294] Moreover, multicomponent crystal engineering is a suitable method for improving the physicochemical properties of phytochemicals, such as compressibility, permeability, stability, dissolution rate, solubility, and melting point.[294,295] Nernst–Brunner or Noyes–Whitney equations for the solubility of phytochemicals are given by eqn (14):

$$\frac{dM}{dt} = \frac{D \cdot A}{h}(C_s - C_t) \quad (14)$$

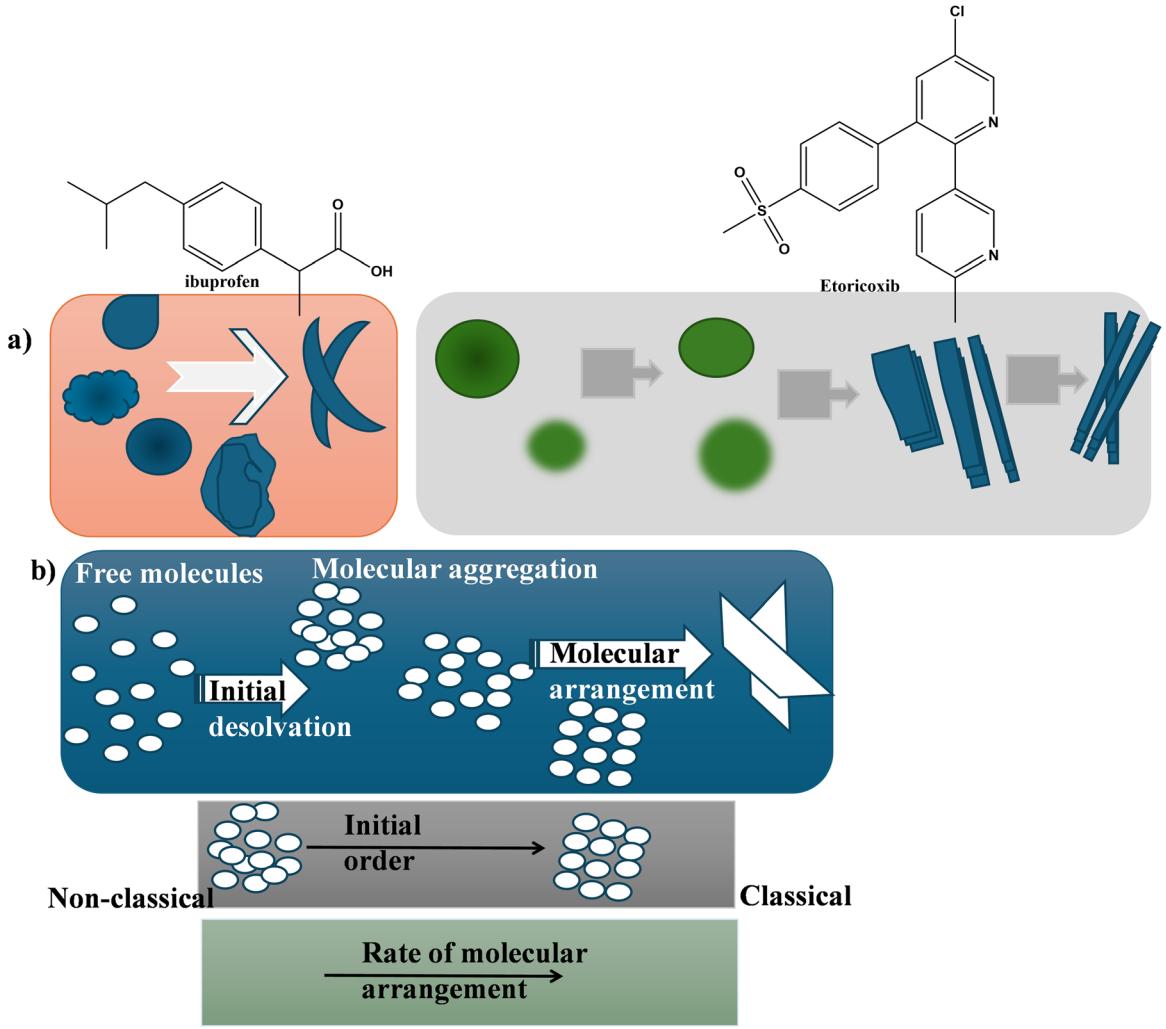

Fig. 10 Crystallization of organic molecules: a) order evolution of ibuprofen and (b) etoricoxib, where continuum crystallization depends on the crystallization of initial intermediates' degree of order evolution, reproduced from ref. 298 with permission from the American Chemical Society, Copyright 2021.

where h is the thickness of the diffusion layer, D is the diffusion coefficient, dM/dt is the dissolution rate, A is the solid surface area, C_s and C_t are the concentrations of phytochemicals in solution at equilibrium and t is the time.[296]

Therefore, crystal engineering is the mechanism for obtaining high-quality organic crystals and purifying organic compounds.[297] In this case, Fig. 10a and b show that the crystallization mechanism is not yet clear, but crystallization occurs through two mechanisms: classical crystallization and non-classical crystallization.[298] Classical crystallization occurs when the crystal order increases from the molecular dissolved state, while non-classical crystallization occurs in an amorphous intermediate state. There is also a type of inclusive crystallization known as continuous crystallization, in which non-classical crystallization and classical crystallization occur simultaneously. This crystallization provides new insights into the novel mechanisms underlying the formation of phytochemical compounds. Moreover, such co-crystallization of phytochemicals has the ability to encapsulate other compounds (possibly bioactive compounds or perovskites) to stabilize these compounds, forming a porous matrix in which perovskites or other bioactive compounds are integrated. Therefore, phytochemical engineering is useful for the formation of larger grains, fewer grain boundaries, lower defect density and the inhibition of particle aggregation.[268,299,300] Phytochemicals may interact with central atoms (such as Pb^{2+}, Sn^{2+}, and Cu^{2+}) in perovskite materials to form larger grains with lower defect density.[301] The inhibition of particle aggregation is achieved through the use of reducing agents and capping agents and the control of surface properties, shape, and size to prevent aggregation and ultimately stabilize active nanomaterials.[300,302,303]

Furthermore, this co-crystallization enhances the encapsulated material's flowability, stability, anti-caking properties, hygroscopicity, dispersibility, homogeneity, and wettability.[304] There are two main encapsulation methods: thin-film encapsulation and glass encapsulation. Among these, thin-film encapsulation is highly recommended due to

its performance improvements,[305] making phytochemicals a viable thin-film encapsulation method for PSCs. Likewise, the advantages of organic crystal engineering include: 1) crystallization-induced properties, such as changes in intermolecular interactions, chemical properties, non-radiative decay pathways, enhanced photoluminescence, water dispersion, and optical waveguide effects and 2) morphology-dependent properties.[306] Moreover, organic optical properties, such as amplified spontaneous emission and optical waveguides, are highly dependent on crystallinity, molecular arrangement, and crystal morphology.[307,308]

4.1.6. Self-assembling small-molecules and polymer heterointerface bridges. Functional additives, spacer ions, ionic liquids, capping layers, and phytochemicals significantly contributed to perovskite crystallisation and protection from environmental and stress factors. The design of PSCs faces not only challenges such as crystallisation and instability of the perovskite active layer but also numerous bottleneck issues across surfaces and interfaces, including those of the remaining constituent materials (ITO, FTO, HTM, and ETL) and the interfaces with the perovskite layer. Overcoming these surface and interface bottlenecks strongly necessitates further innovation in small molecules, such as self-assembling molecules, as well as larger polymer crosslinks and hetero-interface bridges.[309–315] Furthermore, as shown in Scheme 1a, bridging structures such as the heparin sodium polymer heterointerface constitute multifunctional intermediate layers characterized by SO_3^- and COO^- functional groups that interact with metal cations such as Na^+.[314] These bridges possess a bottom surface, main backbone, and top surface that promote interaction with electron transport layers such as SnO_2 and perovskite active layers, forming robust bonds, passivating defects, enhancing interfacial adhesion, and facilitating electron transport. Meanwhile, crosslinked polymers are essential for improving solvent resistance and high mechanical stability by forming a 3D network (Scheme 1b). In particular, crosslinked polymers are useful for forming interfacial contacts between 2D and 3D perovskite layers, creating an environment conducive to charge transport.[313] Hyperbranched polymers are also crucial for reducing current leakage and enhancing mechanical toughness in flexible perovskite solar cells.[316] This innovative technology is indispensable for achieving the optimal trade-off between efficiency, stability, and scalability in further improvements towards the commercialization of PSCs.

Furthermore, self-assembled and co-assembled molecules form ultra-thin, strongly ordered layers, achieving excellent orientation and uniformity by adjusting the interfacial energy

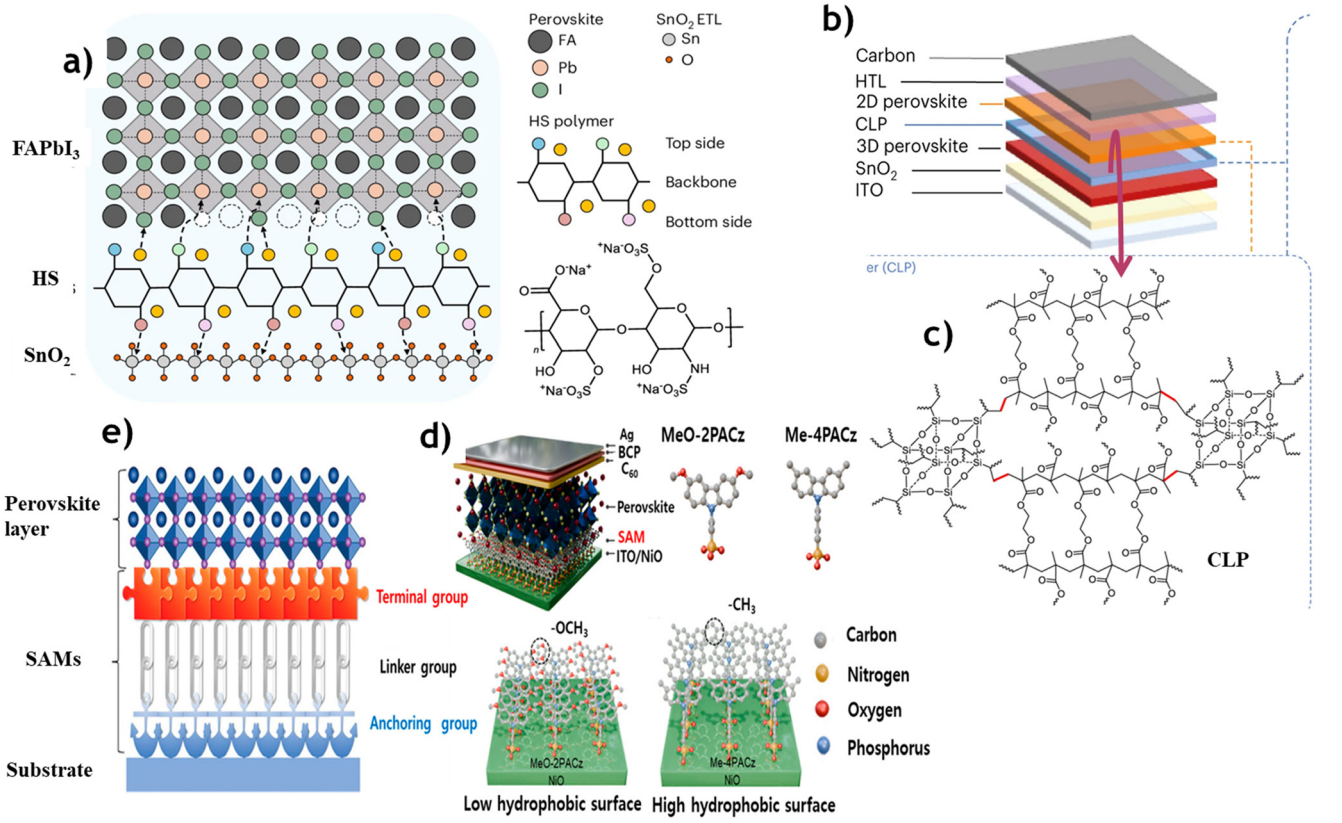

Scheme 1 a) Schematic of the mechanism by which HS connects SnO_2 and perovskite layers and passivates defects at the buried interface, reproduced from ref. 314 with permission from Nature publishing group, Copyright 2025. b and c) Schematic of the device structure, the deposition of the 2D perovskite layer and the molecular structures and synthesis process of POSS, EDMA and the CLP, reproduced from ref. 313 with permission from Nature publishing group, Copyright 2023. d) Schematic of the p–i–n structure of PSCs, including the molecular structures of carbazole-based MeO-2PACz and Me-4PACz, reproduced from ref. 317 with permission from Wiley, Copyright 2024. e) Structure of the self-assembling molecule, reproduced from ref. 323 with permission from Wiley, Copyright 2025.

level, thereby improving the trade-off between efficiency and stability (see Scheme 1d).[317–322] Such molecules possess terminal groups interacting with perovskites, anchor groups interacting with the hole transport layer, and spacers linking the terminal and anchor groups, forming vertical or slightly inclined angles (see Scheme 1e).[323] These self-assembled molecules also exhibit hydrophobicity, with their hydrophobicity varying from low to high, as shown in Scheme 1d. This is an essential property for the development of moisture-resistant PSCs. This orientation provides excellent adhesion, coverage, and ultra-thin film layers for hole transport. Furthermore, π–π interactions within the self-assembled molecules promote the formation of ordered monolayers or bilayers with hydrophilic surfaces. This enables large-area, high-quality formation with reduced defects while pre-enhancing efficient charge extraction and transport at the interface.[310]

Furthermore, the chemical limitations of surfaces and interfaces present an urgent challenge requiring surface and interface engineering using small molecules, such as self-assembled monolayers (SAMs)[324] and bilayer films,[325] with the aim of enhancing both efficiency and stability. As shown in Fig. 11a, the functionalisation of self-assembled materials fundamentally involves: 1) terminal groups that interact with perovskite materials to determine interfacial and surface properties, functioning as functional groups of the structured organic molecules; 2) spacers: components that bind to the perovskite *via* weak interactions such as van der Waals forces, linking the terminal groups and anchor groups to ensure functionality; 3) anchoring groups: components that interact with the substrate *via* coordinate or covalent bonds, enabling high substrate transparency. The primary reasons for applying these self-assembled layers are their low cost, their non-acidic nature within the system, and the improvement in device efficiency and stability afforded by the chemical bonding that facilitates their coupling with the substrate.

The ultimate goal of applying SAMs is to overcome both surface and interfacial chemical limitations that inhibit efficient charge transport characteristics: 1) dysfunction at buried interfaces due to suboptimal energy levels, defects, stress, and potential-induced degradation and 2) high carrier recombination at vacancy sites caused by imperfect lattice structure crystalline surfaces, ion migration, dangling bonds, and chemical corrosion across the entire interfacial layer. Consequently, understanding the concept of self-organizing materials and their impact on overcoming the limitations of interfacial chemistry is imperative, with research underway to realize efficient and stable devices, as depicted in Fig. 11b and c. The unique property of self-assembling materials is based on their 'three-in-one strategy'. This strategy combines three functional approaches: 1) achieving transmittance and stabilization of the surface atoms of the substrate, which is part of the concept of anchoring chemistry, 2) maintaining the tight packing barrier, which is part of the linker or spacer, and 3) improving surface and interfacial properties. A particularly striking way to express this concept is through the "three birds with one stone" strategy. This strategy applies an "integrated

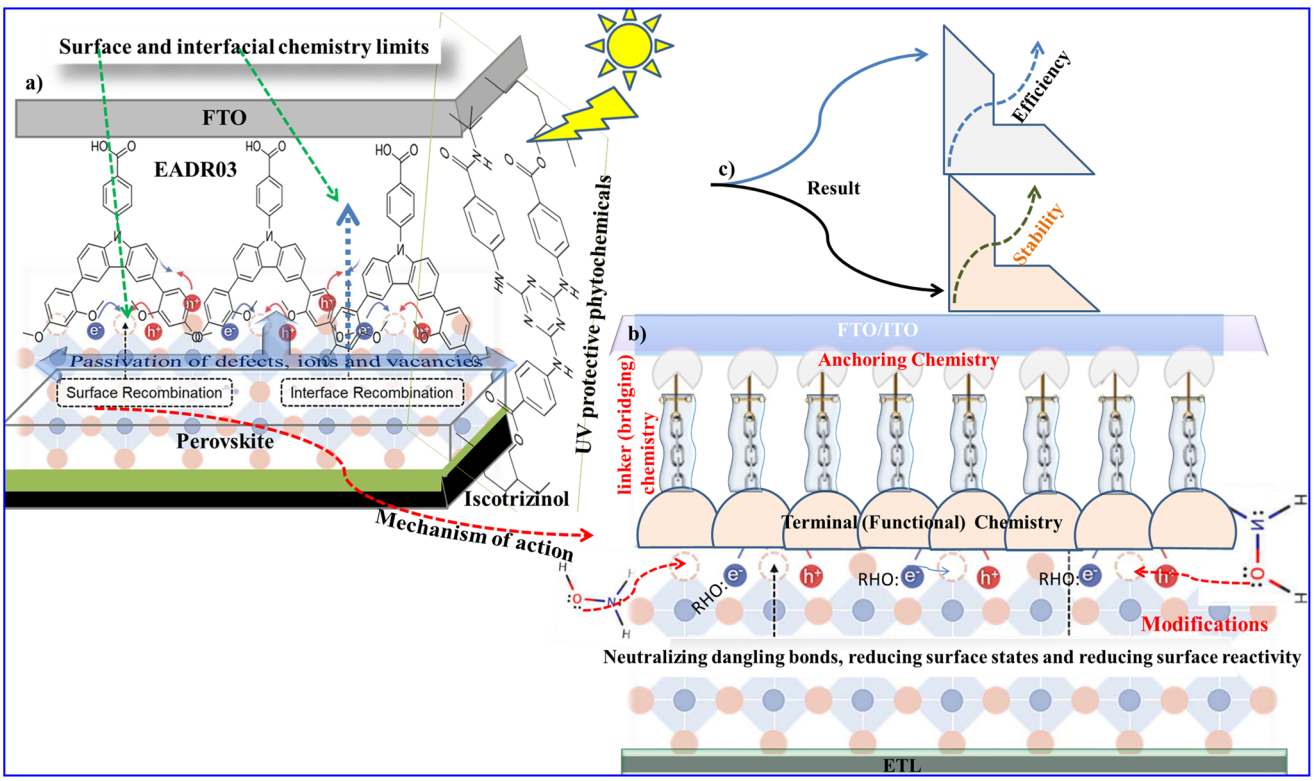

Fig. 11 Schematic of the highly efficient and stable PSCs: a) device configuration, b) mechanism of action and c) demonstration of enhanced trends in efficiency and stability.

approach concentrating three or more functions within a single molecule": a) structural design that suppresses carrier recombination and achieves uniform electric field distribution by expanding the electrode area. b) Optimization of self-assembled molecular layers: reduction of surface and interfacial defects, prevention of reactions between methylammonium/formamidinium and the substrate due to voltage bias, and realisation of thin-film formation through the morphological arrangement of crystallites. Furthermore, this integrated strategy achieves surface and interfacial defect reduction, prevents corrosion-inducing side reactions, and realises surface atomic-level stability through the formation of thin films *via* the morphological arrangement of crystallites. c) Optimization of self-assembled molecular layers: reduction of surface and interfacial defects, prevention of corrosion-inducing side reactions, and realization of thin-film formation through morphological alignment of crystallites. Furthermore, this integrated strategy provides novel solutions to interfacial chemical constraints (such as interfacial side reactions), ultimately enhancing carrier transport by preventing ion migration, thereby simultaneously improving device efficiency and stability. Furthermore, appropriately designed molecular structures facilitate the formation of high-density monolayers and the removal of steric hindrance, enabling optimized SAMs to achieve complete area coverage and attain a tightly packed structure with high density.

Therefore, the degree of coverage, amphiphilic nature leading to unwanted self-aggregation, close packing, acidity, density and ordering of SAMs are important aspects to be considered in the optimization of SAMs.[324] On the other hand, thermal stability, chemical reactivity in aqueous solutions and at ambient temperature, the process on irregular and planar surfaces, the limits of interfacial chemistry and the structure of self-assembling molecules such as dithiols, carbazole, and thiols deserve much attention and remain unclear.[326] Therefore, economical and scalable large-scale fabrication and susceptibility to degradation under extreme weather conditions are also important issues that require careful attention to advance the energy application of SAMs and multilayer molecules in optoelectronic devices. Note that the functionality of the head group, chain length and molecular mobility are useful for the molecular design of self-assembled layers. The introduction of hydroxyl, amino groups, 1-ethyl-3-methylimidazolium tetrafluoroborate, diamine hydrobromide, organic salts, ionic liquids, MABr and MACl, halogens, $-SCH_3$, *etc.* would improve the homogeneity of SAMs on MOs, the wettability of perovskite on SAMs, and the interaction between perovskite and SAMs (Fig. 11b).[327–329] Consequently, special attention should be paid to the 'three fly with one flap' strategy or the 'all-in-one integration' strategy when dealing with self-assembling monolayers and multilayers in the field of energy applications.[330]

The mechanism of action of SAMs in inverted PSCs is as follows: i) stabilization through increasing electron density and enriching molecules with electrons, particularly *via* their electron-donating effect;[331] ii) stabilization of molecules *via* the mesomeric effect, specifically through their ability to delocalize electrons;[332] iii) the p–n homojunction between the perovskite layer and the hole transport layer generates an internal electric field within the perovskite layer, promoting charge carrier transport.[333,334] This generates an internal electric field within the perovskite layer, enhancing charge carrier transport;[333,334] and iv) functional chemical modification or activation of the terminal regions of self-assembled molecules. This improves interactions with the perovskite. The application of SAMs and understanding their induced effects on PSC performance remain a challenging and confusing topic. To simplify this confusion, the structure of PSCs (planar and inverted types) in particular the types and functions of induction effects on molecular electron density and charge transport capability. Specifically, factors such as the types of substituents on molecules (electron-donating groups, electron-withdrawing groups, *etc.*) and their combinations enhance hole and electron extraction, improve charge transport properties between layers, and enable optimal arrangement and compatibility to overcome the chemical limitations of hidden interfaces. These elements turn out to be more important than researchers often expect. More specifically, the induction effect utilizes the phenomenon of permeation bonding, which influences the electron density of the sigma bond, thereby promoting charge transport between interfacial layers. Conversely, the conjugation effect (resonance effect), as shown in Fig. 12, utilises the phenomenon of spatial permeation, which influences the delocalized π-electron density.[335]

The electron-donating properties of the inductive effect enhance the resonance effect, whereas its electron-withdrawing properties inhibit it. In specific organic molecules where both electron-donating inductive effects and resonance effects are present, the increased electron density stabilises the molecule, promotes charge injection and extraction at the interface, and ultimately enhances the device efficiency and stability. For example, as shown in Fig. 12a and b, the combination of the presence of amino, methyl, and methoxy groups with resonance effects improves charge transport, enhancing both device efficiency and stability. Conversely, electron-withdrawing nitro groups inhibit resonance effects, reducing charge transport within the device and consequently diminishing both device efficiency and stability. Based on this understanding, the order of molecules from those exhibiting low to high levels of electron-donating induction effects and conjugation effects is: Ph < –OCOR < –NHCOR < –OR < NH_2 < –O. Conversely, the order of electron-withdrawing effects that inhibit conjugation, from low to high, is: $-CONH_2$ < –COOH < –COOR < –COR < –CHO < $-SO_3H$ < –CN < $-NO_2$ (see Table 4). The electron density of aromatic rings is enhanced and activated by electron-donating groups, thereby increasing the reaction rate of electrophilic substituent. This is highly beneficial in inverted PSCs. Conversely, the electron density of aromatic rings is reduced and deactivated, inhibiting the reaction rate of electrophilic substituent.

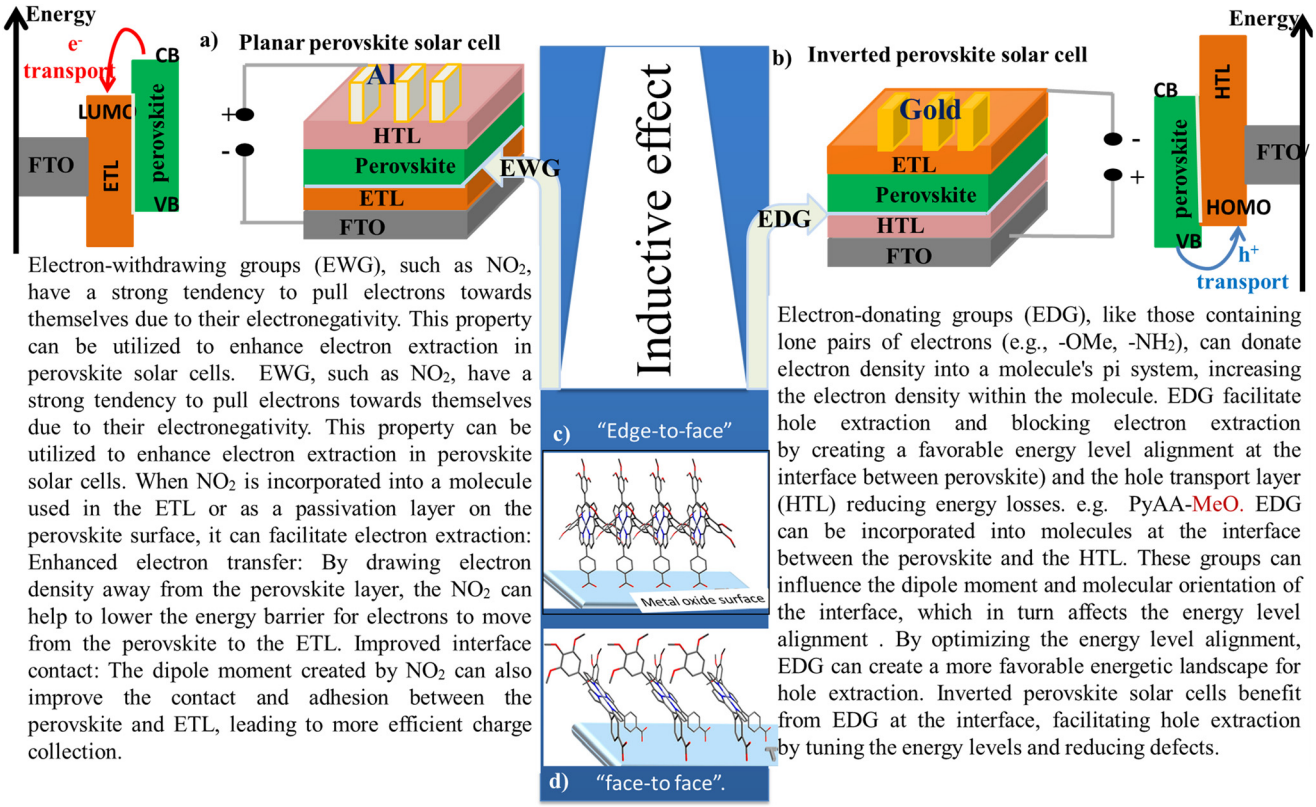

Fig. 12 Proposed application of electron-withdrawing (a) and electron-donating (b) groups in the PSC device architecture; c) edge-to-edge manner and d) face-to-face manner of interaction of anchoring group to the metal oxide surface, reproduced from ref. 336 with permission from MDPI, Copyright, 2019.

Table 3 Basic concepts for the selection of substituents and self-assembling molecules with the impact shown in Fig. 13 as an example[107]

Impact on electron density of the core	Substituent in SAMs	Type of inductive effect	*ortho*-, *para*- and/or *meta*-Directors
Very strongly activating	O^-	(+) I, (+) M	
Strongly activating	$-NR_2$, $-NHR$, $-NH_2$, $-OH$, $-OR$	(−) I< (+) M	*o*, *p*-Directors
Moderately activating	$-OCOR$, $-NHCOR$, $-C_6H_5$	(−) I< (+) M	*o*, *p*-Directors
Weakly activating	$-CH_3$, $-CR_3$	(+) I	*o*, *p*-Directors
Weakly deactivating	$-F$, $-Cl$, Br, I $-CH_2Cl$, $-CH{=}CH-COOH$ $-CH{=}CH-NO_2$	(−) I, (+) M	*o*, *p*-Directors
Strongly deactivating	$-COR$, $-CHO$, $-COOR$, $-CONH_2$, $-COOH$, $-SO_3H$, $-CN$, $-NO_2$	(−) I > (+) M	*m*-Directors
Very strongly deactivating	$-NH_3$, $-NR_3$	(−)I	*m*-Director

The presence of an electron-withdrawing group at the anchor site enhances the molecule's electron affinity, thereby strengthening its bond to the substrate. Conversely, the presence of an electron-donating group increases the molecule's electron density, reducing its electron affinity and weakening its bond to the substrate. This can potentially affect the molecular orientation at the surface, the overall packing density of the self-assembled monolayer (SAM) and its stability. Conversely, when an electron-withdrawing group is present at one end and an electron-donating group at the opposite end, a dipole moment (pull–push system) arises, improving the hole injection efficiency between layers. Furthermore, the presence of an electron-donating group at the end increases the molecule's electron-donating ability, promoting charge injection and extraction by adjusting the molecule's HOMO level. In planar PSC devices, employing electron-withdrawing groups as the electron transport layer enhances electron extraction while using electron-donating groups, as the hole transport layer improves hole extraction. Furthermore, this approach can enhance the morphological quality of the thin film.

Table 4 Classification of X substituents according to their behaviour in aromatic electrophilic substitution reactions, reproduced from ref. 346 with permission from MDPI, Copyright 2021

X	Activation	Electronic effect	Directing effect
O^-	+e	+I/+M	*o*/*p*
NH_2	+s	−I/+M	*o*/*p*
SH	+m	−I/+M	*o*/*p*
CH_3, R	+w	+I	*o*/*p*
F[a]	+w	−I/+M	*p*
F[a]	−w	−I/+M	*o*
Cl, Br, I	−w	−I/+M	*o*/*p*
NO_2, CN	−s	−I/−M	*m*
CF_3, NH_3^+	−s	−I	*m*

[a] F group is understood to be a weak activating substituent in the *para* position and a weak deactivating substituent in the *ortho* position. The e, s, m and w labels refer to the extreme, strong, medium and weak effects, respectively, while + and − are the signs of activating and deactivating groups, respectively. Likewise, the ± indicates whether the group donates or extracts electronic charge from the ring, whereas M and I refer to the mesomeric and inductive effects.

Understanding the influence of interactions between anchoring and terminal ends on SAM properties, and grasping the selection and impact of electron-withdrawing or electron-donating groups strategically applied to either device structure (inverted or planar), is crucial for optimizing essential parameters such as charge extraction, injection, and transport, preventing ion migration, reducing recombination through interface energy level alignment, and enhancing device efficiency and stability by eliminating surface trap states. Advantageously, control over molecular orientation on the substrate surface, work function adjustment, and charge transport enhancement are customisable.[337] Furthermore, as shown in Table 4, considering the influence of substituent positions on the anchor and terminal groups on molecular stability and acidity is also highly beneficial. For example, *meta*- or *para*-substituted nitro groups enhance acidity by stabilising the negative charge of specific anchor anions and removing electron density, whereas *para*- and *meta*-substituted methoxy and amino groups reduce anion acidity, thereby destabilising the molecule. Compared to *meta* and *para* positions, the ortho effect stabilizes the anion by enhancing the acidity of the molecule.

Fig. 12c and d indicate that the positional alignment of the anchor group with the metal surface is a critical consideration requiring greater attention to achieve high V_{OC} and photocurrent associated with dense coverage on metal oxide surfaces. Edge-to-edge interactions are preferable to face-to-face interactions as they yield superior coverage.[336,338] Conjugated effects enhance stability by reducing bond-length alternation, amplified by the delocalization of cyclic π electrons. Conversely, the cyclic delocalization of substituted π electrons induced a non-additive energy effect, as shown in Fig. 13a, arising from interactions between the reactive site functioning as the transfer portion and different substituents assigned as *x*, *y*, and *z*. This non-additive energy is termed the substituent effect stabilization energy, the principle being that 'the greater the substituent effect stabilization energy, the stronger the stabilizing effect conferred by the substituent effect'.[339] Such transfer groups contribute to efficiency enhancement in solar cells by allowing light transmission to promote charge separation at the donor–acceptor interface, generating free charge carriers, and transporting these free carriers across the layer to their respective charge collection electrodes. Charge collection, charge generation, and light absorption are key requirements necessitating optimization. Furthermore, charge transport within the perovskite layer, energy levels (HOMO/LUMO), and light absorption are critical points requiring careful selection of the transparent base layer to enhance the device efficiency and stability. For instance, furans and thiophenes lower the energy of effective charge transport transitions while providing efficient conjugation, whereas benzo[1,2-*b*:4,5-*b*′] dithiophene[340] and indacenodithiophene[341] are effective electron-donating groups. Such substituents are necessary to improve the solubility and morphology of thin films for enhanced solar cell performance. For this purpose, longer-chain alkyl groups and phenyl groups prove beneficial. In this context, the crucial activity for researchers lies in the selection and arrangement of these moieties within the molecule.

Furthermore, as shown in Table 3 and Scheme 2, the highest degree of mesomeric effect fictionalization to enhance charge transport processes is achieved at the ortho and para positions of the ring, whereas it is weak at the *meta* position. In addition, the inductive effect and mesomeric effect depend on the position of the anchor group intended to form a bond to the substrate surface (Fig. 13b). A long linker induces strong intermolecular packing to avoid intermolecular interactions, causing chains to spread apart and widening the tunneling barrier, thereby inhibiting charge transport and rendering charge injection and extraction inefficient.

Conversely, a short linker increases intermolecular interactions, bringing the anchor group and terminal group closer together. This weakens molecular packing with the perovskite, accelerating charge tunneling and enabling an efficient charge transport process. For example, the methoxy group at the 4-position in MeO-4PACz achieves a weaker electron-donating effect than that of the methoxy group at the 2-position in MeO-2PACz, thereby readily enhancing the charge transport process.[331] The primary roles of methoxy substituent are electron donation, significant intermolecular charge transfer, non-additivity of the electric dipole moment, and changes in geometric structure that enhance stability (Fig. 13c). However, when both substituents possess electron-donating properties, the system becomes unstable due to electrostatic repulsion and the formation of high electron density. The introduction of electron-withdrawing groups can stabilize the molecule through their ability to reduce electron repulsion. This arises from their property of pulling electron density away from the positively charged centre, thereby

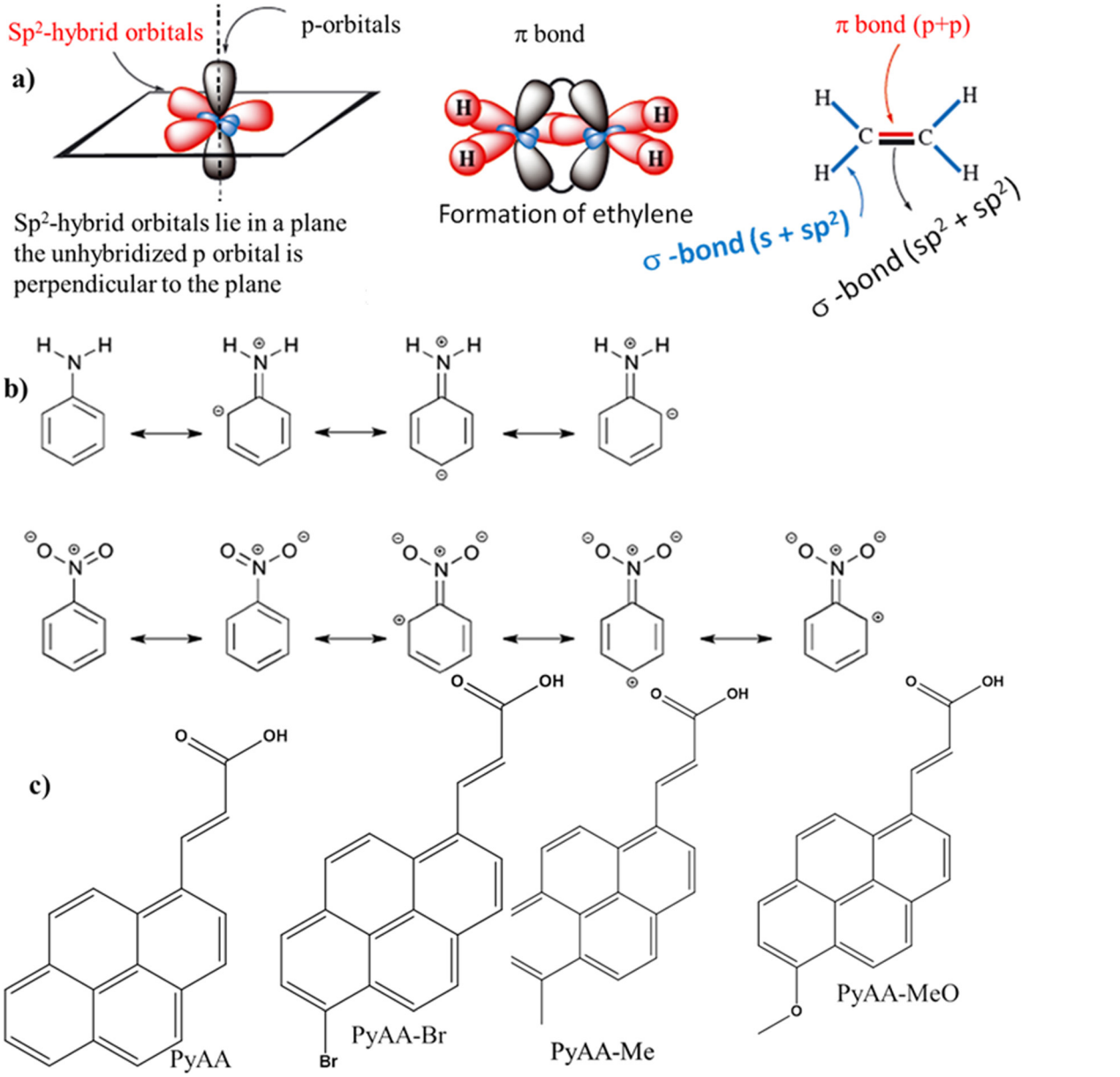

Fig. 13 Inductive and mesomeric effects: representation of a) localized sigma bond electron density and delocalized π-electron density orientation for polarization, reproduced from ref. 342 with permission from Wiley-VCH, Copyright 2022. b) Inductive and mesomeric effects with the inductive effect of the electron-donating amino and electron-withdrawing nitro substituents in aniline and nitrobenzene; reproduced from ref. 343 with permission the Royal Society of Chemistry, Copyright, 2016. c) Inductive effect of bromine, methyl and methoxy substituent groups in stabilizing the (*E*)-3-(pyren-1-yl)acrylic acid (PyAA), (*E*)-3-(6-bromopyren-1-yl)acrylic acid (PyAA-Br), (*E*)-3-(6-methylpyren-1-yl)acrylic acid (PyAA-Me), and (*E*)-3-(6-methoxypyren-1-yl)acrylic acid (PyAA-MeO) conjugated systems, reproduced from ref. 331 with permission from Nature publishing group, Copyright 2025.

contributing to the overall stabilization of the molecular system.

Understanding the inductive effects of the substituent groups on the anchoring group such as cyanoacetic acid (–CH_2(CN)COOH), phosphonic acid (–PO_3H_2), and carboxylic acid (–COOH), which matters its interaction with the substrate (such as NiO_x, FTO, ITO), is highly necessary. For instance, introducing an F atom into acetic acid reduces the pK_a value from 4.86 to 2.59. Introducing a Cl atom into butanoic acid reduced the pK_a value from 4.06 to 2.84.[342] Halogens are atoms with high electronegativity, acting as aromatic deactivating groups by repelling electron density, thereby promoting electron extraction from n-type semiconductors to the corresponding electrodes. The effect of halogen-containing SAMs in n-type semiconductors is to lower the LUMO energy, facilitating energetically favorable electron extraction from the perovskite (see Table 4 and Scheme 2).[344,345]

Conversely, electron-donating groups increase electron density on the aromatic ring, promoting hole extraction. In p-type HTLs, electron-donating groups increase the HOMO

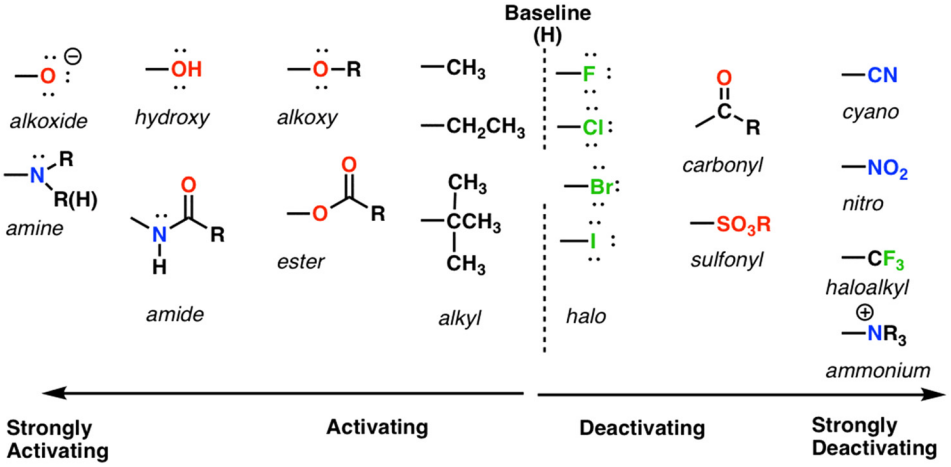

Scheme 2 Activating and deactivating groups in electrophilic aromatic molecules, reproduced from ref. 349 with permission from Master Organic Chemistry LLC, Copyright 2025.

energy, reducing the energy barrier for holes by better aligning energy levels, thereby favoring hole extraction (see Scheme 2).[331,347] Crucial here is understanding the position of the substituent, the type of substituent, and the effect the substituent has on the anchor group's interaction capability, bond-forming ability, and interface stabilization capability with the substrate.[348]

Furthermore, it is crucial and cannot be overlooked to understand the substituent's interaction capacity with the perovskite at the terminal or functional group, its ability to stabilize the interface with the perovskite, and its ultimate impact on the charge transport properties of the self-assembled molecules within the device performance. This leads to a big question: how can self-assembled molecules overcome the energy mismatch and barriers arising at the interface? This concern is a critical issue, necessitating the elucidation of the operating mechanisms within the interfacial layer. This is because, if appropriately optimized, it can contribute to enhancing the performance of PSCs. Consequently, understanding the charge extraction and injection characteristics of SAMs becomes an essential research topic for PSCs. Therefore, the intrinsic properties of self-assembled molecules—namely, the alignment of the HOMO–LUMO gap with the metal electrode or metal oxide substrate, the electron–hole tunneling effect *via* the transfer site, and the molecular length—influence the charge transport characteristics of the target molecule.[350] Electron-donating groups lower the HOMO level, reducing energy loss by bringing it closer to the perovskite Fermi level, decreasing the work function, and improving junction characteristics. This enhances the hole extraction efficiency, thereby improving device performance. In this case, the molecular level near the Fermi level, namely the HOMO, governs the tunneling process, and the tunneling decay depends on the energy separation $\Delta = E\_(\text{Fermi}) - E\_(\text{HOMO})$.[350]

Generally, the principles governing strong acids and strong bases, as well as weak acids and weak bases, influence the formation and application of self-assembled molecular structures. Similar to weak acids and weak bases, strong bases and strong acids promote mutual interactions, forming specific structures in self-assembled molecules. This principle proves useful for monitoring and predicting diverse nanostructures, ranging from simple to complex. Hard bases are species with low polarizability, high electronegativity, and low molecular weight, such as anions containing F^- or O^-. Conversely, hard acids are species with low polarizability, high charge density, and low molecular weight, such as highly oxidised metal cations or H^+.[342]

A key principle of this acid–base theory is that hard bases favour interactions with hard acids, primarily forming strong ionic bonds, whereas soft bases favour interactions with soft acids, typically forming strong covalent bonds.[351] Such favourable interactions serve as the driving force inducing specific structures in self-assembled molecules and monolayers. A crucial point that this review should address is the significant influence of the hard acid–hard base principle in SAMs on buried interface design aimed at improving energy matching in PSCs. Among self-assembling molecules, those possessing strong acids exhibit high LUMO due to their strong electron-withdrawing properties. Conversely, self-assembling molecules containing strong bases such as NH_3, Cl^-, F^-, or HO^- exhibit low HOMO due to their electron-donating properties towards metal cations or H^+. The introduction of strong bases into PSCs induces three major effects: i) energy level alignment *via* electron donation from the hard base due to polarisation or charge transfer at the interface. This shifts the energy levels of the participating materials. ii) Hard base-induced interfacial dipoles arising from polarisation or charge transfer at the interface, which either lower or raise the energy levels depending on the nature of the interaction. iii) Modification of the electronic structure due to interactions between the hard base at the interface and the electronic structure of other layers. This leads to a revision of the existing energy levels. The

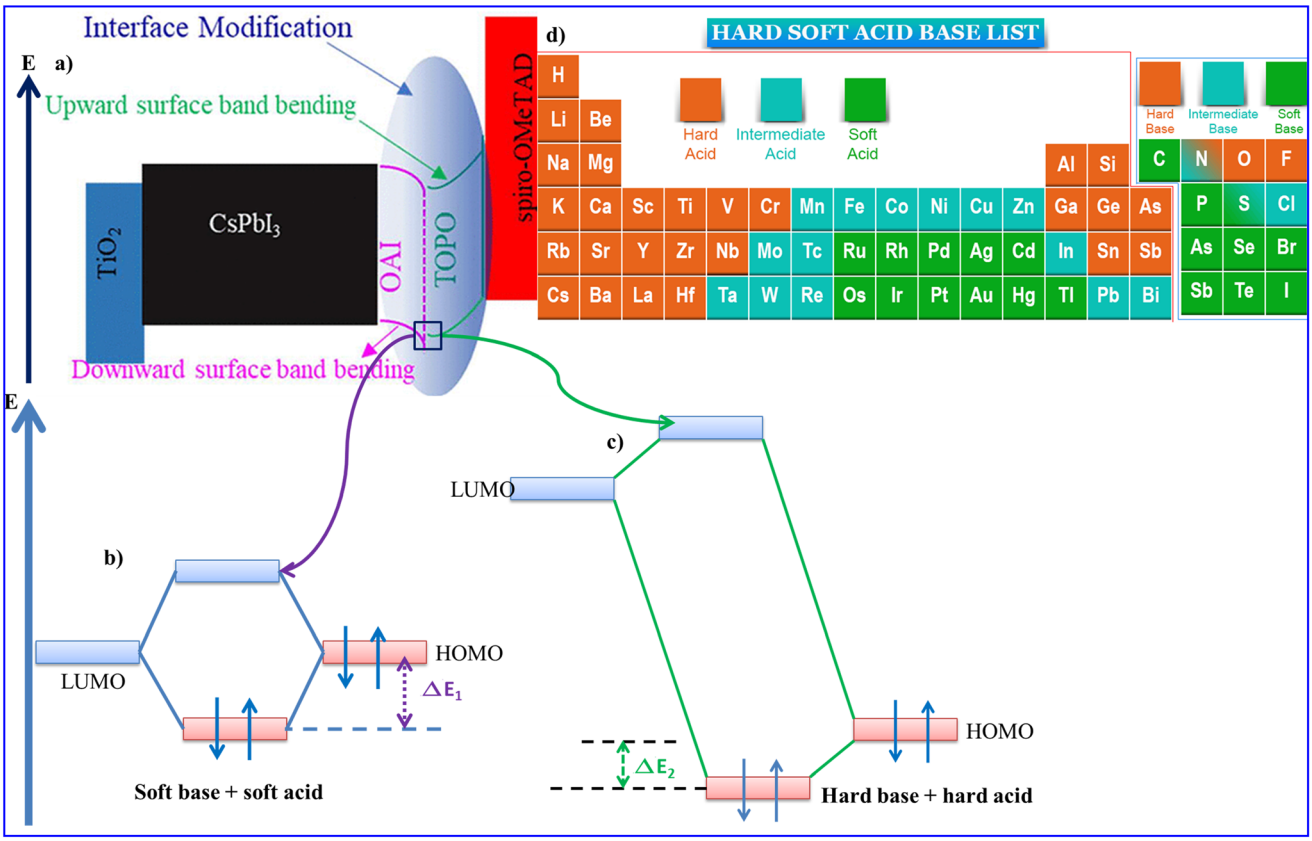

Fig. 14 Mechanism of action of the hard base and soft base-induced energy level alignment between the perovskite and the hole transport layer in the n–i–p device architecture (a), reproduced from ref. 352 with permission from the American Chemical Society, Copyright 2023. Formation of molecular orbitals by the interaction of HOMOs and LUMOs with different energy levels and energy release (b) and energy gain (c) along with periodic table of hard soft acid–base theory (d), reproduced from ref. 342 with permission from WILEY-VCH GmbH, Copyright 2022.

mechanism of action induced by hard bases involves bending of the surface band and creation of new energy states, promoting alignment of energy levels, as shown in Fig. 14.[352] Trioctylphosphine oxide is a hard base, whereas *n*-octylammonium iodide is a soft base, enabling optimisation of the energy levels between the perovskite and HTL interface, as shown in Fig. 14a.

The soft base *n*-octylammonium iodide influences the I/Pb ratio, inducing Donnes-type band bending at the perovskite semiconductor interface. This alters the energy alignment, improving charge transport in planar PSCs (Fig. 14b).[352] Furthermore, the *n*-octylammonium iodide soft base reacts with soft acids or boundary line acids present at the interface, such as Pb^{2+}, inducing weakly covalent interactions. The participating atomic orbitals have closely spaced energy levels, and the strong covalent bond formed by the corresponding molecular orbitals results in a small energy gap. Consequently, significant energy release occurs, as shown in Fig. 14b. Electron emission from the hard base of trioctylphosphine oxide induces band bending and level shifting of the HOMO level near the valence band of the perovskite, creating a state favourable for hole injection. Conversely, interaction with the molecule raises the energy of the LUMO level, levelling it far from the perovskite conduction band, thereby inhibiting electron injection. The oxygen atom in trioctylphosphine oxide possesses strong electronegativity and interacts with strong acids such as boundary acids like Pb^{2+}, H^+, and $CH_3NH_3^+$. Demonstrating strong electrophilicity, this leads to intense ionic interactions. The participating orbital possesses a large energy gap, allowing molecular orbitals to form with a smaller energy increase, as shown in Fig. 14c. Fig. 14d presents the periodic table based on the hard–soft acid–base theory classification of elements. This table assists researchers in understanding the characteristics of each element, aiding comprehension of the nature of bonds formed and interaction tendencies during reactions.

Understanding the nature of the HOMO–LUMO gap in self-assembling molecules is crucial, as it provides a fundamental criterion for efficient charge transport processes.[353] This gap reflects how readily a molecule can participate in charge transport processes. A smaller gap indicates a more reactive molecule, while a larger gap signifies a more stable, less reactive molecule. A smaller gap facilitates faster charge transport, requiring less energy for the free movement from the HOMO to the LUMO. Conversely, a larger gap slows the charge transfer process, necessitating greater energy for the free electron movement from the HOMO to the LUMO. Furthermore, the greater the energy difference between a molecule's HOMO and a semiconductor's valence band, or between a molecule's LUMO

and a semiconductor's conduction band, the greater the energy required to transport holes and electrons between these respective energy bands and orbitals. Conversely, a smaller energy difference necessitates less energy for electrons to move between these energy bands and orbitals. Furthermore, molecules with a large HOMO–LUMO energy gap and a small energy difference between the HOMO and valence band in the semiconductor, or between the LUMO and the semiconductor's conduction band, are favorable for solar cells. This large HOMO–LUMO energy gap renders the molecule a more stable HTL or ETL, while the small energy difference between its HOMO and the semiconductor's valence band, or between its LUMO and the semiconductor's conduction band, means that the energy required for hole and electron transport within the energy band gap is low, making the molecule an efficient HTL or ETL. This characteristic makes spiro-OMeTAD a more suitable HTL in perovskite solar cells. Specifically, this is because it possesses a large HOMO–LUMO energy gap of 2.7 eV and a small energy difference between its HOMO level and the valence band of the perovskite. That is, as shown in Fig. 15,[354] it is 0.09 eV from the VB of $CsPbI_3$, 0.23 eV from the VB of $MAPbI_3$, and 0.3 eV from the VB of $AFPbI_3$. This fundamental principle provides a useful guideline for material selection aimed at PSC applications. Furthermore, the HOMO–LUMO energy gap of a molecule is determined by the strength of the interaction energy between the donor and the acceptor and the energy difference between the donor's HOMO and the acceptor's LUMO. Here, the interaction energy is inversely proportional to the HOMO–LUMO energy gap.[355]

4.2. Innovative interfacial chemistry engineering approaches

Innovative approaches may be interpreted in the development of novel manufacturing techniques, device structure design, surface and interface modification technologies, and the creation of new alternative semiconductor materials. Optimizing and integrating all these innovative approaches would constitute a superior strategy for researchers, industry, and enterprises to pursue, thereby charting a path towards successful commercial viability in the marketplace. In advancing these challenging yet necessary new innovative approaches, it is essential to clearly identify bottlenecks involving trade-offs between efficiency, stability, and scalability. Considering device structures, inverted PSCs represent an attractive new research area, possessing unique advantages and potential despite acknowledging their weaknesses. Challenging yet indispensable innovative approaches, specifically tailored to this device structure, are being designed to achieve future commercialization.

Inverted PSCs represent the most promising type of PSCs due to their potential stability, scalability, and the possibility of rapid efficiency improvements. However, they face inherent bottlenecks that require resolution. The main challenges are as follows: i) low efficiency due to chemical

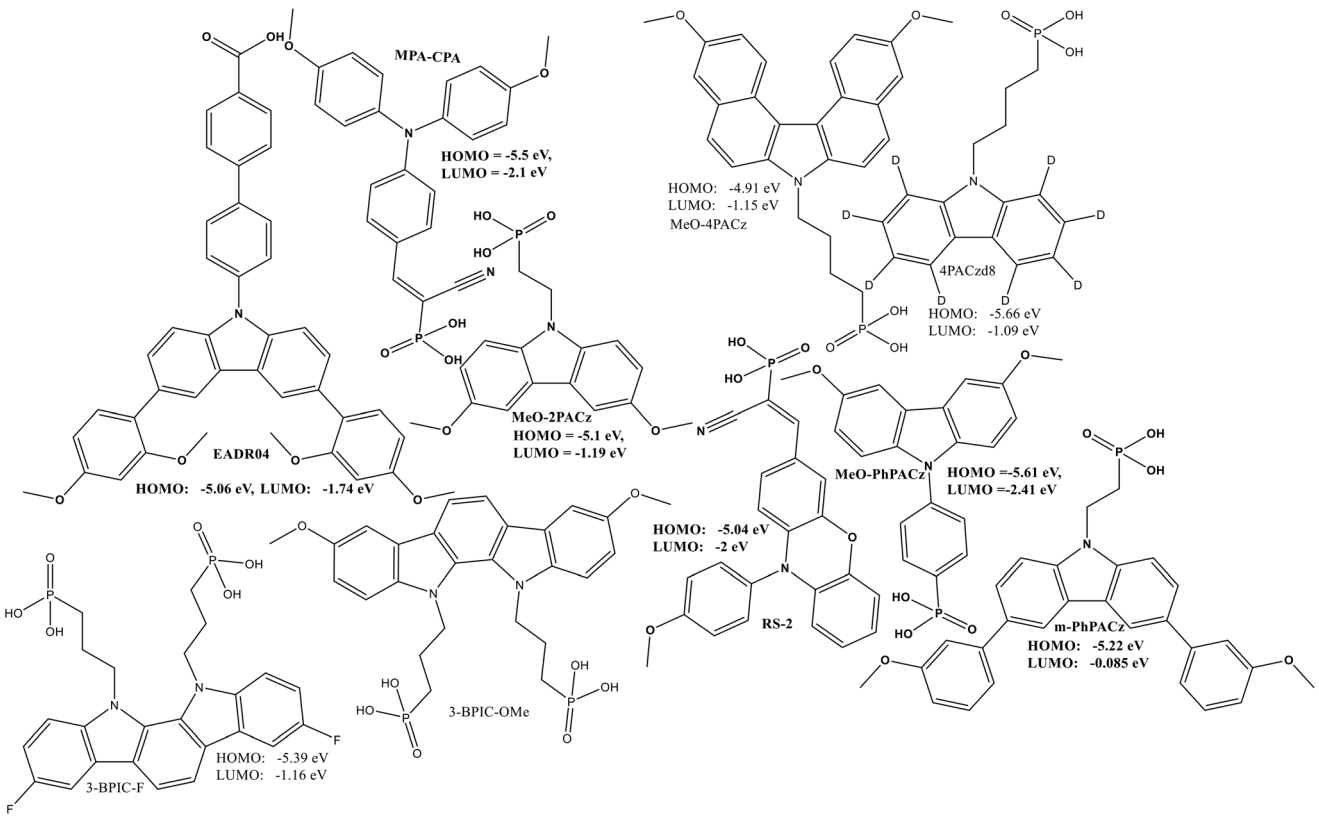

Fig. 15 Self-assembling organic molecules.

limitations at interfaces (charge accumulation, defect formation, recombination promotion by surface states, mismatched interface energy levels, *etc.*). The buried interface between the perovskite and the substrate is particularly problematic, and strategies to minimise this are underway.[356] ii) Increased series resistance due to poor contact between the perovskite layer and the charge transport layer; this impedes efficient charge extraction and reduces device efficiency.[357] iii) Ion migration induced by tensile strain from the firing temperature, which degrades device efficiency; as reported elsewhere, this necessitates advanced control techniques.[358] iv) Poor interface alignment. Energy level mismatches between the charge transport layer and perovskites inhibit charge extraction and increase non-radiative recombination.[359] v) Formation of built-in potentials at weak bonding sites in homojunctions; this arises from the differences in work function and energy levels. While control *via* work function adjustment is considered feasible, it is reported as a potential issue. It may induce defect generation and extensive depletion layer formation, thereby degrading device performance.[360] This occurs at the perovskite/HTL interface due to mismatched work functions and energy levels, strain, homojunction and inhomogeneity, forming a broad, defective depletion layer that compromises device stability and efficiency.[361] vi) Inconsistent or non-uniform and poor quality film is common in PSCs, hindering its reproducibility and performance enhancement.[362] vii) Potential-induced degradation under operating conditions exposed to light and voltage can cause efficiency losses, particularly in short-circuit current.[363] viii) Unsaturated dangling bonds and non-ideal crystallisation are the root causes of imperfect lattice structures and defective surface lattice arrangements, leading to environmental degradation, ion migration, and carrier recombination, which compromise device efficiency and stability.[364] ix) Poor wettability of perovskites, stemming from inadequate interaction between perovskite ink and SAMs, results in the formation of perovskite films riddled with morphological pinholes.[327,365] Furthermore, as shown in Table 4, the success of inverted PSCs depends on understanding the following performance bottleneck issues: a) nature of the ITO/NiO_x interface; b) nature of the NiO_x/perovskite interface; c) selection and electron-donating properties of hole-selective SAMs; d) selection and electron-accepting properties of electron-selective SAMs; e) properties of the perovskite/ETL interface; f) properties of the electron-selective interlayer/Ag/Au interface; and g) properties of nucleation and SAM growth orientation during the deposition process. The proposed bottleneck issues arise at the ITO/NiO_x interface and the NiO_x/perovskite interface, and are related to the following factors: a) the inherently low conductivity of NiO_x, oxidation of I^- by Ni^{3+} and the deprotonation of amines (creating a barrier rich in PbI_{2-}_xBr_x), b) formation of excess oxygen vacancies due to non-stoichiometric Ni^{2+}/Ni^{3+}, c) diffusion outflow of VNi, d) difficulty in controlling the Ni^{3+} concentration, e) poor adhesion to ITO, f) heterogeneous NiO_x films with variations in thickness and coverage, and g) energy level mismatch at the ITO/NiO_x interface, unrealistic maximum valence band energy of NiO_x, substrate surface OH groups, particle aggregation, and incomplete coverage of the transparent conductive oxide (TCO) substrate due to poor dispersion of NiO_x nanoparticles. Peroxide modification[366] and surface redox control are proposed as two approaches.[366–370] Furthermore, the orientation of molecular dipoles (away from or towards metal oxide surfaces such as NiO_x) arising from electron-donating and electron-withdrawing groups is highly confusing, as reported in the discussion concerning phenylphosphonic acids. The molecular dipole effects of MPPA–NiO_x and CNPPA on the p–i–n device structure[371] differ from the results observed in the n–i–p device structure.[372] These bottlenecks in inverted PSCs suggest that researchers should urgently seek sustainable solutions to bring inverted solar cells to the practical stage. To enhance progress in inverted PSCs and disseminate the achievements to the scientific community, Table 5 systematically summarizes the latest research results largely unreported in other literature reviews.[329,373–375] Consequently, intensive efforts are being directed towards surface nanostructuring techniques,[376] embedded interface design techniques,[377] surface redox control technologies, and the application of peroxide metal oxide surface modification strategies. These approaches are anticipated to substantially improve the weaknesses currently impeding the practical implementation of reverse PSCs.

4.2.1. Flawless and surface-nanostructured film strategy. The existence of thin films possessing these two characteristics is highly sought after in high-performance energy devices. Whilst continuous, smooth, defect-free thin films with reduced imperfections are essential for efficient charge collection, nanostructured layers achieving increased surface area *via* nanocrystalline solution processes are necessary for improved interlayer and surface contacts. This synergistic coexistence constitutes the requirement for solar cell devices that deliver enhanced stability, reduced recombination, and improved performance (Scheme 3a).[376]

4.2.2. Buried interface engineering strategy. This type of technology is highly useful for overcoming the interfacial chemical limitations at the buried interface between the primary electron transport layer, hole transport layer, and perovskite active layer, thereby achieving optimized interfacial contact, crystallisation control, energy level matching, and defect passivation.[378] This enhances the stability, performance, and durability of PSCs, strengthens the mechanical properties of the perovskite thin film layer, reduces recombination between the interface layers, and promotes charge extraction between multiple layers (Scheme 3b).[377,379]

4.2.3. Surface redox engineering strategy. Understanding the redox behaviour on metal oxide surfaces is beneficial for manipulating intrinsic properties such as electronic structure and surface composition, and further enhances the potential

Table 5 Current progress in efficiency and stability of inverted PSCs

Self-assembling molecule	Inverted device structure	Efficiency/%	V_{OC}/V	J_{SC}/mA cm^{-2}	FF	Stability	Ref.
MeO-2PACz	Glass/ITO/MeO-2PACz/AL_2O_3/PVK/PEAI/PCBM/BCP/Ag structure	26.37	1174	26.59	84.48	5000 h	382
Poly ferrocenyl	ITO/PTAA/perovskite/fc-derived molecules/C60/BCP/Ag	24.51	1.190	25.30	80.82	2000 h	383
Dual host molecule (DB21C7) with guest I (Cs^+) or guest II (PEA^+)	FTO/c-TiO_2/m-TiO_2/$(FAPbI_3)_{0.97}(MAPbBr_3)_{0.03}$ perovskite layer/spiro-OMeTAD/Au	25.55	1.181	26.414	81.84	1050 h	185
MeO-2PACz	Glass/ITO/MeO-2PACz/perovskite/PC61BM/BCP/Ag	24.6	1.177	24.8	84.3	1000 h	384
C60	FTO/MeO-2PACZ/Me-4PACZ/perovskite/C60/ALD-SnO_x/Ag	25.5	1.16	25.9	84.9	2100 (94.5%)	385
CPMAC	FTO/MeO-2PACZ/Me-4PACZ/perovskite/CPMAC/ALD-SnO_x/Ag	26.1	1.18	26.0	85.5	2100 (97.6%)	385
Ferrocenyl molecules	(ITO)/PTAA/perovskite/fc-derived molecules/C60/BCP/Ag	26.08	1.194	25.93	84.24	1000 h	383
NA-Me-4PACz	ITO/NiO/NA-Me/perovskite/PI/PCBM/BCP/bi/Ag	26.69	1.201	26.30	84.5	2400 h	379
	Hydroxylation-etched ITO ITO/SAM/perovskite/PCBM/BCP/Ag	26.55, certified	1.192	26.47	84.11	T_{96} = 2400 h (65 °C))	379
Hydroxylation pretreatment of TCO	Perovskite/C60 layer/ALD-SnO_x, 1-sun operation at 65 °C	26.6, certified 26.44	1.190	26.2	85.3	2800 h, only loses 4% of its initial efficiency after 2800 h	380
c-SAM or a-SAM	FTO/c-SAM or a-SAM/$Cs_{0.1}FA_{0.9}PbI_3$/C60/BCP/Ag	25.20	1.175	25.6	84.0	1000 h at 85 °C	309
Me-4PACz	(FTO)/NiO_x or ATO_x/Me-4PACz/$Cs_{0.1}FA_{0.9}PbI_3$/C60/BCP/Ag	25.7	1.17	25.67	85.3	500 h under LED light and 2000 h without light	386
	Co-SAM (CbzNaph:JJ24)	26.92	1.185	26.18	86.75	85 °C for 1000 h	387
Me-4PACz	$Cs_{0.05}FA_{0.9}MA_{0.05}PbI_3$/(with or without 3PDPA)/C60/BCP/Cu	26.82	1.18	26.32	86.5	10% decay, T_{90} of 1000 h	388

for significantly influencing the performance of optoelectronic devices such as solar cells, light-emitting diodes, and transistors (Scheme 3c). Such enhancements are engineered through surface redox engineering, which modifies the oxidation state at the surface or outermost layer of metal oxides where interface contacts and interactions occur, *via* doping, acid–base treatment, or plasma processing. Techniques such as acid–base treatment and plasma processing aim to improve surface energy, energy level alignment, conductivity, and the scalability of the methods.[367] This provides a powerful toolkit for modifying the surface properties of metal oxides applicable to perovskite solar cells, batteries, and catalytic systems, enabling the enhancement of advanced energy materials for multifunctional energy applications.

4.2.4. Hydroxylation-based surface modification strategy. Hydrogen peroxide is a reagent applied to accelerate hydroxylation while the process of introducing hydroxyl groups onto the surface metal oxide is hydroxylation surface modification. This strategy is established not only by chemical treatment using hydrogen peroxide, piranha solution (hydrogen peroxide plus sulfuric acid)[381] or ozone but also by electrochemical methods and plasma treatments. Recently, reports have been published concerning the hydroxylation of ITO through bonding site design for robust and uniform SAMs (Scheme 3d),[380] and the homogenisation of NiO_x using hydrogen peroxide (Scheme 3e and f)[366] for high-performance inverted PSCs. Furthermore, considering a 'three birds with one stone' strategy to overcome the bottlenecks in inverted PSCs, there is an urgent need for a 'single self-assembling molecule' capable of addressing three bottlenecks:[330] i) photo-stability, ii) moisture resistance, and iii) air stability.

4.2.5. Selective templating perovskite layer growth strategy. The design of perovskite layers is a primary focus for improving the trade-off between efficiency, stability, and scalability in perovskite solar cells. To this end, constructing and accessing low-dimensional interfaces—0D/3D, 1D/3D, and 2D/3D—have attracted significant interest and growing attention. Consequently, both high- and low-reactivity bulk organic cation salts have been employed.[389,390] For example, 4-(aminomethyl)piperidinium ($4AMP^{2+}$), n-butylammonium (BA^+), and phenethylammonium (PEA^+) are highly reactive bulk cations, whereas 2-piperidine-1-yl-ethylammonium ($PiEA^{2+}$), 2-pyrrolidine-1-yl-ethylammonium ($PrEA^{2+}$), biphenyl-4-ylmethylammonium ($BPMA^+$), and 3-(methylthio) propylammonium ($3MTPA^+$) are low-reactivity bulk cation salts (see Scheme 4a). Due to the solubility constraints and the low reactivity of bulk cations, low-dimensional interfaces have been inaccessible and a cause of interface instability in PSCs. The low-dimensional interface is inaccessible and also the root cause of interface instability in PSCs due to solubility constraints and the low reactivity of bulk cations. The former bulk cation salts react with the 3D perovskite, causing

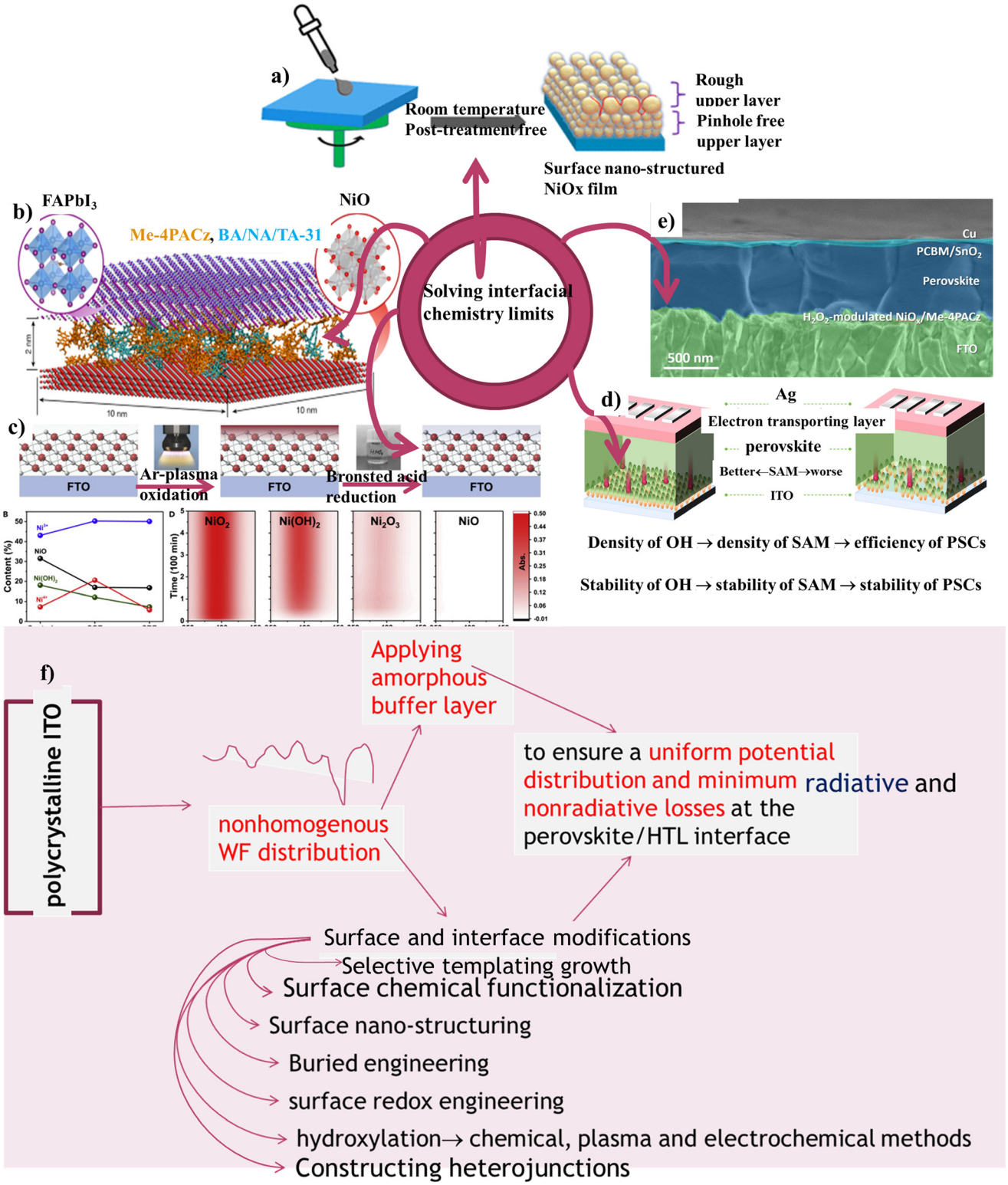

Scheme 3 Schematic of the surface nano-structuring (a), reproduced from ref. 376 with permission from the American Chemical Society, Copyright 2016, buried interface engineering (b), reproduced from ref. 379 with permission from Nature publishing group, Copyright 2024, surface redox engineering (c), reproduced from ref. 367 with permission from Cell Press, Copyright 2022, hydroxylation of ITO (d), reproduced from ref. 380 with permission from Nature publishing group, Copyright 2025, and H_2O_2 homogenized NiO_x (e), reproduced from ref. 366 with permission from AAAS, Copyright 2023. Schematic representation summarising the key concepts of development trends (f).

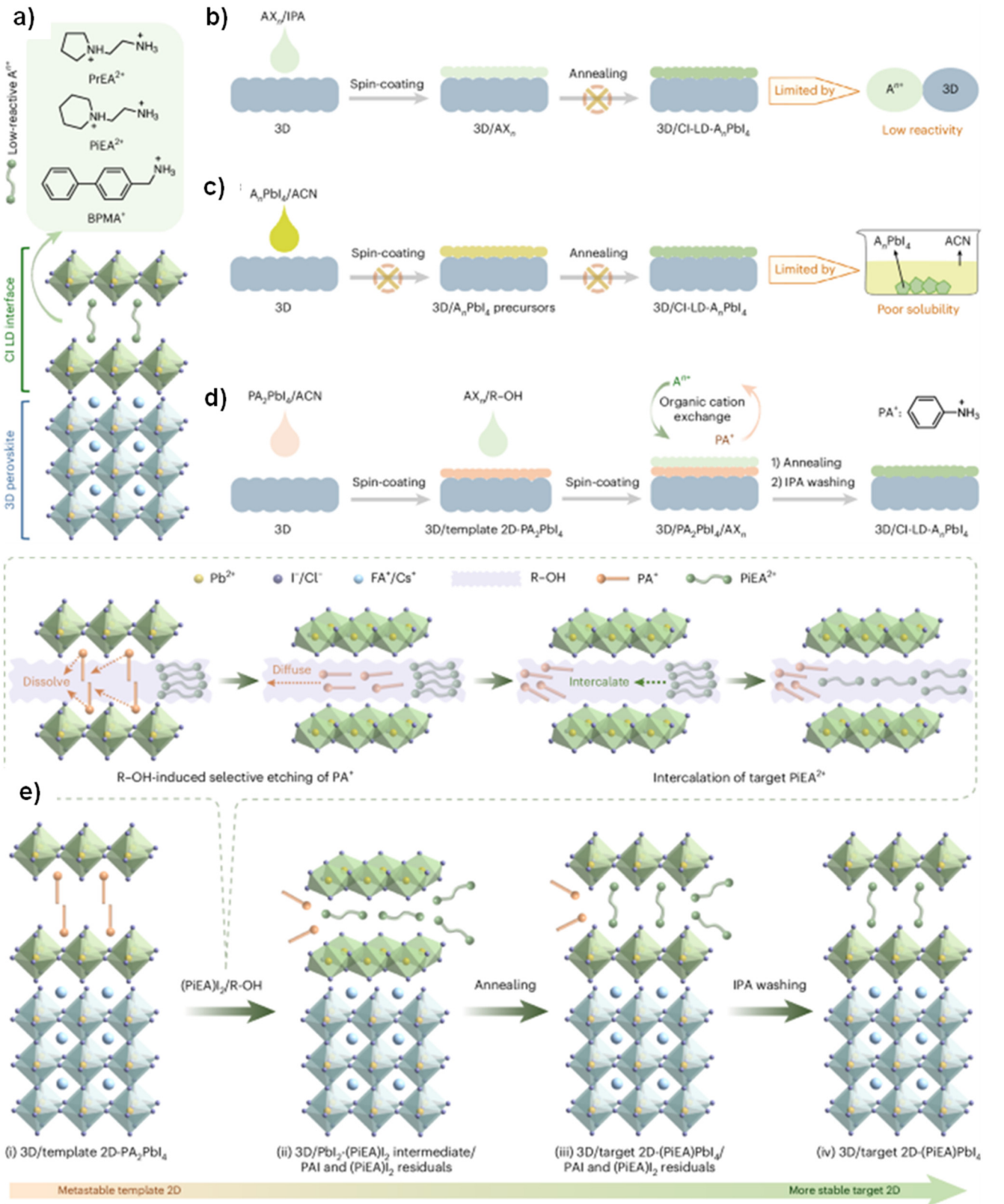

Scheme 4 Schematic of the 3D/CILDI heterostructure (a–d); reproduced from ref. 402 with permission from Nature publishing group, Copyright 2025. Possible mechanism for accessing low-dimensional perovskites (e), reproduced from ref. 402 with permission from Nature publishing group, Copyright 2025.

interface instability due to their high reactivity. Consequently, they form low-dimensional interfaces with limited effectiveness despite their high conductivity.[391–394] Conversely, bulk cation salts with low reactivity do not react with the 3D perovskite. However, they function as insulating interface layers with low conductivity, limiting the insulating effect, and exhibit excellent stability.[395–399]

Regardless of their promises, persistent challenges have hindered the realization of chemically inert low-dimensional interfaces (CILDI) due to the lack of effective growth techniques. Semi-precursor and fully precursor solution-based approaches have attempted to resolve this issue, yet have not succeeded in practice. The former semi-precursor approach failed due to extremely low reactivity characteristics despite widespread adoption.[400] Conversely, the latter full-precursor approach failed because the resulting chemically inert low-dimensional interfaces exhibited insufficient solubility (see Scheme 4b and c).[401] Presently, collaborative development of a new trend in PSCs has made it possible to overcome this bottleneck. Selective template growth (STG), as illustrated by the procedure in Scheme 4d, has achieved an efficiency of 25.1%,[402,403] opening the door to accessing these chemically inert, low-dimensional interfaces. Enabling access to chemically inert low-dimensional interfaces opens new avenues for advancing perovskite solar cells. Beyond this access, understanding the potential mechanisms of this strategy and the lattice compatibility of low-dimensional perovskite-like materials constitutes a significant contribution.

The potential mechanism for constructing the 3D/STG-targeted 2D-(PiEA)PbI_4 structure *via* this selective template growth involves composition and structural evolution. As shown in Scheme 4e, depositing 2D PA_2PbI_4 onto a 3D perovskite yields a 3D/template 2D-PA_2PbI_4 multilayer. This outcome is facilitated by the selective etching of the template's macrocation PA^+ by R–OH, followed by the simultaneous insertion of the macrocation $PiEA^{2+}$. This yields a 3D/PbI_2-(PiEA)I_2 intermediate multilayer rich in (PiEA)I_2 and PAI. A post-processing annealing step fully converts PbI_2-(PiEA)I_2 to (PiEA)PbI_4, yielding the purified 2D-(PiEA)PbI_4 multilayer structure, the 3D/STG target.

This is a promising technique, not limited to spin coating, but extendable to other solution-based processing methods such as blade coating. The advantages of this approach are: i) access to chemically inert low-dimensional interfaces, ii) improved thermal stress and stability under operating conditions, which were lacking in conventional methods, iii) the establishment of a solution processing system, iv) potential scalability for large-area manufacturing, and v) cost-effectiveness compared to conventional methods. This innovation is remarkable, and lattice matching conditions require further verification. Therefore, understanding atomic arrangement and crystal structure is of paramount importance. Grasping lattice matching opens opportunities to control and adjust interface defects, dislocations, and strains at the interface. These can potentially reduce device efficiency and stability. Furthermore, this lattice matching was confirmed three years prior to this selective approach.[404] As shown in Scheme 5, the findings of this study demonstrate lattice matching between 3D perovskites and low-dimensional perovskite-type materials. This confirmation is based on the alignment or lattice matching at 3D/1D, 3D/0D, and 1D/0D interfaces, exhibiting a favourable device efficiency of 24.18%. The lattice matching between the low dimensional perovskites and the 3D perovskite shown in Scheme 5 follows three unique properties: i) strain is not significant but tolerable; ii) the overall binary complex is stabilized through the regular formation of the Pb–I bond at the interface and hence constructs channels for charge transport; and iii) lattice distortion is not strong because of the moderate density of interfacial Pb–I bonds.

4.2.6. Synergy engineering enabling PSCs. In PSC engineering, particularly in research conducted in 2025–2026, synergy is achieved by optimising multiple components simultaneously. For example, surface defect passivation is combined with bulk crystal growth modulation to overcome the efficiency-stability trade-off. This approach yields PSCs with a high PCE, often exceeding 34%,[12] by improving film quality and energy-level alignment. As shown in Scheme 6, the key synergistic engineering approaches are as follows:

Buried/bulk interface engineering. The synergistic engineering of buried interfaces and the bulk, often referred to as 'buried/bulk interface engineering' or 'dual-site passivation', is a highly effective strategy in PSCs, particularly in inverted (p–i–n) structures.[405–410] This approach simultaneously reduces defects and optimises crystallisation. This approach addresses the limitations of charge transport layers and the poor crystallinity of perovskite films at the bottom interface. This involves combining surface modifiers (*e.g.* thiols or amines) with 2D perovskite seeds or managing the solvent to passivate defects, enhance grain size and reduce lattice strain.

Steric-complementary synergistic strategy (SCSS). This strategy involves using a mixture of compact cations to passivate deep-level surface defects, as well as larger, bulkier organic ions to form a hydrophobic protective layer that ensures efficiency and moisture resistance.[411] The two molecules work together in a hierarchical assembly and the responsible mechanisms are as follows:[410–412] i) *deep-level passivation*: piperazinium chemically neutralises undercoordinated lead defects and suppresses the formation of metallic lead, which are the primary sites for non-radiative recombination. ii) *Physical shielding*: for example, PEA^+ provides a steric barrier that protects the perovskite from moisture, oxygen and thermal stress. It also improves the alignment of the interfacial energy levels, facilitating better electron extraction. iii) *Thermodynamic stability*: theoretical calculations show that pre-adsorption creates energetically favourable sites for attachment, making the combined system more stable than its constituent parts.

A-site/B-site engineering. In A-site/B-site engineering, synergy refers to the simultaneous optimisation of the perovskite crystal lattice by adding or substituting functional agents at both the

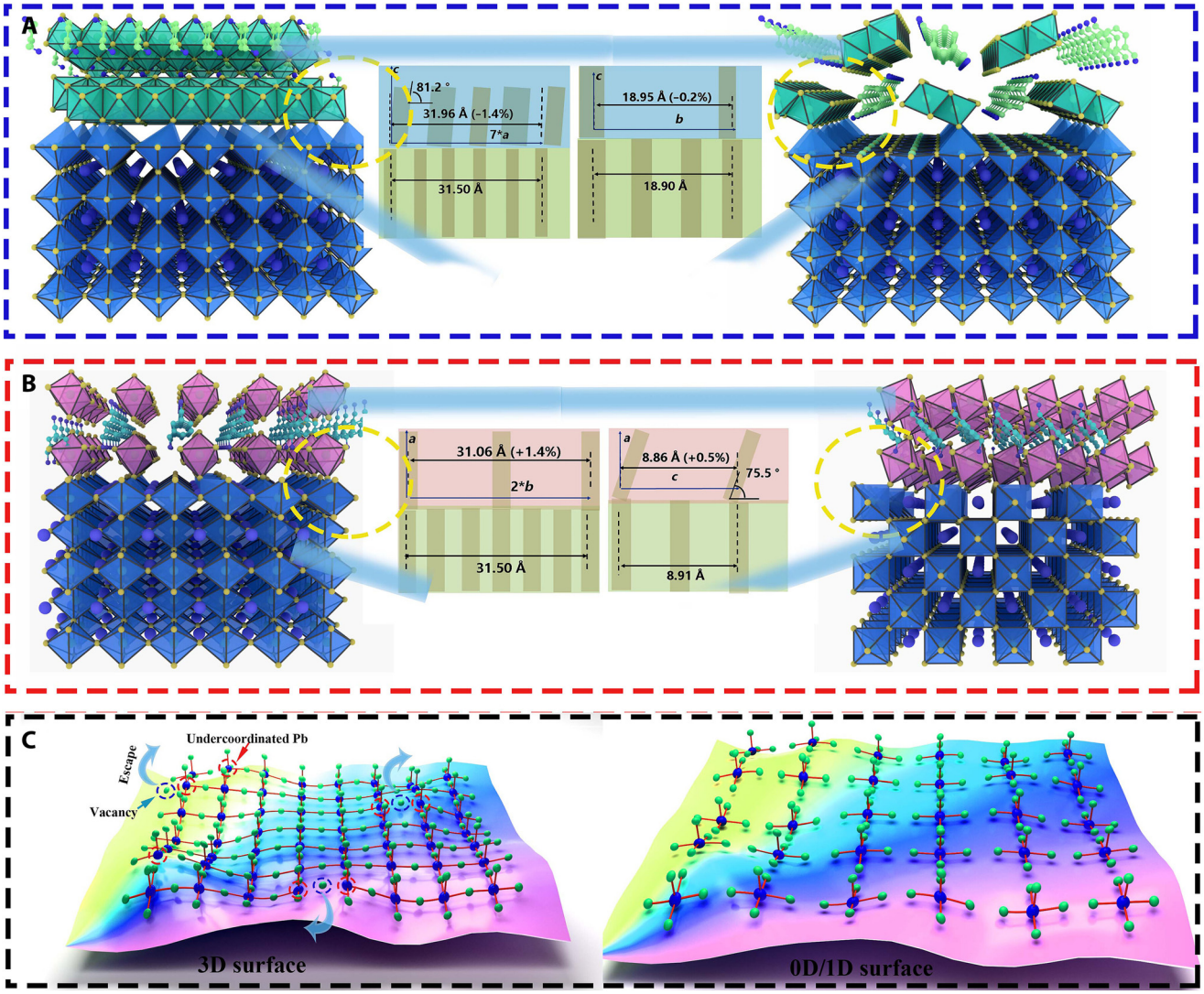

Scheme 5 Low-dimensional perovskite passivation strategy: (A) 3D/1D; (B) 3D/0D; and (C) 1D/0D interfacial alignment for effective passivation, reproduced from ref. 404 with permission from AAAS, Copyright 2022.

organic/inorganic cation site (A-site) and the metal cation site (B-site).[413] This dual-site approach is more effective at addressing defects, stabilising the crystal structure and improving charge carrier dynamics than modifying either site alone, leading to higher efficiency and better stability.

Dipole-defect engineering. In PSCs, synergy in dipole-defect engineering refers to a multifunctional strategy in which a single molecular modifier, or a combination of molecules, simultaneously passivates surface and bulk defects, while also introducing an interfacial dipole moment to improve energy-level alignment.[414] This approach effectively mitigates non-radiative recombination and optimizes carrier extraction, resulting in improved power conversion efficiencies (PCEs), minimal hysteresis and enhanced long-term stability (often exceeding 1000 hours in testing).[415] Using sulfonic or ammonium compounds to create interfacial dipole moments that align energy levels and reduce charge transport barriers while reducing the trap density.

Chemical/molecular bridging. In PSCs, synergy in the chemical/molecular bridging strategy refers to the use of multifunctional molecules (or combinations of molecules) that can simultaneously passivate defects, optimise energy-level alignment and improve crystallisation at the buried interface between the perovskite absorber and transport layers.[416] Designing molecules with dual or multiple functional groups—such as one end that anchors to the electron/hole transport layer (ETL/HTL) and the other that coordinates with perovskite ions (Pb or I)—creates a robust, ordered and conductive interface.[417] This enhances both PCE and long-term stability, often exceeding 26% PCE.[418,419] Dual-molecule passivators connected by functional groups (*e.g.* amino groups and chiral molecules) are used to create an 'electronic bridge' for improved carrier dynamics.[420]

These synergistic strategies lead to superior performance by lowering voltage losses (V_{OC}), increasing fill factors (FF) and boosting overall cell stability. This makes them critical

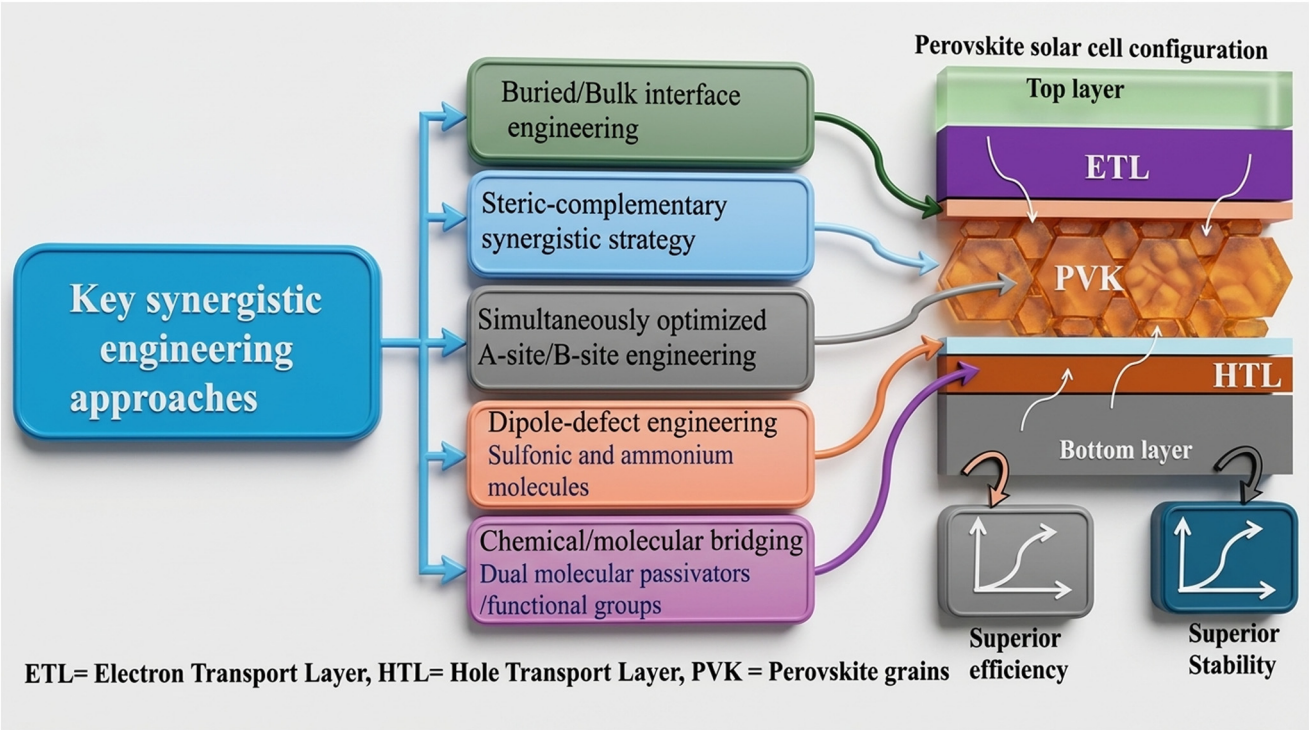

Scheme 6 Schematic representation of synergy engineering in PSCs.

for advances in both single-junction and tandem devices. However, this approach faces significant interconnected challenges that hinder its commercialization, which are proposed as follows:

✓ Balancing efficiency, stability and scalability: one of the core challenges is that strategies that improve one aspect often have a negative impact on another. For instance, long-chain passivating ligands enhance stability but impede charge transport. Achieving high-quality perovskite films over large areas (*i.e.* scaling up) while maintaining the efficiencies achieved in small-area laboratory cells is difficult.

✓ Managing complex interactions in mixed systems: synergistic approaches involving multiple additives, dopants or interfacial layers can lead to unpredictable and undesirable chemical interactions. For instance, Lewis base additives employed to passivate Pb^{2+} defects may result in the detrimental deprotonation of organic cations within the perovskite lattice.

✓ Intrinsic and extrinsic instability: PSCs are highly susceptible to heat, moisture, oxygen and UV light. To address both structural instability (phase segregation) and environmental degradation, synergistic engineering must tackle these issues simultaneously. This often requires complex encapsulation, which raises cost challenges.

✓ Ion migration and hysteresis: even with passivation, mobile ions (Pb^{2+}, MA^{+} and FA^{+}) can still migrate during operation. This results in non-radiative recombination and hysteresis in *J–V* curves, which reduces the cell's efficiency and lifespan.

✓ Interfacial energy alignment and recombination: although interfaces are designed to enhance performance by aligning the energy levels of the perovskite and transport layers (ETL/HTL), the elimination of charge transport barriers and the minimisation of trap states remain challenging.

✓ Reproducibility and standardization: many synergistic strategies depend on precise, non-standardised laboratory techniques, such as anti-solvent dripping. Such techniques are difficult to reproduce on an industrial scale.

4.2.7. Role of interface engineering in bridging the gap between lab-scale efficiency and module performance. The commercialization of PSCs remains the greatest unresolved challenge due to their low stability and poor scalability. The primary obstacle in scaling up PSCs is the decline in efficiency and long-term stability as the device area increases.[88] Maintaining the uniformity of efficiency and stability achieved in laboratories and small-scale manufacturing becomes the bottleneck issue in large-area production. This relates to variations in film quality—such as thickness, pinholes, and defects—and increases in sheet resistance and contact resistance during large-scale manufacturing, compared to results reported by research institutions. Furthermore, the key challenges in scalability are as follows: i) producing high-quality perovskite thin films, ii) establishing the optimum thickness, iii) constructing a large-scale design integration architecture involving adaptation to flexible substrates and dead area reduction, and iv) ensuring high stability against environmental factors such as moisture, temperature, ultraviolet light, and air. This hinders v) the maintenance of efficiencies achieved at the laboratory level and vi) the guarantee of long-term stability.[421]

Therefore, addressing the gap between lab-scale efficiency and module performance becomes crucial this time. Besides, the role of interface engineering in bridging this gap is vital.

Although spin-coating is effective in laboratory setting, *in situ* interface engineering is essential for large-area industrial coating techniques to ensure uniform passivation and the production of stable, high-performance modules.[422,423] Interface engineering plays a crucial role in bridging the gap between laboratory-scale efficiency and module performance in PSCs.[424] It addresses the unique stability and uniformity challenges that arise when scaling up from small cells to large-area modules. It mitigates the high-density interfacial defects, ion migration and energy level misalignment that typically cause severe performance losses during upscaling.[186,425]

4.2.8. Engineering new semiconductors: emergence of copper halide perovskites. Copper–lead halide perovskites are novel perovskite semiconductor materials with significant application potential in perovskite solar cells, batteries and photocatalysts. These materials are classified as direct bandgap semiconductors and promise to overcome the challenges associated with PSCs in terms of stability and toxicity. Beyond stability analysis, bonding chemistry and orbital design, further investigation of design mechanisms is needed to develop stable, environmentally friendly and efficient halide perovskite semiconductors for solar cells. A major challenge for halide perovskites is their degradation under environmental conditions such as humidity, oxygen, light and temperature. Other newly developed halide perovskites suffer from toxicity and efficiency problems. Currently, the most efficient PSCs have the lowest stability, while the most stable ones have low efficiency. This trend can also be observed in silicon solar cells. Over the past 30 years, silicon solar cells have demonstrated significantly higher stability than PSCs. As a result, to develop new semiconductor materials for solar cells, we must identify new materials that satisfy the following five principles: 1) possess efficiency equivalent to current PSCs; 2) possess stability equivalent to current silicon solar cells; 3) meet environmental standards for toxicity; 4) low manufacturing cost; and 5) easy processing and manufacturing using available technologies. By considering these five principles, we must ask ourselves the critical question: 'How should we design new copper halide perovskites that are suitable for the needs of PSCs and can be brought into field operations?'

To answer this, a comprehensive investigation of all conceivable "light-absorbing semiconductor design mechanisms" is essential while acknowledging all possible investigations from scientists. The central challenge is determining the "amount of light a new semiconductor can absorb" to achieve sufficient energy conversion. The most critical issue in material selection that could answer this question is band gap control. Therefore, material selection factors affecting the band gap include nanostructure type, band gap, lattice design, doping, composition, and others.[426–429] The primary role of these factors is to influence light absorption at specific wavelengths within the visible absorption region. Furthermore, bandgap design entails three key requirements: material selection (which semiconductor material to choose?), alloying or composite material design (how to achieve the desired chemical composition of the mixture?), and strain design (how to achieve the required strain?). The selected semiconductor must absorb photon energy ($h\nu$) greater than its bandgap energy (E_g) to generate electron–hole pairs. The remaining energy is emitted as thermal energy. Semiconductor materials with $h\nu$ less than E_g cannot absorb photon energy and therefore cannot generate electron–hole pairs. Consequently, the maximum carrier generation per unit area becomes a function of the bandgap of the selected semiconductor. The number of photons per square centimetre per second is defined as the photon flux and is given by eqn (15):

$$F(x) = F(0)e^{-ax} \quad (15)$$

The rate of carrier generation per unit volume is given by eqn (16):

$$G(x) = -dF(x)/dx = aF(0)e^{-ax} \quad (16)$$

where α is the absorption coefficient of the semiconductor, which is greater than 10^4 cm^{-1} for direct bandgap semiconductors. Therefore, semiconductors used in solar cells shall have the following characteristics: 1) an ideal band gap (0.9 to 1.2 eV),[430] 2) high optical absorption (10^4 cm^{-1}), and 3) good electrical conductivity. Generally, the following main semiconductor parameters determine the design and performance of solar cells: i) band gap energy E_g, absorption coefficient α, and refractive index n; ii) excess carrier diffusion length L and lifetime τ; iii) carrier diffusion coefficient D and mobility μ, which characterize the transport properties of carriers due to drift and diffusion, respectively; iv) dopant concentration, which determines the width of the space charge region at the junction; v) cost; and vi) availability or abundance on earth.[431,432] The ultimate goal of emerging copper halide PSCs is to compete with other existing solar cell technologies and achieve commercialization in the market, just like other solar cell technologies. For instance, the efficiency of CdTe thin-film modules has reached 14%, with a cost of US$0.50 per W, while the total cost of silicon solar cell modules has decreased from US$4 per W in 2008 to only US$1.25 per W in 2011, with the module efficiency improving from 15 to 20%.[433]

For this purpose, copper-based PSCs have recently been reported and have emerged as a new solar material.[434–436] However, most copper halide materials are 2D materials. Now, copper should be introduced in a way that can form 3D perovskite structures. In this case, there are two possibilities: 1) replacing the A-site methylamine in the 3D ABX_3 perovskite;[437] 2) replacing the central Pb^{2+} with CuI_3^{2-} octahedron instead of PbI_3^{2-}, and if possible, form $MCuX_3$ or $MACuI_3$, where M = a metal with a +1 charge, MA = methylamine, and X = a halogen, located at the B-site.[130] Now, it can be proposed that Cu plays a unique role in the band structure. This unique role includes the following:

1. Contribution to the band structure when used in both A- and B-site of ABX_3:[130] Cu contributes to the valence band through its *s* orbitals and d orbitals, influencing the

optoelectronic properties near the Fermi level.[437] The s–p hybridization between Cu and halogen atoms contributes to the band structure, forming a unique band structure. Both the occupied and unoccupied *s* orbitals of copper make unique contributions to the band structure. The effects of the occupied and unoccupied states of Cu on the band structure, overall optoelectronic properties, charge transfer, mobility and extraction are important research topics that have not yet been fully elucidated.

2. Cu can replace Pb atoms to overcome toxicity issues and adjust the bandgap.[438,439] However, its smaller size hinders the formation of a 3D perovskite structure when replacing lead atoms at the central position.[440] Thus, to form a 3D perovskite structure, Cu^+ shall replace methylamine rather than Pb. Placing Cu^+ at the A-site while ensuring that the atomic size of the central atom is similar to that of lead remains a major unsolved challenge. Potential atoms with similar sizes include Sn and Bi. Due to Sn instability under external conditions, Bi may be the optimal candidate atom.

3. By modifying the chemical environment with halogens, Cu perovskites offer multiple alternative solutions. Due to its high copper content, environmental friendliness, and stability toward moisture, it can replace methylamine, addressing issues such as stability, toxicity, and cost associated with methylamine.

4. The oxidation state and octahedral distortion are also important variables influencing the performance of engineered copper halide perovskite properties.

5. Generally, when engineering copper halide perovskites (Table 6), numerous factors require consideration and optimization.[441] These factors include crystal growth, composition, doping, nanostructure, carrier concentration, carrier mobility, diffusion and drift currents, absorption coefficient, and ambipolar diffusion length. Therefore, none of these variables have been optimized for this emerging copper halide perovskites. This indicates that there remains a significant amount of work to be done in the field of PSCs.

6. Copper halide perovskites have been reported for use in photovoltaic materials and other electronic devices.

Engineering strategies for copper halide perovskite solar materials involve nucleation engineering of the ABX_3 perovskite structure. Nucleation engineering is an engineering technique used to control the shape, size and crystal structure of materials during their crystallization process.[446,447]

The stability of the ABX_3 perovskite structure is determined by the Goldschmidt tolerance factor given by eqn (17):

$$t = \frac{r_A + r_X}{\sqrt{(r_B + r_X)}} \quad (17)$$

where r_A, r_B, and r_X are the ionic radii of A, B and X atoms in the ABX_3 perovskite structure, respectively. A stable perovskite structure exists in the range of $0.8 < t < 1$.

5. Copper semiconductor orbital mixing, bonding chemistry and orbital engineering

What is the possible strategy to realize a stable PSC with better efficiency in the real field of practical operation? In front of us, there is a new and unexplored potential room for Cu-based photovoltaic and other optoelectronic applications!

Semiconductors' property is determined by its orbital mixing in its band structure formation while molecular orbital mixing determines a molecule's reactivity, stability and shape. The difference also lies in the semiconductor orbital overlapping connecting vast number of atoms interacting to configure continuous band of energy levels, which determines its optoelectronic properties. The bonding chemistry in semiconductor materials involves the atomic orbital connectivity and orbital hybridization information that determine the specific optoelectronic properties of semiconductors. Such information and understanding elucidate the concept of orbital connectivity that regulates structural dimensions. For instance, in $Cs_2AgBiBr_6$ double halide perovskites, the $[BiBr_6]$ octahedral isolated the $[AgBr_6]$ octahedral, causing their valence bands and conduction bands to connect at a lower electronic dimension rather than in 3D. Compared to 3D halide perovskites such as $CH_3NH_3PbI_3$, this characteristic results in disappointing optoelectronic properties in the lower-dimensional dihalide clathrates, despite their better stability and lower toxicity.

Table 6 Recently reported Cu-based halide perovskite materials with their efficiencies

Semiconductor	Absorption coefficient, α	Band gap, E_g/eV	Efficiency	Ref.
$CuPbI_3$, $CuPbI_3$, $CuPbI_3$	—	1.45–2.0	—	68
$MACu_xI_3$	—	—	4.0	130
$MAPbI_3$:$MACu_xI_3$	—	—	12.43	130
$MAPb_{1-x}Cu_xI_3$	—	—	12.85	130, 442
$C_6H_4NH_2CuBr_2I$	—	1.65	0.63	430
$(CH_3NH_3)_2CuCl_2Br_2$	—	1.04	0.99	443
$(CH_3NH_3)_2CuCl_2I_2$	—	1.99	1.75	443
$CuCaCl_3$	—	1.536	—	437, 444, 445
$CuFeCl_3$	—	1.533	—	437, 444, 445
$CuSnCl_3$	—	1.697	—	437, 444, 445
$CuCoCl_3$	—	1.78	—	
$CuCuCl_3$	—	1.98	—	
$CuGaCl_3$	—	1.861	—	

For inorganic semiconductor materials, although some standards have been reported elsewhere, selecting appropriate criteria remains a challenge.[448] These criteria include: 1) valency: most reported inorganic semiconductors exhibit ionic properties. These semiconductors include PbS, CuBr, GaAs, ZnSe, bornite, pyrites, and stannite. 2) Covalency: the electronegativity difference of the bonds should be between 0.8 and 1.0. The electronegativity difference shall be considered before atoms form semiconducting bonds. 3) Phase diagram or line phase rule: the phase diagram of the system should show line phases with low solubility. If the semiconductor is a mixture of two other semiconductors, this rule may be violated. Other indicators for semiconductor materials include resistivity, high thermoelectric power, dielectric constant, and point contact rectification.[448]

5.1. Orbital occupation and orbital engineering

At thermal equilibrium, the orbital occupancy is expressed by the Fermi–Dirac distribution function $f(E)$, as shown in eqn (18):

$$f(E) = 1/(1 + \exp^{(E-E_F)/KT}) \quad (18)$$

where E_F is the Fermi energy or Fermi level, k_BT is the thermal energy, and k_B is the Boltzmann constant. Thus, the distribution of carriers in a semiconductor is solely determined by the Fermi level, with E_F located between the valence band and the conduction band. Each energy level E is either occupied by an electron (with probability $P(E)$) or left empty. Thus, the vast differences in chemical and physical properties, ranging from energy storage and electrocatalysis to spin–orbit coupling, valleytronics, charge density waves, and superconductivity, all stem from orbital occupancy.[449] This indicates that material properties are directly or indirectly related to electronic structure. This electronic structure depends on the shape and size of the Fermi surfaces and the position of the Fermi level. Therefore, the functionalization of continuous electron filling orbitals can serve as an operational strategy to functionalize electronic states, thereby functionalizing the chemical and physical properties of specific semiconductor materials.

The properties of high-performance materials require various engineering strategies, such as strain, doping, interface and band structure engineering. These engineering strategies aid in designing material properties to achieve suitable applications with enhanced efficiency and stability. Consequently, band structure engineering strategies are highly useful for various applications, including ferroelectrics, microelectronics, optoelectronics, catalysis, storage devices and thermoelectric applications. To implement this strategy, orbital engineering is of great importance. As shown in Fig. 16a–d, this orbital engineering depends on orbital interactions (Fig. 16a), such as s, p, d, f, and p–d (Fig. 16b), s–p (Fig. 16c), and d–sp orbital hybridization in the band structure shown in Fig. 16d. Such orbital interactions are essential for designing valence bands, conduction bands, and band gaps, which are crucial for designing properties such as charge carrier excitation, transfer, energy emission, and absorption.

5.2. Role of orbitals in halide perovskites

Understanding the orbital role and the properties associated with this orbital role is crucial for designing new materials for novel applications. Therefore, understanding contributing orbitals in the new semiconductor material $CuPbX_3$ is essential for designing these materials for potential new applications. $CuPbX_3$ has an ABX_3 perovskite structure. To describe the properties of this material, it is essential to understand the role of each orbital in the Cu, Pb and X atoms of $CuPbX_3$. This is because the energy band structure of $CuPbX_3$ is formed based on the contributions of each atom. For instance, in $CuAlO_2$, the $3d^{10}$ closed-shell orbitals from Cu^+ hybridized with the 2p orbitals of O. This hybridization alters the valence band maximum, making holes easier to excite. This results in high hole mobility.[25] The Cu $3d^{10}$ energy level is close to the oxygen X p orbital, enabling this hybridization. This makes $CuAlO_2$ a p-type semiconductor. Similarly, in $CuPbX_3$, the Cu^+ $3d^{10}$ and 4s orbitals are close to the halogen X p orbital, enabling hybridization, and $CuPbX_3$ becomes a p-type semiconductor similar to $CuAlO_2$. As shown in Fig. 17a–c, the valence band is primarily composed of Cu 4s, 3d and X p orbitals, as well as s–p and p–d hybridization, while the conduction band is primarily composed of Pb 6p orbitals. In $CH_3NH_3PbI_3$, the conduction band minimum is dominated by Pb 6p orbitals, while the valence band maximum consists of the Pb 6s and X p orbitals.[68] In the band structure of $CsPbX_3$, the role of Cu^+ is very significant, while in the band structure of CH_3NH_3-PbX_3 and $CsPbX_3$, the roles of $CH_3NH_3^+$ and Cs^+ are not significant. Moreover, the total state density of $CuPbX_3$ involves Cu-s, Cu-d, Pb-s, Pb-p and X-p.

5.3. Dual nature of cu d orbitals

The amount of Cu required depends on the d configuration that it contributes to the bond. Its role in bond formation within the perovskite structure depends on its oxidation states, such as +1, +2, or +3.[450] Considering Cu's chemical properties, Cu has five d orbitals, labeled as d_{xy}, d_{zy}, d_{yz}, d_{z^2} and $d_{x^2-y^2}$. Depending on the position of the Cu atom, there are two positions: intercalated Cu^+ and center-positioned Cu^{2+}. Its intercalation matters its position. Intercalated Cu^+ is not located at the center but connects the octahedral MX_6^{2-}, while the non-intercalated Cu^{2+} is located at the center, forming the geometric shapes of the octahedral CuX_6^{2-} or tetrahedral CuX_4^{2-}, as shown in Fig. 18. It can also create square planar shapes when forming Cu complexes. Intercalated copper forms $CuPbX_3$ or $CuMX_3$ perovskites, where M represents metal cations such as Sn^{2+} and Pb^{2+}. The central Cu^{2-} complexes form perovskites such as $MCuX_3$ or M_2CuX_6 (Cs^+, Cu^+, Ag^+, *etc.*)

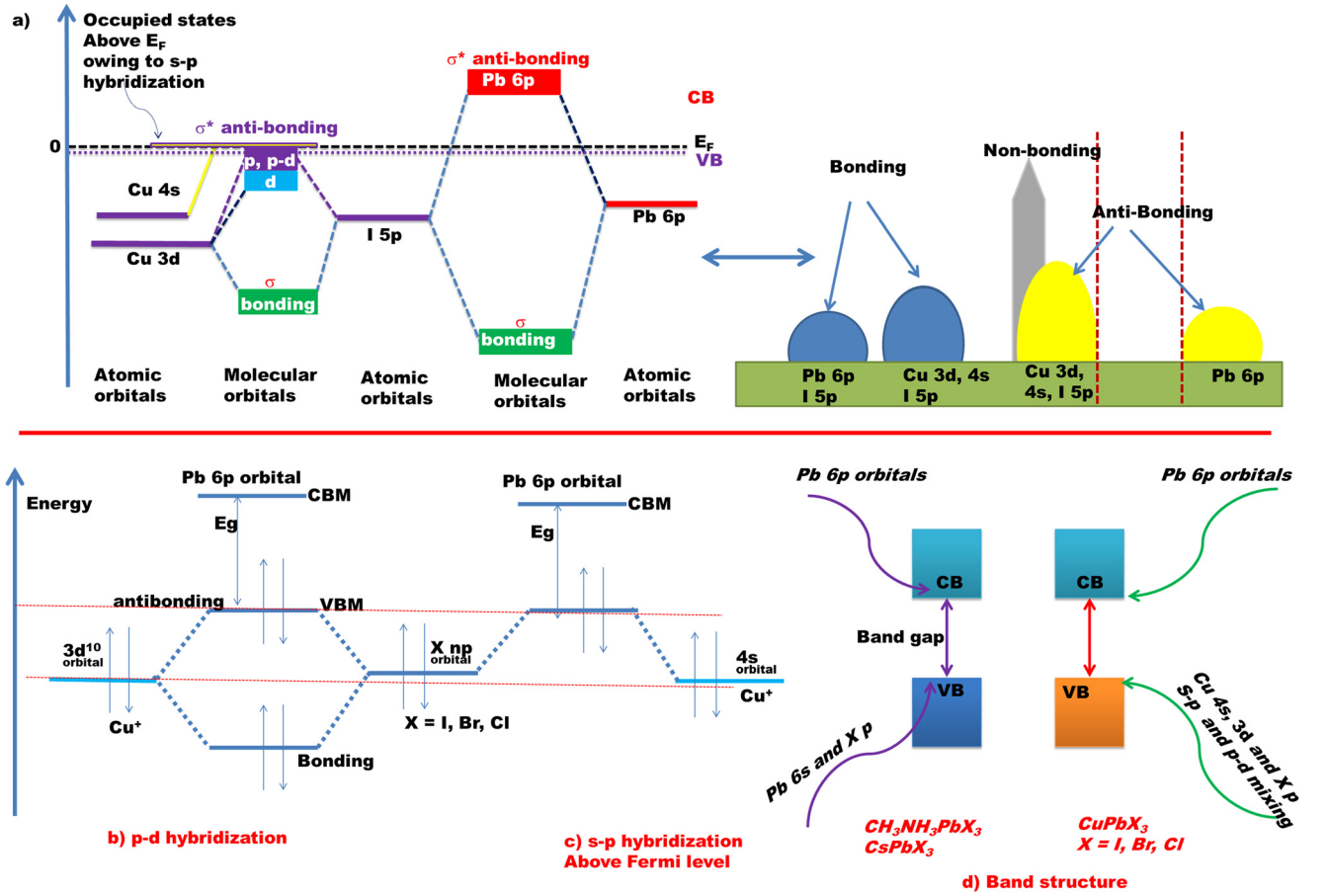

Fig. 16 a) Schematic of bonding and anti-bonding in $CuPbI_3$. b) Band structure contribution orbitals of $CH_3NH_3PbX_3$ and $CuPbX_3$. c) s–p and p–d orbital hybridization formed in $CuPbX_3$. d) Orbitals contributing to the valence band and conduction band in $CuPbX_3$.

or $MCuX_2$ (M = Al, Fe, *etc.*), where M stands for metal cations, such as $AgCuX_3$ and $CsCuX_3$, proposing new halide perovskites.[450,451] Furthermore, the mixed-valent $Cu^{+/2+}$ double perovskite structure can also form layered structures.[452,453]

In copper chemistry, the five d orbitals have the same energy and are initially degenerate. When six halide negative charges are uniformly distributed above the spherical surface, the d orbitals remain degenerate. However, due to the repulsive electrostatic interactions between the electrons in the d orbitals and the spherical shell of negative charges, the energy of the d orbitals increases (Fig. 18a). Distributing the six halide negative charges at the *vertices* of an octahedron does not change the average energy of the d orbitals but eliminates their degeneracy: the five d orbitals are split into two groups, whose energies depend on their orientations. As shown in Fig. 18b, the d_{z^2} and $d_{x^2-y^2}$ orbitals point directly toward the six negative charges located along the *x*, *y* and *z* axes. Consequently, due to increased electrostatic repulsions, the energy of electrons of these two orbitals (collectively referred to as the e_g orbitals) is higher than that in the spherical distribution of negative charges. In contrast, the other three d orbitals (d_{xy}, d_{xz}, and d_{yz}, collectively referred to as the t_{2g} orbitals) are oriented at 45° angles to the coordinate axes, thus pointing toward the six negative charges. The energy of electrons in any of these three orbitals is lower than that of the spherical distribution of negative charges in halides. In the octahedral symmetry of Cu^{2+}, the energy of the anti-bonding e_g hybrids $\left(e_g^*\right)$ is higher than that of the anti-bonding t_{2g} hybrids $\left(t_{2g}^*\right)$, because σ-anti-bonding interaction is feebler than π-anti-bonding interactions (Fig. 18c).[454] the energy of these e_g and t_{2g} are inversely related to the octahedral and tetrahedral structured copper compounds, as shown in Fig. 18c. The Cu^+ ion contributes to the valence band through s–p and p–d hybridisation. It also contributes to the unoccupied states above it by creating an empty band from the partially occupied s orbital. In contrast, Cu^{2+}, a central atom in $MCuX_3$, contributes to the conduction band because the X anions contribute to the valence band.[68] Moreover, understanding semiconductor orbital mixing, bonding chemistry and orbital engineering based on copper chemistry stimulates researchers, industries and enterprises to awaken their energetic motivation to explore $CuBX_3$ (B = divalent metal and X = halide ions) and or $ACuX_3$ (A is monovalent metal) more and bring them to be part of the new-generation energy materials to benefit UN sustainable development goals.

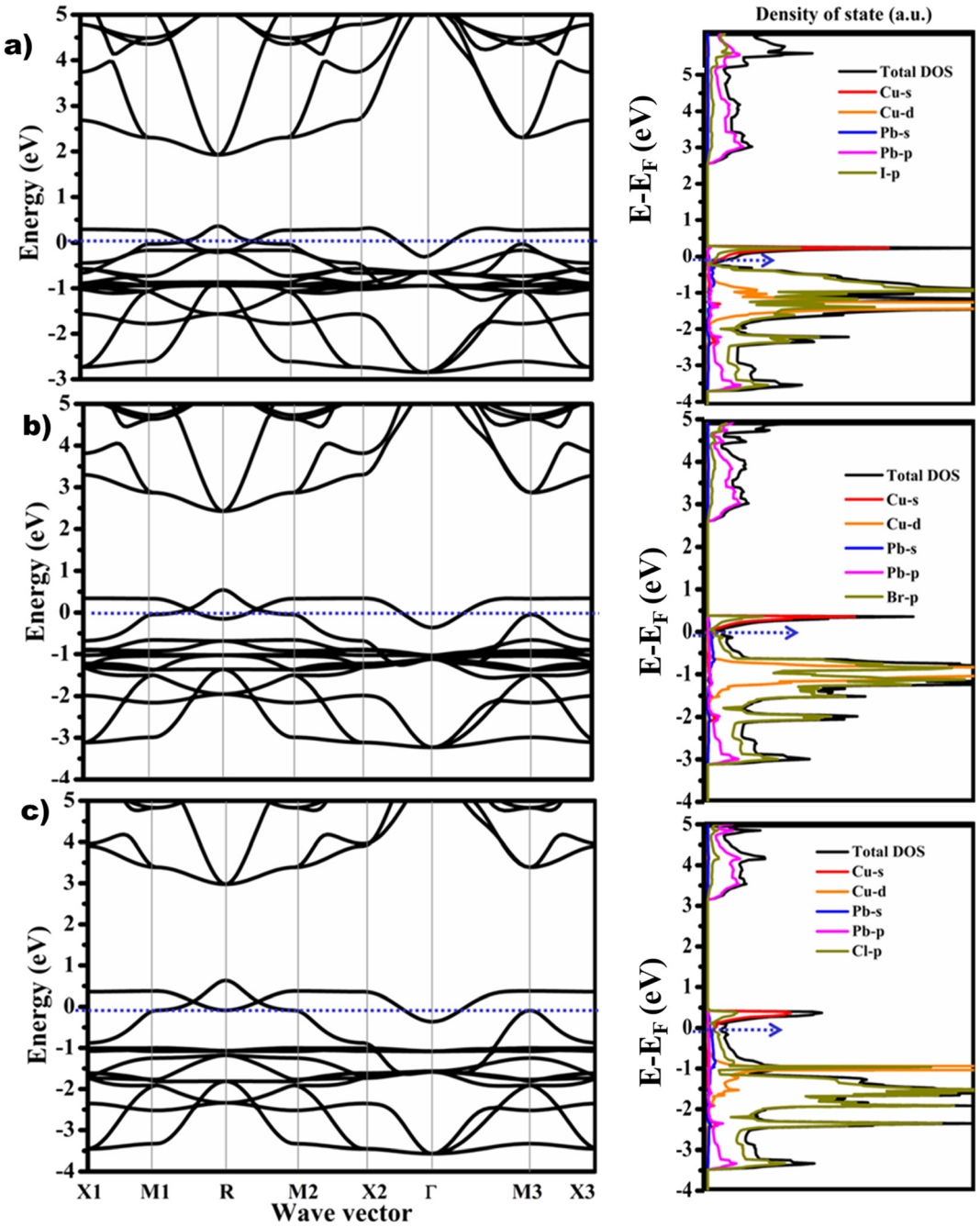

Fig. 17 Band structure engineering: a) schematics of the band structure and PDOS of a) $CuPbI_3$, b) $CuPbBr_3$ and c) $CuPbCl_3$ structures, reproduced from ref. 68 with permission from the National Taiwan University of Science and Technology, Electronic Thesis, Copyright, 2017.

6. Awakening towards exploring $CuPbX_3$ and $MACuX_3$

Are there any revolutionary opportunities to shift from CH_3NH_3-PbX_3 to $CuBX_3$ and/or $ACuX_3$? What intriguing optoelectronic properties enlighten $CuBX_3$ and $ACuX_3$ to ignite the potential light from within and achieve a new paradigm shift of igniting light in a wide range of energy applications?

Proposing research topics to the scientific community has been highly praised by researchers. For this reason, the authors propose potential research topics in the study of $CuBX_3$ and $ACuX_3$ semiconductor materials that have not yet been well explored:

1. From this perspective, the next hot research area will be manufacturing technologies such as smart manufacturing, inkjet printing, roll-to-roll printing, 3D printing, and solution processing technology. These technologies should be economical, simple, sustainable, and scalable to a wider range of applications. Which processing technology will be prioritized for the manufacture of $CuBX_3$ and $ACuX_3$ perovskite future solar

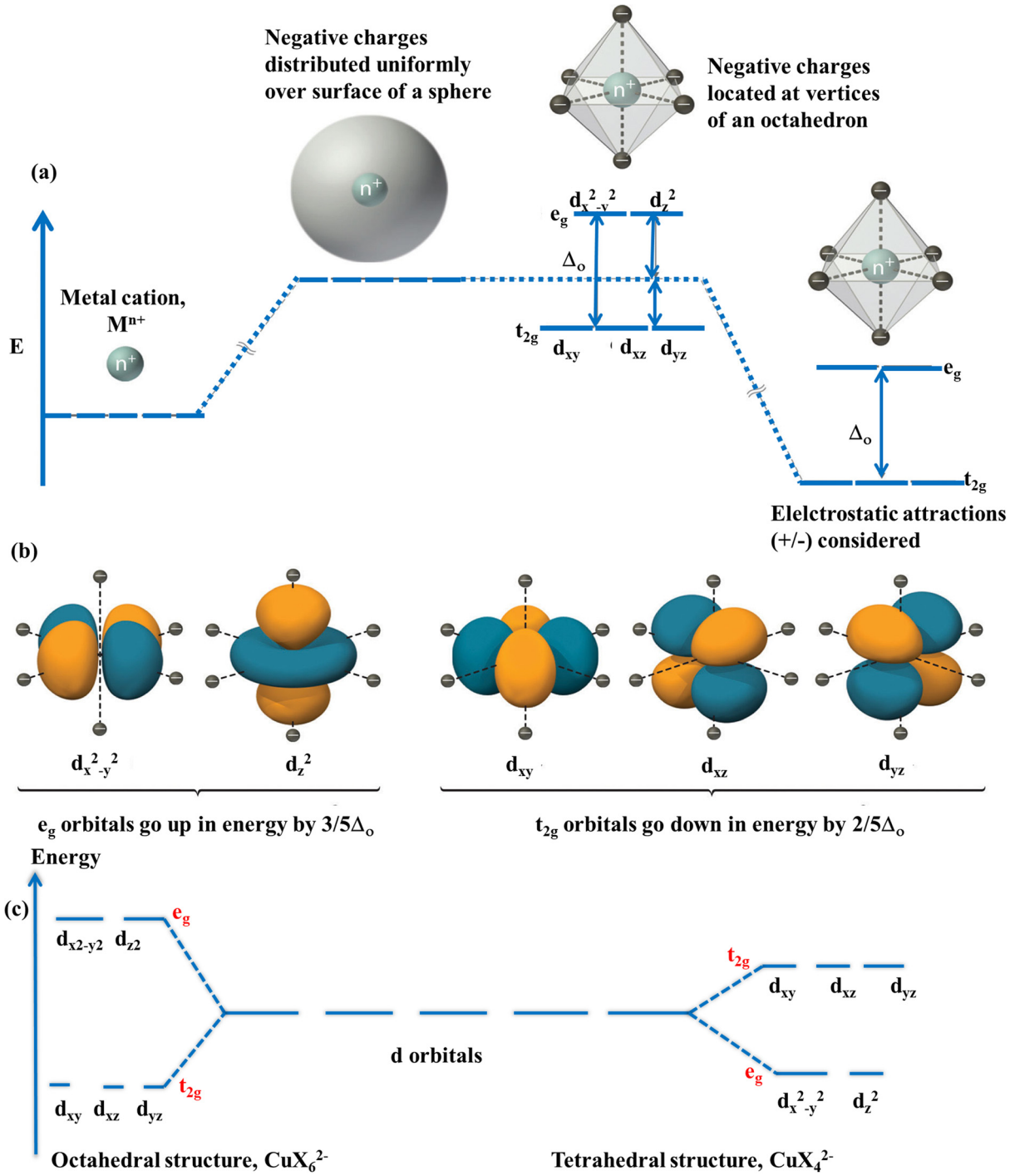

Fig. 18 Octahedral arrangement of six negative charges around a metal ion causes the five d-orbitals to split into two sets with different energies. (a) Distributing the −6 charge uniformly on the spherical surface around the metal ion increases the energy of all the five d orbitals due to electrostatic repulsions, but the five d orbitals remain degenerate. (b) Two e_g orbitals (left) point directly toward the six negatively charged ligands, resulting in increased energy compared to the spherical charge distribution. Conversely, the three t_{2g} orbitals (right) point between the negatively charged ligands, resulting in decreased energy compared to the spherical charge distribution. (c) Cu 3d orbitals split into octahedral and tetrahedral structures. Moreover, chalcogenides such as $CuGaS_2$ and Cu_2SnSe_3 benefit from the unique properties of Cu 3d orbitals due to their dual characteristics (*i.e.* localization effect and delocalized orbitals). Reproduced from ref. 455 with permission from Elsevier, Copyright 2015.

materials in solar material technology? To give a clue that might lead researchers to synthesize $CuBX_3$ and $ACuX_3$, as shown in Fig. 19, $CuBX_3$ can be synthesized from dissolving CuX and BX_2 in a solution while $ACuX_3$ can be synthesized by dissolving $CuCl_2$ in a given solvent and then adding BX into the solution.[456] The copper(I) halides are prepared from the reduction of copper(II) halides or $[Cu(MeCN)_4]PF_6$ reacted with 2,5-bis[(diphenylphosphino)methyl]thiophene.[457] PSC with the

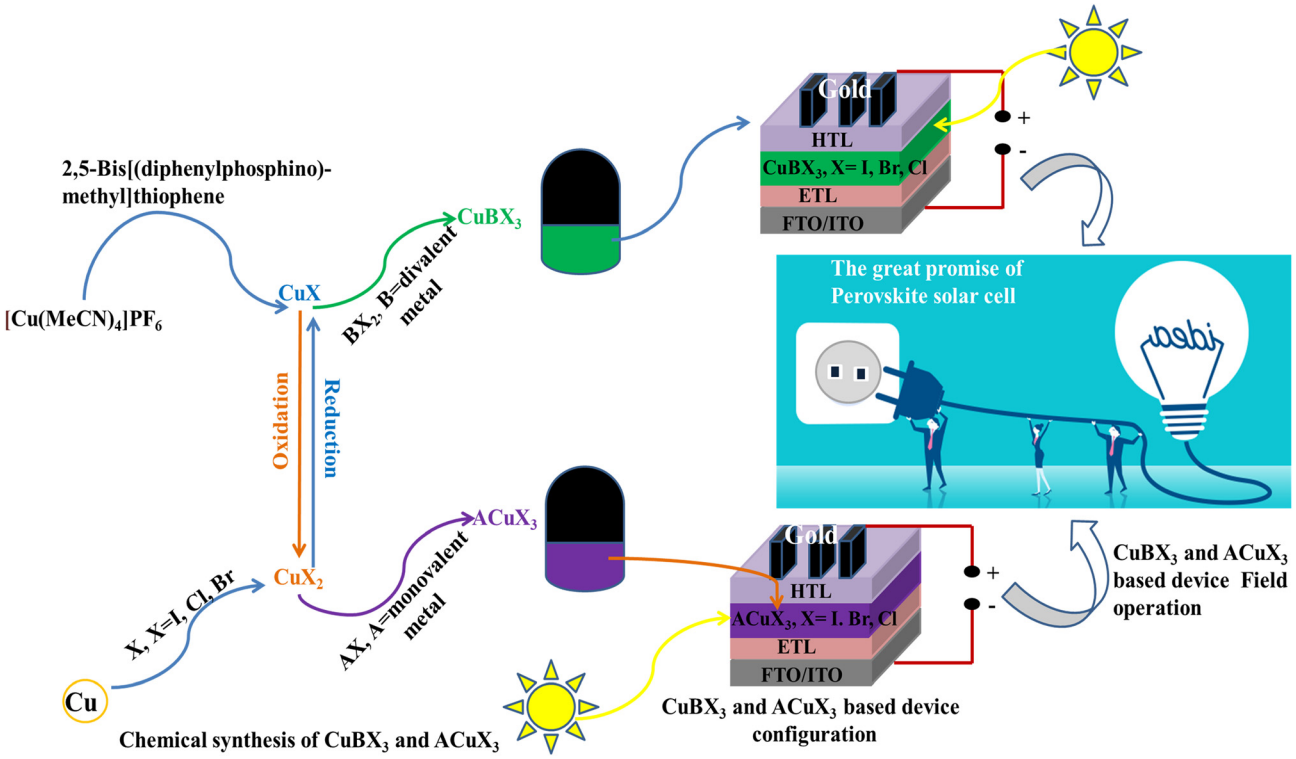

Fig. 19 Chemical synthesis and potential device architectures for $CuBX_3$ and $ACuX_3$ solar cells.

planar[458,459] and inverted[460,461] architectures can be developed to configure the solar cell in the practical application, as shown in Fig. 19. In this research direction, extensive research will be conducted in the future to drive revolutionary developments in solar energy research through new research directions, material design, and performance studies.

2. Copper perovskites are emerging materials for future PSCs. In this structure, Cu is located at the corners of the octahedral PbX_3^{2-} unit, replacing the water-soluble methylamine, or at the center, replacing the toxic Pb metal in the perovskite crystal structure. The core challenges in studying Cu-based perovskites for PSCs lie in: 1) the interplay between localized and delocalized Cu-3d and halide p orbitals; 2) Cu-s orbital interactions with a halide p orbital, *i.e.*, s–p hybridization; 3) in the band structure, the Cu s band replaces the methylamine cations in the perovskite structure; and 4) Cu^{2+} interacts with halide anions to form either octahedral or tetrahedral structures, replacing Pb^{2+} cations. Moreover, there is a potential issue regarding whether the Cu 3d state in Cu-based perovskites exhibit the same dual nature as those in Cu-chalcogenides. The dual natures of Cu 3d states in chalcogenides stems from the inherent localization of the 3d states and p–d hybridization, which arises from the localization of the *e* sub-states and the hybridization of the t_2 sub-states.[455] Do these dual properties of the Cu 3d states also exist in Cu-based perovskites, just as they do in Cu-chalcogenides? This requires detailed experimental and computational studies.

3. The study of the d orbital orders of Cu^+ cations offers opportunities for achieving novel physical and chemical properties, making it an urgent topic that requires clarification. The d orbital possesses dual properties of localization and delocalization. This dual nature is crucial for verifying the properties of $CuPbX_3$ materials in various applications, thereby necessitating further investigation.

4. Spin–orbit coupling: a hidden force that not only affects the band structure but also influences properties such as singlet-triplet splitting, spin lifetime, and magneto-resistance. Hence, studying spin–orbit coupling in $CuPbX_3$ halide perovskites is highly required. The effect of Cu^+ intercalation in the $CuPbX_3$ structure and the origin of the Rashba effect have not yet been investigated.

5. The hybridization driven by orbital overlap in 3D Cu-based halide perovskites requires advanced tools such as X-ray absorption spectroscopy, direct visualization of orbital electron occupancy, resonant inelastic X-ray scattering (RIXS) at the Cu edges, and density functional theory (DFT) to investigate the hybridization mechanisms and bonding information.

6. Another study with significant implications will involve replacing lead in $CuPbX_3$ with other elements. Potential candidate elements include M^{2+} metal cations, such as Cu^{2+} and Sn^{2+}. The reason is that $CuMX_3$ possesses advantages such as green nature, stability, environment-friendliness, low cost, and easy processability, making it suitable for the development of solar cell technology.

7. In the research and development of copper halide PSCs, understanding the coordination engineering, coordination chemistry, and electronic interactions present in the crystal structures of $CuBX_3$ and/or $ACuX_3$ (where A represents a metal

replacing the methylamine cation, and M can be Pb, Sn, Cu, Ag, *etc.*) is crucial for addressing the aforementioned nine research questions. This research area is still in its infancy and is expected to undergo further development over the next few years and beyond. In these structures, the sizes of the A, B, and X atoms are critical and must be considered for their suitability for perovskite structures, as these atoms are the primary sources of structural distortion, strain, stress, defects, and vacancies, which directly influence the thermodynamic stability of the structure, the formation of the band structure, light absorption, and charge carrier transport properties.

8. According to experimental and computational studies, the spin-polarized photoemission, the spin degrees of freedom of charge carriers within electronic devices, the band edges, recombination process, electronic coupling, spin–orbit interactions, charge transfer processes, charge carrier dynamics and charge separation, power conversion efficiency, lifetime, absorption and emission properties, catalytic properties, ion exchange, and anisotropic properties are responsible for various applications and represent the current research topics in these Cu halide perovskite materials.

7. Encouraging multifunctional properties and energy applications of copper halide perovskites

The perovskite community is looking for exploring a better stable, green, economical and energy-efficient perovskite energy materials. The question of this revolution is that will $CuPbI_3$ and its derivatives revolutionize the wide-ranging energy applications of the conventional $CH_3NH_3PbI_3$ perovskite and its derivatives? Thus, scientists have two tasks: making $CH_3NH_3^+$ free stable copper halide perovskites and lead-free user-friendly copper halide perovskites, at the same time, for efficient, stable and green energy applications.

Multifunctional energy applications of semiconducting materials, ranging from energy harvesting, conversion, generation to storage, depend on their potential multifunctional properties, as indicated by Fig. 20. Highly useful multifunctional properties of semiconducting materials for multifunctional energy applications that this review wants to stimulate are of degree of ionic conductivity, nature of the tunable band gap and band structure, thermal properties, electrochemical stability window, non-flammability, tunable optoelectronic properties, optical and electrochemical properties, photodetection and sensing, charge transport properties and solution processability. Based on these properties, copper halide perovskites such $CuPbI_3$, $MACuI_3$ and other derivatives have key properties that make them potential for energy applications. Such potential properties are as follows:

Direct bad gap property

Copper halide perovskites have direct band gap properties,[437] which may bring new research horizon in various efficient energy absorbing and emitting applications such as optoelectronic devices owing to their efficient absorption and

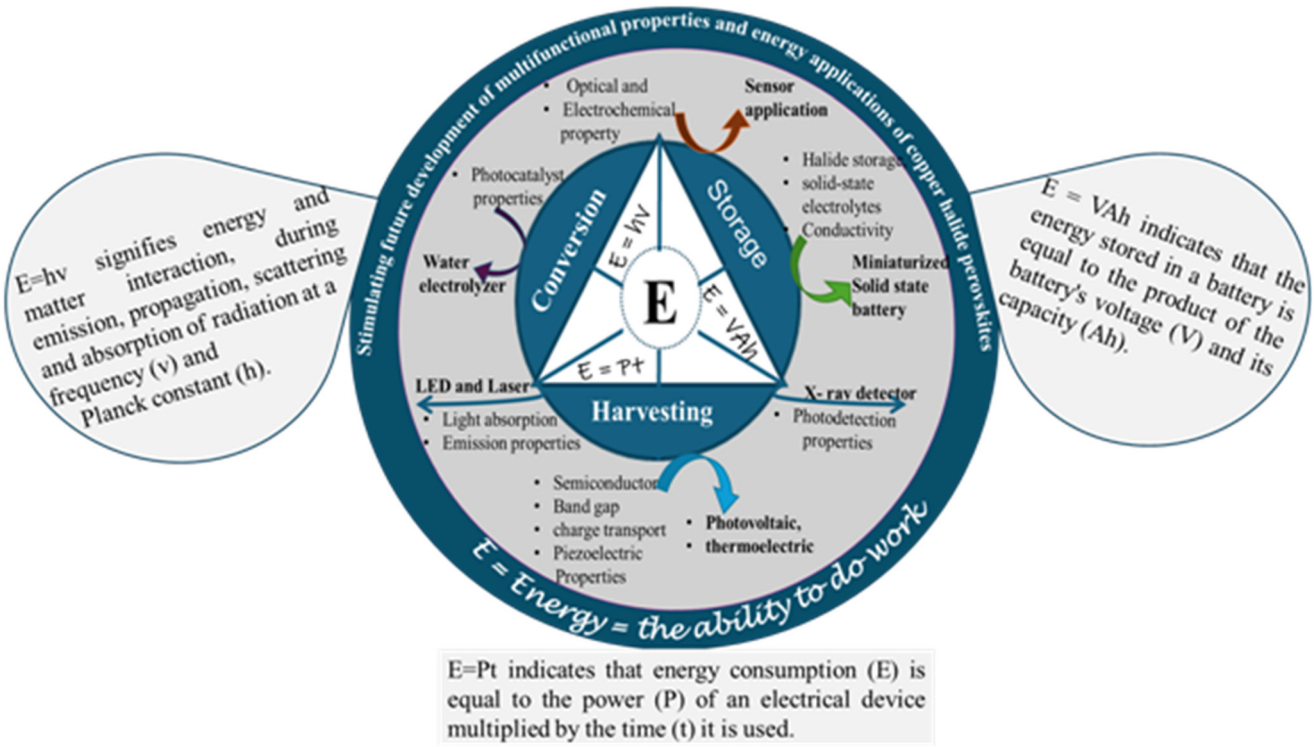

Fig. 20 Promoting the development of multifunctional energy applications of copper halide perovskite materials for future generations.

emission of light. Such optoelectronic devices are solar cells, light-emitting diodes, lasers, thin-film transistors, *etc.*, which are not benefited from the new timely research paradigm of copper halide perovskites. Their direct electron transition and recombination make copper halide perovskites promising semiconducting materials in this field. Moreover, $CuPbI_3$ has been used for water splitting owing to its direct band gap that can drive hydrogen evolution at a voltage of 0.62 V and 216 μA cm^{-2} current density using a 0.1 M Na_2SO_4 solution.[462] There are performance improvement and stability challenges in the liquid electrolytes, which need further optimization. Thus, the future research is aimed at improving the stability and efficiency of photoelectrochemical water splitting for efficient solar hydrogen generation. The reason to apply for photochemical water splitting is that photoelectrochemical water splitting is responsible for the zero emission energy carrier stated in the sustainable development goals. The main goal here is achieving high solar-to-hydrogen efficiency through the following strategies: (1) band gap position alignment appropriate for photoelectrochemical water splitting into oxygen and hydrogen half reactions, (2) inserting narrow band gap and enhanced ability of absorbing visible light, (3) improved electron–hole (charge carrier) separation in semiconductors such as $CuBX_3$ or $ACuX_3$ perovskites, and (4) designing photocorrosion-resistant stable photoelectrodes and economical semiconductors as primary criteria.[463]

Basically, to fully convert H_2O into its component parts H_2 and $1/2O_2$, the semiconductor shall absorb photon energy (ΔE) of greater than 1.23 eV per electron transferred with a free energy change (ΔG) = 237.2 kJ mol^{-1}. The semiconductor photoelectrode shall have an energy of 1.6–2.4 eV per electron–hole pair produced.[464] Thus, a series of semiconductors with suitable alignments are required to effectively operate water splitting solar cells. Eqn (19)–(21) show the photoelectrochemical water splitting process:

$$H_2O + 2h^+ \rightarrow H^+ + 1/2O_2 \quad (19)$$

$$H^+ + 2e^- \rightarrow H_2 \quad (20)$$

$$H_2O \rightarrow H_2 + 1/2O_2, (\Delta G = 237.2 \text{ kJ mol}^{-1} \text{ and } \Delta E > 1.23 \text{ eV} \quad (21)$$

Perovskite semiconductors with a band gap of 1.6 eV can be an ideal material for hydrogen molecule production, solving stability issues in the liquid electrolyte and interfacial alignments. Furthermore, $CsPbI_3$, $KPbI_3$, $LiPbCl_3$, $NaPbI_3$ and $LiPbI_3$ having a band gap energy in the range of 1.31–1.43 eV are not only useful for solar cells but also highly useful semiconductors for photoelectrochemical water splitting and solid-state batteries (Fig. 21).[465–467]

Tunable optoelectronic properties, high optical emission and absorption properties

copper halide perovskites have direct and tunable band gaps of 1.82 eV,[462] 2.1 eV,[468] and 1.55–2.33 eV,[68] which make them optical emitters and absorbers. This is owing to the direct recombination of electrons and holes, enabling the emitting photon energy applicable in laser, light-emitting diode and

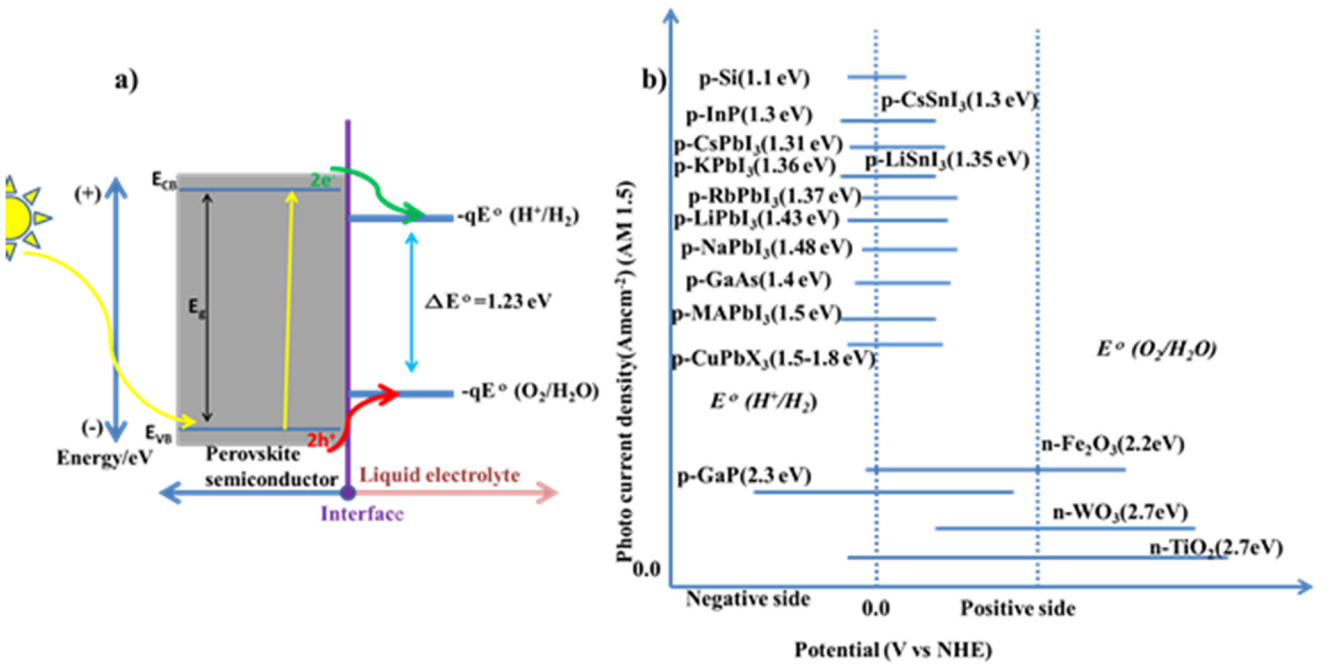

Fig. 21 A proposed schematic representation of the photo-electrochemical water splitting process is shown below: a) A diagram showing an ideal ABX_3 halide perovskite semiconductor for water splitting. b) The proposed position of the perovskite band gap for water splitting alongside that of other common semiconductors in the thermodynamic potential of the water redox process.

transistors. However, their high optical absorption is facilitated by efficient electron–hole separation and injection and electron transition from a lower energy band to a higher energy band to boost the power conversion efficiency. Although copper halide perovskites have these new research opportunities, researchers are not yet focusing on such promising semiconductors, and thus, this review is calling them to shine their research life with new breakthroughs in this field of study.

Copper-based perovskites can be classified into two perovskite structures: 1) Cu^{2+} at the B site of ACu_xX_3 such as in $MAPb_{1-x}Cu_xI_3$ with a PCE of 12.85%, $Cs_{0.12}FA_{0.88}Pb_{0.99}Cu_{0.01}I_{2.99}$ (ref. 469) and $MACuI_3$ with a PCE of 4.0% ref. (130, 442 and 470) and 2) Cu^+ at the A sight of the $CuBX_3$ structure such as $CuPbCl_3$, $CuPbI_3$, and $CuSnI_3$.[437,471,472] Above all, there is also a conclusion that Cu, Ag and Tl are candidates to interact with the BX_3^- cage in the ABX_3 structure, occupying the A site to create $CuPbI_3$, $AgPbI_3$ and $TlPbI_3$ with relatively better covalence.[473] This makes these materials applicable in various energy application fields of operations.

Electrical and photocatalytic properties

copper halide perovskites such as $CuCdCl_3$ and $CuSnI_3$ have catalytic and electrical properties. The room-temperature conductivities are 2.62×10^{-9}, 7.1×10^{-8} and 1.11×10^{-5} (Ω cm) for $KPbI_3$, $CuPbI_3$ and $CuSnI_3$, respectively.[471] At higher temperatures of 300 and 400 °C, the conductivity values for $CuCdCl_3$ are 5.80×10^{-3} and 1.54×10^{-2} $(\Omega\ cm)^{-1}$, respectively.[474] The catalytic research opportunity is open for research this time, calling researchers to investigate and put their great effort to flourish new research dimensions (see Fig. 21). There has been one report showing increased crystallite size and unit cell volume upon doping with Eu^{2+}/Eu^{3+}. This indicates that there is a possibility to boost the catalytic property of $CuPbI_3$ through doping and other material engineering strategies.[475]

Radiation dosimetry

Cu-based perovskite films showed great response when exposed to gamma radiation.[468] The response had been reported as the change in morphology, crystallinity, optical, electrical and structural properties, suggesting the potential for use in dosimetry and radiation detection from $CuPbI_3$ thin films.[468,476] This is owing to its capability to produce and separate electron–hole pairs upon interaction with the photon energy, and hence, this makes such semiconductors appropriate for the detection of radiation multifunctionalities. Consequently, the radiation induced mechanisms and changes, and the specific dose ranges are yet to be optimized for the betterment of this field. Furthermore, the ideal factor obtained indicates the presence of radiation induced defects, which are useful in the application of dosimetry owing to the $CuPbI_3$/P–Si heterostructure showing acceptable diode property.[477]

Ionic conductivity

Copper halide perovskites, particularly $CuPbI_3$, had been employed in the galvanic electrolytic cell as solid electrolytes with a cell configuration of Pb/$CuPbI_3$/AgI/Ag, providing a cell open circuit voltage of 0.211 V and a capacity of 6.6 μAh at an ionic transference number >0.99 as well as a lower activation energy of 0.29 eV, responsible for iodine ion migration or iodine ion vacancy migration, showing relatively easy ionic conduction at room temperature within a geometrical cell area of 0.36 cm^2.[478] $CuPbI_3$ thin films are required in galvanic electrochemical cell applications because of the need for 'developing miniaturized batteries' having: 1) long shelf life, 2) wide operating temperature and 3) high energy density configured using the combination solid thin-film semiconductors such as $CuPbI_3$ with solid electrolytes. This embraces great promise of realizing 'miniaturized solid batteries' with the application of copper halide perovskites owing to its 'mixed ionic-electronic conductivity' properties at a lower activation energy than that of $CH_3NH_3PbI_3$ (0.6 eV).[479]

Moreover, is it possible for copper halide perovskites to have the synergy nature of ferroelectric polarization and semiconducting properties to achieve the ferroelectric-semiconductor solar cell type and open a new avenue for a higher PCE to revolutionize the field of organic–inorganic hybrid PSCs? In case if this question gets answered by copper halide PSCs, then it will be the end of history for organic–inorganic hybrid PSCs. Therefore, this nature of copper halide PSCs matters the continuity or discontinuity history of organic–inorganic hybrid PSCs in this era. To this end, ferroelectric solar cells can achieve high power conversion efficiency if the following four scientific aspects are well understood: 1) bulk photovoltaic effect; 2) depolarization field effect; 3) Schottky barrier effect and 4) domain wall effect.[480] Above all, machine learning methods with the potential for further development of perovskite photovoltaics are urgently required.[481,482] The exploration of perovskite photovoltaic, particularly, the new rise of copper halide perovskites, for various optoelectronic advancements necessary modern technological demands,[483] thereby the new breakthroughs revolutionize the research and development.

8. Concluding remarks and future outlooks

What future developments could accelerate the advancement of copper–lead halide perovskites and their lead-free derivatives? The development of efficient, stable and environmentally friendly perovskite solar cells (PSCs) must be encouraged to enable more effective energy applications and help solve the world's energy problems.

Despite their high PCE or energy efficiency and low cost of solution processing opportunities, PSCs faced two major

bottlenecks with regard to the issues of sustainable operation and environment. These bottlenecks include *poor stability of operation and toxicity to living beings*. Overcoming these bottlenecks has become a hot research topic attracting widespread attention from the perovskite scientific community. This review aims to explore possibilities and lead the way toward overcoming the stability and scalability challenges, and if beyond, the toxicity challenge too. To realise this vision and further advance related research, this review focuses on six dynamic and promising solutions: 1) development of contributing functional molecular bridges, modifiers and stabilizers such as application of additives, ionic liquid, spacer ions, capping agents, and its role in crystal engineering; 2) development of innovative approaches headed to overcome surface and interfacial limits as well as device engineering limits; 3) engineering new perovskite semiconductor with the vision to develop efficient, stable, green and economical semiconductor solar materials replacing the conventional methylamine and Pb in the CH_3-NH_3PbX_3 framework *via* chemical methods at the same time; 4) awakening ideas to stimulate the PSC community to re-explore copper halide perovskites and innovate them in various energy applications as has been done to the conventional PSC materials; and 5) stimulating multifunctional properties and energy applications of copper halide perovskites to broaden the field in multidimensional wide range applications and show the future platform of the field for researchers, developers such as industries and enterprises with the believe that a new horizon of research for new advancements, opportunities and perspectives may open, visualizing the unseen horizon of potential research to be seen. 6) the sixth contribution stems on comprehensive solution strategies such as one stone: three bird strategies and/or an all in one integrated innovative approaches that have been more demanding in this research filed and yet this strategy is better to bring PSC to commercial viability, wondering with this idea led us to design the aim of this review article.

In nurturing the development trends of the PSC nexus, the limits of surface and interfacial chemistry, together with those of device engineering, become urgent topics in need of urgent solutions. For this purpose, designing flawless and surface nanostructuring, self-assembling layers for buried interface engineering, surface redox engineering, hydroxylation-based surface and interface homogenization and developing selective templating growth to access low-dimensional interfaces and create better lattice matching have been implemented, and research is ongoing with great promises. This paradigm shift has seen inverted perovskite solar cells (PSCs) emerge as a hot research breakthrough, achieving record efficiencies of 27% in single-junction devices and 34.85% in tandem devices. For unknown reasons, the performance of such inverted PSCs is not well established to come to the practical applications. This requires identifying and understanding key performance bottlenecks hampering their practical applications.

Moreover, developing 'triple-E solar cell' devices requires an understanding of trends in nexus development. This includes surface nanostructuring, self-assembling layers, surface redox engineering, and peroxide surface homogenisation. It also involves identifying new opportunities, such as designing halide perovskite energy materials that are as efficient as current organic-inorganic halide perovskites (*e.g.* $CH_3NH_3PbI_3$) or full inorganics (*e.g.* $CsPbI_3$), but which are more stable and environmentally friendly. These materials are urgently needed to advance the use of PSCs. Consequently, the emergence of copper halide perovskite become possible to be an alternative halide perovskite energy materials expected to boost efficiency, stability and environment issues together for future generation PSC development. Thus, triple-E-solar cell devices require understanding not only the role of semiconductor orbital mixing rules, orbital engineering, bonding chemistry and band structure formation but also the abundance and environmental issues of the raw semiconductor materials, economics of processing, and sustainability of working in real-time operations to continue and stimulate applied and fundamental research on further development of copper halide PSCs. Based on this philosophy of triple-E-solar cell devices and its core requirement, this review wants to introduce a new research horizon and a copper lead halide perovskite. Moreover, copper and its derivative semiconductors are environmentally friendly, durable, recyclable, abundant, healthier and vital to operate efficiently with a great promise to future low carbon economy, energy generation and delivery of electricity to respond to human energy demands and realize a greener future. This makes working with copper and its derivative semiconductors safe and robust. Therefore, now is a reasonable and practical time to discover copper halide perovskites and develop them for use in energy-efficient, economical and ecological applications.

Conflicts of interest

The authors declare no conflicts of interest.

Data availability

No primary research results, software or codes have been included, and no new data were generated or analysed as part of this review.

Acknowledgements

C. C. C. thanks the financial supports from the NSTC in Taiwan (112-2223-E-002-008-MY4, 113-2628-E-002-015-MY3, and 114-2124-M-027-001) and the Top University Project of National Taiwan University (115 L7722, 115 L893903, and 115 L104305). T. A. B. thanks the financial support from Adigrat University (AGU/RCSD/DDM-6724c2b/2024) and Addis Ababa University (TR/525/2023).

References

1 H. Dong, *et al.*, Metal Halide Perovskite for next-generation optoelectronics: progresses and prospects, *eLight*, 2023, **3**, 3, DOI: 10.1186/s43593-022-00033-z.

2 R. Pandey, *et al.*, Mutual Insight on Ferroelectrics and Hybrid Halide Perovskites: A Platform for Future Multifunctional Energy Conversion, *Adv. Mater.*, 2019, **31**, 1807376, DOI: 10.1002/adma.201807376.

3 T. A. Berhe, W.-N. Su and B. J. Hwang, Halide Perovskites' Multifunctional Properties: Coordination Engineering, Coordination Chemistry, Electronic Interactions and Energy Applications beyond Photovoltaics, *Inorganics*, 2024, **12**, 182.

4 T. A. Berhe, E. K. Ashebir, W.-N. Su and B. J. Hwang, Nano-engineering halide perovskites: towards energy harvesting, nano-plasmonic sensing and photoflexoelectric applications, *Energy Adv.*, 2025, **4**, 469–517, DOI: 10.1039/D4YA00442F.

5 A. Kojima, K. Teshima, Y. Shirai and T. Miyasaka, Organometal Halide Perovskites as Visible-Light Sensitizers for Photovoltaic Cells, *J. Am. Chem. Soc.*, 2009, **131**, 6050–6051, DOI: 10.1021/ja809598r.

6 J. Y. Kim, J.-W. Lee, H. S. Jung, H. Shin and N.-G. Park, High-Efficiency Perovskite Solar Cells, *Chem. Rev.*, 2020, **120**, 7867–7918, DOI: 10.1021/acs.chemrev.0c00107.

7 W. Shen, Y. Zhao and F. Liu, Highlights of mainstream solar cell efficiencies in 2025, *Eng. Energy*, 2026, **20**, 10508, DOI: 10.1007/s11708-026-1050-8.

8 K. Wang, *et al.*, Overcoming Shockley-Queisser limit using halide perovskite platform?, *Joule*, 2022, **6**, 756–771, DOI: 10.1016/j.joule.2022.01.009.

9 S. Rühle, Tabulated values of the Shockley–Queisser limit for single junction solar cells, *Sol. Energy*, 2016, **130**, 139–147, DOI: 10.1016/j.solener.2016.02.015.

10 M. Nayak, A. J. Akhtar and S. K. Saha, Theoretical estimation to double the performance of perovskite solar cells using a graded absorber layer, *Sustain. Energy Fuels*, 2025, **9**, 1305–1316, DOI: 10.1039/D4SE01271B.

11 R. Liu, *et al.*, Precisely Tuning 3D/Quasi-2D Perovskite Heterojunctions in Wide-Bandgap Perovskites for High-Performance Tandem Solar Cells, *Adv. Mater.*, 2025, **37**, 2504321, DOI: 10.1002/adma.202504321.

12 LONGI, 34.85%! LONGi Breaks World Record for Crystalline Silicon-Perovskite Tandem Solar Cell Efficiency Again. LONGi News (2025.4.15).

13 C. Marchant and R. M. Williams, Perovskite/silicon tandem solar cells-compositions for improved stability and power conversion efficiency, *Photochem. Photobiol. Sci.*, 2024, **23**, 1–22, DOI: 10.1007/s43630-023-00500-7.

14 F. Xu, *et al.*, Monolithic perovskite/perovskite/silicon triple-junction solar cells with cation double displacement enabled 2.0 eV perovskites, *Joule*, 2024, **8**, 224–240, DOI: 10.1016/j.joule.2023.11.018.

15 G. E. Eperon, M. T. Hörantner and H. J. Snaith, Metal halide perovskite tandem and multiple-junction photovoltaics, *Nat. Rev. Chem.*, 2017, **1**, 0095, DOI: 10.1038/s41570-017-0095.

16 X. Zhao, T. Liu and Y.-L. Loo, Advancing 2D Perovskites for Efficient and Stable Solar Cells: Challenges and Opportunities, *Adv. Mater.*, 2022, **34**, 2105849, DOI: 10.1002/adma.202105849.

17 A. M. Oni, A. S. M. Mohsin, M. M. Rahman and M. B. Hossain Bhuian, A comprehensive evaluation of solar cell technologies, associated loss mechanisms, and efficiency enhancement strategies for photovoltaic cells, *Energy Rep.*, 2024, **11**, 3345–3366, DOI: 10.1016/j.egyr.2024.03.007.

18 Y. Li, M. Li, P. Fu, R. Li, D. Song, C. Shen and Y. Zhao, A comparison of light-harvesting performance of silicon nanocones and nanowires for radial-junction solar cells, *Sci. Rep.*, 2015, **5**, 11532.

19 H. J. Lee, *et al.*, Absorption Coefficient of Bulk III-V Semiconductor Materials: A Review on Methods, Properties and Future Prospects, *J. Electron. Mater.*, 2022, **51**, 6082–6107, DOI: 10.1007/s11664-022-09846-7.

20 M. C. Gupta and J. Ballato, *III–V Semiconductor Materials in The Handbook of Photonics*, CRC Press, Boca Raton, 2nd edn, 2006.

21 M. W. Dashiell, *et al.*, Quaternary InGaAsSb Thermophotovoltaic Diodes, *IEEE Trans. Electron Devices*, 2006, **53**, 2879–2891, DOI: 10.1109/TED.2006.885087.

22 D. Zheng, T. Pauporté, C. Schwob and L. Coolen, Models of light absorption enhancement in perovskite solar cells by plasmonic nanoparticles, *Exploration*, 2024, **4**, 20220146, DOI: 10.1002/EXP.20220146.

23 V. C. Nikolis, *et al.*, Reducing Voltage Losses in Cascade Organic Solar Cells while Maintaining High External Quantum Efficiencies, *Adv. Energy Mater.*, 2017, **7**, 1700855, DOI: 10.1002/aenm.201700855.

24 R. Kumar and R. Gupta, Shunts in crystalline silicon PV modules: A comprehensive review of investigation, characterization, and mitigation, *Sol. Energy Mater. Sol. Cells*, 2024, **277**, 113121, DOI: 10.1016/j.solmat.2024.113121.

25 E.-C. Cho, *et al.*, Silicon Quantum Dots in a Dielectric Matrix for All-Silicon Tandem Solar Cells, *Adv. OptoElectron.*, 2007, **2007**, 069578, DOI: 10.1155/2007/69578.

26 Y. Ji, L. Xu, X. Hao and K. Gao, Energy Loss in Organic Solar Cells: Mechanisms, Strategies, and Prospects, *Sol. RRL*, 2020, **4**, 2000130, DOI: 10.1002/solr.202000130.

27 J. Li, *et al.*, Unveiling microscopic carrier loss mechanisms in 12% efficient Cu2ZnSnSe4 solar cells, *Nat. Energy*, 2022, **7**, 754–764, DOI: 10.1038/s41560-022-01078-7.

28 Q. Dong, *et al.*, Electron-hole diffusion lengths >175 μm in solution-grown $CH_3NH_3PbI_3$ single crystals, *Science*, 2015, **347**, 967–970, DOI: 10.1126/science.aaa5760.

29 S. R. Kumavat, Y. Sonvane, D. Singh and S. K. Gupta, Two-dimensional CH3NH3PbI3 with high efficiency and superior carrier mobility: a theoretical study, *J. Phys. Chem. C*, 2019, **123**, 5231–5239.

30 M. Rani, *et al.*, Breaking barriers: Addressing challenges in perovskite solar cell development, *J. Alloys Compd.*, 2025, **1010**, 177648, DOI: 10.1016/j.jallcom.2024.177648.

31 B. Kayes, *et al.*, 27.6% Conversion efficiency, a new record for single-junction solar cells under 1 sun illumination, 2011.
32 N.-G. Park, Perovskite solar cells: an emerging photovoltaic technology, *Mater. Today*, 2015, **18**, 65–72, DOI: 10.1016/j.mattod.2014.07.007.
33 P. Ščajev, *et al.*, Impact of dopant-induced band tails on optical spectra, charge carrier transport, and dynamics in single-crystal CdTe, *Sci. Rep.*, 2022, **12**, 12851, DOI: 10.1038/s41598-022-16994-7.
34 K. Suzuki, S. Seto, T. Sawada and K. Imai, in *2001 IEEE Nuclear Science Symposium Conference Record (Cat. No.01CH37310)*, 2001, vol. 2394, pp. 2391–2395.
35 First Solar Press Release, *First Solar Achieves Yet Another Cell Conversion Efficiency World Record*, https://www.eqmagpro.com/first-solar-achieves-yet-another-cell-conversion-efficiency-world-record/, (accessed February 26, 2016).
36 M. Ochoa, S. Nishiwaki, S.-C. Yang, A. N. Tiwari and R. Carron, Lateral Charge Carrier Transport in Cu(In,Ga)Se2 Studied by Time-Resolved Photoluminescence Mapping, *Phys. Status Solidi RRL*, 2021, **15**, 2100313, DOI: 10.1002/pssr.202100313.
37 J. Kaur, *et al.*, Optimization of Photovoltaic Characteristics of CIGS/Si Heterojunction Solar Cells, *ES Energy Environ.*, 2022, **17**, 56–63, DOI: 10.30919/esee8c743.
38 K. Keller, K. Kiselman and O. Donzel-Gargand, *et al.*, High-concentration silver alloying and steep back-contact gallium grading enabling copper indium gallium selenide solar cell with 23.6% efficiency, *Nat. Energy*, 2024, **9**, 467–478.
39 S. Lou, H. Zhu, S. Hu, C. Zhao and P. Han, Investigation of diffusion length distribution on polycrystalline silicon wafers *via* photoluminescence methods, *Sci. Rep.*, 2015, **5**, 14084, DOI: 10.1038/srep14084.
40 N. D. Arora, J. R. Hauser and D. J. Roulston, Electron and hole mobilities in silicon as a function of concentration and temperature, *IEEE Trans. Electron Devices*, 1982, **29**, 292–295, DOI: 10.1109/T-ED.1982.20698.
41 M. Schleuning, *et al.*, Generalized Method to Extract Carrier Diffusion Length from Photoconductivity Transients: Cases of ${\mathrm{BiVO}}_{4}$, Halide Perovskites, and Amorphous and Crystalline Silicon, *PRX Energy*, 2022, **1**, 023008, DOI: 10.1103/PRXEnergy.1.023008.
42 H. C. Kang, Silicon *vs.* Amorphous Silicon: the Significance of Structural Differences in Photovoltaic Applications, *IOP Conf. Ser.: Earth Environ. Sci.*, 2021, **726**, 012001, DOI: 10.1088/1755-1315/726/1/012001.
43 Q. Zhou, *et al.*, Additive-assisted perovskite crystallization on industrial TOPCon silicon for tandem solar cells with improved efficiency, *Nat. Energy*, 2026, DOI: 10.1038/s41560-026-02010-z.
44 P. Löper, *et al.*, Organic–Inorganic Halide Perovskites: Perspectives for Silicon-Based Tandem Solar Cells, *IEEE J. Photovolt.*, 2014, **4**, 1545–1551, DOI: 10.1109/JPHOTOV.2014.2355421.
45 L. W. Aukerman, M. F. Millea and M. McColl, Diffusion Lengths of Electrons and Holes in GaAs, *J. Appl. Phys.*, 1967, **38**, 685–690, DOI: 10.1063/1.1709396.
46 R. D. Ryan and J. E. Eberhardt, Hole diffusion length in high purity n-GaAs, *Solid-State Electron.*, 1972, **15**, 865–868, DOI: 10.1016/0038-1101(72)90022-6.
47 *Gallium Arsenide (GaAs) Semiconductors*, https://www.azom.com/article.aspx?ArticleID=8349 (accessed March 27 2013).
48 T. Li and J. Zhu, Research of Enhancing the Light Absorption and Strengthen GaAs Thin Film Solar Cells with Metallic Ti Material Based on Grating Structure and Surface Plasmon Resonance Effect, *Plasmonics*, 2025, **20**, 8145–8154.
49 L. Hafaifa, *et al.*, Enhanced CZTSSe Thin-Film Solar Cell Efficiency: Key Parameter Analysis, *Phys. Status Solidi A*, 2025, **222**, 2400332, DOI: 10.1002/pssa.202400332.
50 R. Adhi Wibowo, E. Soo Lee, B. Munir and K. Ho Kim, Pulsed laser deposition of quaternary Cu2ZnSnSe4 thin films, *Phys. Status Solidi A*, 2007, **204**, 3373–3379, DOI: 10.1002/pssa.200723144.
51 J. Zhou, *et al.*, Control of the phase evolution of kesterite by tuning of the selenium partial pressure for solar cells with 13.8% certified efficiency, *Nat. Energy*, 2023, **8**, 526–535, DOI: 10.1038/s41560-023-01251-6.
52 J. Lee, J. D. Cohen and W. N. Shafarman, The determination of carrier mobilities in CIGS photovoltaic devices using high-frequency admittance measurements, *Thin Solid Films*, 2005, **480-481**, 336–340, DOI: 10.1016/j.tsf.2004.11.087.
53 J. Keller, *et al.*, High-concentration silver alloying and steep back-contact gallium grading enabling copper indium gallium selenide solar cell with 23.6% efficiency, *Nat. Energy*, 2024, **9**, 467–478, DOI: 10.1038/s41560-024-01472-3.
54 O. Gunawan, T. Gokmen and D. B. Mitzi, Suns-VOC characteristics of high performance kesterite solar cells, *J. Appl. Phys.*, 2014, **116**, 084504.
55 Avancis claims 19.64% efficiency for CIGS module, PV Magazine International, https://www.pv-magazine.com/2021/03/04/avancis-claims-19-64-efficiency-for-cigs-module/, (accessed March 4, 2021).
56 J. Zhang, *et al.*, Highly efficient narrow bandgap Cu(In,Ga)Se2 solar cells with enhanced open circuit voltage for tandem application, *Nat. Commun.*, 2024, **15**, 10365, DOI: 10.1038/s41467-024-54818-6.
57 O. Gunawan, *et al.*, Carrier-resolved photo-Hall effect, *Nature*, 2019, **575**, 151–155, DOI: 10.1038/s41586-019-1632-2.
58 A. Tombak, T. Kilicoglu and Y. S. Ocak, Solar cells fabricated by spray pyrolysis deposited Cu2CdSnS4 thin films, *Renewable Energy*, 2020, **146**, 1465–1470, DOI: 10.1016/j.renene.2019.07.057.
59 X. Cui, K. Sun and J. Huang, *et al.*, Cd-Free Cu2ZnSnS4 solar cell with an efficiency greater than 10% enabled by Al2O3 passivation layer, *Energy Environ. Sci.*, 2019, **12**(9), 2751–2764, DOI: 10.1039/C9EE01726G.
60 S. Dadgostar, *et al.*, A Cathodoluminescence Study on the Diffusion Length in AlGaInP/InGaP/AlInP Solar Cell Heterostructures, *J. Electron. Mater.*, 2020, **49**, 5184–5189, DOI: 10.1007/s11664-020-08176-w.

61 H.-H. Huang, *et al.*, *Effective mobility map for InGaP/InGaP multiple quantum-well-based solar cells*, SPIE, 2019, p. 1091310, DOI: 10.1117/12.2508592.
62 NREL, Private Communication, 2019.
63 T. Takamoto, H. Juso and K. Ueda, *et al.*, IMM triple-junction solar cells and modules optimized for space and terrestrial conditions, *Proceedings of the 44th IEEE Photovoltaic Specialist Conference (PVSC)*, 2017, DOI: 10.1109/PVSC.2017.8366097.
64 M. A. Green, E. D. Dunlop and G. Siefer, *et al.*, *Prog. Photovolt.: Res. Appl.*, 2023, **31**, 3–16, https://global.sharp/corporate/news/220606-a.html (Press Release, 21 November 2022).
65 R. Lin, *et al.*, All-perovskite tandem solar cells with dipolar passivation, *Nature*, 2025, **648**, 600–606, DOI: 10.1038/s41586-025-09773-7.
66 W. Dawidowski, *et al.*, Tunnel junction limited performance of InGaAsN/GaAs tandem solar cell, *Sol. Energy*, 2021, **214**, 632–641, DOI: 10.1016/j.solener.2020.11.067.
67 J. F. Geisz, *et al.*, Building a Six-Junction Inverted Metamorphic Concentrator Solar Cell, *IEEE J. Photovolt.*, 2018, **8**, 626–632, DOI: 10.1109/JPHOTOV.2017.2778567.
68 T. A. Berhe, Room Temperature Synthesis, Mechanism and Stability Analysis of $CH_3NH_3PbI_3$ and the Development of Transition metal (I) cation based New Inorganic Perovskites, *Electronic Thesis and Disertations Service*, National Taiwan University of Science and Technology, 2017, https://etheses.lib.ntust.edu.tw/detail/a96e1afdc5a1f2264629170caaf710fc/.
69 C. Geng, *et al.*, Crystallization Modulation and Holistic Passivation Enables Efficient Two-Terminal Perovskite/CuIn(Ga)Se2 Tandem Solar Cells, *Nano-Micro Lett.*, 2024, **17**, 8, DOI: 10.1007/s40820-024-01514-1.
70 B. Kang and F. Yan, Emerging strategies for the large-scale fabrication of perovskite solar modules: from design to process, *Energy Environ. Sci.*, 2025, **18**, 3917–3954, DOI: 10.1039/D4EE05613B.
71 L. Liu, *et al.*, 4-Terminal Inorganic Perovskite/Organic Tandem Solar Cells Offer 22% Efficiency, *Nano-Micro Lett.*, 2022, **15**, 23, DOI: 10.1007/s40820-022-00995-2.
72 J. Huang, *et al.*, Perovskite–organic tandem solar cells with superior reverse-bias stability, *Nat. Mater.*, 2026, DOI: 10.1038/s41563-026-02541-6.
73 M. Minbashi, A. Ghobadi, E. Yazdani, A. A. Kordbacheh and A. Hajjiah, Efficiency enhancement of CZTSSe solar cells *via* screening the absorber layer by examining of different possible defects, *Sci. Rep.*, 2020, **10**, 21813.
74 J. Han, K. Park, S. Tan, Y. Vaynzof, J. Xue, E. W.-G. Diau, M. G. Bawendi, J.-W. Lee and Il. Jeon, Perovskite solar cells, *Nat. Rev. Methods Primers*, 2025, **5**, 3.
75 R. Vaillon, O. Dupré, R. B. Cal and M. Calaf, Pathways for mitigating thermal losses in solar photovoltaics, *Sci. Rep.*, 2018, **8**, 13163, DOI: 10.1038/s41598-018-31257-0.
76 H. Xiang, *et al.*, Tackling Energy Loss in Organic Solar Cells *via* Volatile Solid Additive Strategy, *Adv. Sci.*, 2024, **11**, 2401330, DOI: 10.1002/advs.202401330.
77 J. Wang, *et al.*, Highly efficient all-inorganic perovskite solar cells with suppressed non-radiative recombination by a Lewis base, *Nat. Commun.*, 2020, **11**, 177, DOI: 10.1038/s41467-019-13909-5.
78 D. B. Mitzi, O. Gunawan, T. K. Todorov, K. Wang and S. Guha, The path towards a high-performance solution-processed kesterite solar cell, *Sol. Energy Mater. Sol. Cells*, 2011, DOI: 10.1016/j.solmat.2010.11.028.
79 S. Reykandeh, M. Vahedpour, H. Douroudgari, A. Razavizadeh and S. Asgharzadeh, Computational study of the mechanism, reaction rate and Thermochemistry of atmospheric oxidation of methylamine with singlet oxygen, *Phys. Chem. Res.*, 2016, **4**, 191–208, DOI: 10.22036/pcr.2016.13575.
80 M. R. Dash and M. A. Ali, Can a single ammonia and water molecule enhance the formation of methanimine under tropospheric conditions?: kinetics of ·CH2NH2 + O2 (+NH3/H2O), *Front. Chem.*, 2023, **11**, 1243235.
81 Q. Akkerman and L. Manna, What Defines a Halide Perovskite?, *ACS Energy Lett.*, 2020, **5**, 604–610, DOI: 10.1021/acsenergylett.0c00039.
82 T. A. Berhe, *et al.*, Organometal halide perovskite solar cells: degradation and stability, *Energy Environ. Sci.*, 2016, **9**, 323–356, DOI: 10.1039/C5EE02733K.
83 T. Wu, *et al.*, The Main Progress of Perovskite Solar Cells in 2020–2021, *Nano-Micro Lett.*, 2021, **13**, 152, DOI: 10.1007/s40820-021-00672-w.
84 X. Zhao, *et al.*, Accelerated aging of all-inorganic, interface-stabilized perovskite solar cells, *Science*, 2022, **377**, 307–310, DOI: 10.1126/science.abn5679.
85 S. M. Park and E. H. Sargent, Navigating the path to stability in perovskite solar cells, *Matter*, 2023, **6**, 2488–2490, DOI: 10.1016/j.matt.2023.06.007.
86 J. Li, *et al.*, Cs2PbI2Cl2, All-Inorganic Two-Dimensional Ruddlesden–Popper Mixed Halide Perovskite with Optoelectronic Response, *J. Am. Chem. Soc.*, 2018, **140**, 11085–11090, DOI: 10.1021/jacs.8b06046.
87 S. Liu, V. P. Biju, Y. Qi, W. Chen and Z. Liu, Recent progress in the development of high-efficiency inverted perovskite solar cells, *NPG Asia Mater.*, 2023, **15**, 27, DOI: 10.1038/s41427-023-00474-z.
88 S. Khatoon, *et al.*, Perovskite solar cell's efficiency, stability and scalability: A review, *Mater. Sci. Energy Technol.*, 2023, **6**, 437–459, DOI: 10.1016/j.mset.2023.04.007.
89 H. Zhang and N.-G. Park, Progress and issues in p-i-n type perovskite solar cells, *DeCarbon*, 2024, **3**, 100025, DOI: 10.1016/j.decarb.2023.100025.
90 R. K. Battula, G. Veerappan, P. Bhyrappa, C. Sudakar and E. Ramasamy, Stability of MAPbI3 perovskite grown on planar and mesoporous electron-selective contact by inverse temperature crystallization, *RSC Adv.*, 2020, **10**, 30767–30775, DOI: 10.1039/D0RA05590E.
91 J. Yang, K. M. Fransishyn and T. L. Kelly, Comparing the Effect of Mesoporous and Planar Metal Oxides on the Stability of Methylammonium Lead Iodide Thin Films, *Chem. Mater.*, 2016, **28**, 7344–7352, DOI: 10.1021/acs.chemmater.6b02744.
92 J. H. Kim, *et al.*, High-Performance and Environmentally Stable Planar Heterojunction Perovskite Solar Cells Based

on a Solution-Processed Copper-Doped Nickel Oxide Hole-Transporting Layer, *Adv. Mater.*, 2015, **27**, 695–701, DOI: 10.1002/adma.201404189.

93 W. Chen, *et al.*, A comparative study of planar and mesoporous perovskite solar cells with printable carbon electrodes, *J. Power Sources*, 2019, **412**, 118–124, DOI: 10.1016/j.jpowsour.2018.11.031.

94 W. Qin, *et al.*, in *2015 IEEE 42nd Photovoltaic Specialist Conference (PVSC)*, 2015, pp. 1–5.

95 M. V. Khenkin, *et al.*, Consensus statement for stability assessment and reporting for perovskite photovoltaics based on ISOS procedures, *Nat. Energy*, 2020, **5**, 35–49, DOI: 10.1038/s41560-019-0529-5.

96 M. U. Ali, H. Mo, Y. Li and A. B. Djurišić, Outdoor stability testing of perovskite solar cells: Necessary step toward real-life applications, *APL Energy*, 2023, **1**, 020903, DOI: 10.1063/5.0155845.

97 H. J. Kim, G. S. Han and H. S. Jung, Managing the lifecycle of perovskite solar cells: Addressing stability and environmental concerns from utilization to end-of-life, *eScience*, 2024, **4**, 100243, DOI: 10.1016/j.esci.2024.100243.

98 C. Fei, *et al.*, Highly Efficient and Stable Perovskite Solar Cells Based on Monolithically Grained CH3NH3PbI3 Film, *Adv. Energy Mater.*, 2017, **7**, 1602017, DOI: 10.1002/aenm.201602017.

99 L. Zuo, H. Guo, D. W. deQuilettes, S. Jariwala, N. De Marco, S. Dong, R. DeBlock, D. S. Ginger, B. Dunn, M. Wang and Y. Yang, Polymer-modified halide perovskite films for efficient and stable planar heterojunction solar cells, *Sci. Adv.*, 2017, **3**, e1700106.

100 J. Duan, *et al.*, Lanthanide ions doped CsPbBr3 halides for HTM-free 10.14%-efficiency inorganic perovskite solar cell with an ultrahigh open-circuit voltage of 1.594 V, *Adv. Energy Mater.*, 2018, **8**, 1802346.

101 W. Xiang, *et al.*, Europium-doped CsPbI2Br for stable and highly efficient inorganic perovskite solar cells, *Joule*, 2019, **3**, 205–214.

102 M. Abdi-Jalebi, *et al.*, Maximizing and stabilizing luminescence from halide perovskites with potassium passivation, *Nature*, 2018, **555**, 497–501.

103 N. Li, *et al.*, Cation and anion immobilization through chemical bonding enhancement with fluorides for stable halide perovskite solar cells, *Nat. Energy*, 2019, **4**, 408–415.

104 J. Jin, *et al.*, Enhanced Performance of Perovskite Solar Cells with Zinc Chloride Additives, *ACS Appl. Mater. Interfaces*, 2017, **9**, 42875–42882, DOI: 10.1021/acsami.7b15310.

105 R. Wang, *et al.*, Caffeine Improves the Performance and Thermal Stability of Perovskite Solar Cells, *Joule*, 2019, **3**, 1464–1477, DOI: 10.1016/j.joule.2019.04.005.

106 F. Zhang, *et al.*, Suppressing defects through the synergistic effect of a Lewis base and a Lewis acid for highly efficient and stable perovskite solar cells, *Energy Environ. Sci.*, 2018, **11**, 3480–3490.

107 C. Li, J. Yin, R. Chen, X. Lv, X. Feng, Y. Wu and J. Cao, Monoammonium Porphyrin for Blade-Coating Stable Large-Area Perovskite Solar Cells with >18% Efficiency, *J. Am. Chem. Soc.*, 2019, **141**, 6345–6351, DOI: 10.1039/C9TA04486H.

108 T. Wu, *et al.*, Efficient defect passivation for perovskite solar cells by controlling the electron density distribution of donor-π-acceptor molecules, *Adv. Energy Mater.*, 2019, **9**, 1803766.

109 X. Zheng, *et al.*, Managing grains and interfaces *via* ligand anchoring enables 22.3%-efficiency inverted perovskite solar cells, *Nat. Energy*, 2020, **5**, 131–140.

110 S. Fu, *et al.*, Multifunctional liquid additive strategy for highly efficient and stable CsPbI2Br all-inorganic perovskite solar cells, *Chem. Eng. J.*, 2021, **422**, 130572, DOI: 10.1016/j.cej.2021.130572.

111 T. Li, S. Wang, J. Yang, X. Pu, B. Gao, Z. He, Q. Cao, J. Han and X. Li, Multiple functional groups synergistically improve the performance of inverted planar perovskite solar cells, *Nano Energy*, 2021, **82**, 105742, DOI: 10.1007/s12598-020-01691-z.

112 S. Akin, Hysteresis-free planar perovskite solar cells with a breakthrough efficiency of 22% and superior operational stability over 2000 h, *ACS Appl. Mater. Interfaces*, 2019, **11**, 39998–40005.

113 W. Yu, S. Yu, J. Zhang, W. Liang, X. Wang, X. Guo and C. Li, Two-in-one additive-engineering strategy for improved air stability of planar perovskite solar cells, *Nano Energy*, 2018, **45**, 229–235.

114 H. Tsai, *et al.*, High-efficiency two-dimensional Ruddlesden–Popper perovskite solar cells, *Nature*, 2016, **536**, 312–316.

115 H. Zhai, F. Liao, Z. Song, B. Ou, D. Li, D. Xie, H. Sun, L. Xu, C. Cui and Y. Zhao, 2D PEA2PbI4–3D MAPbI3 Composite Perovskite Interfacial Layer for Highly Efficient and Stable Mixed-Ion Perovskite Solar Cells, *ACS Appl. Energy Mater.*, 2021, **4**, 13482–13491.

116 R. Yang, *et al.*, Oriented quasi-2D perovskites for high performance optoelectronic devices, *Adv. Mater.*, 2018, **30**, 1804771.

117 H. Ren, *et al.*, Efficient and stable Ruddlesden–Popper perovskite solar cell with tailored interlayer molecular interaction, *Nat. Photonics*, 2020, **14**, 154–163, DOI: 10.1038/s41566-019-0572-6.

118 T. Niu, *et al.*, High performance ambient-air-stable FAPbI 3 perovskite solar cells with molecule-passivated Ruddlesden–Popper/3D heterostructured film, *Energy Environ. Sci.*, 2018, **11**, 3358–3366.

119 G. Grancini, *et al.*, One-Year stable perovskite solar cells by 2D/3D interface engineering, *Nat. Commun.*, 2017, **8**, 15684.

120 D. H. Kim, *et al.*, Bimolecular additives improve wide-band-gap perovskites for efficient tandem solar cells with CIGS, *Joule*, 2019, **3**, 1734–1745.

121 S. Bai, P. Da, C. Li, Z. Wang, Z. Yuan, F. Fu, M. Kawecki, X. Liu, N. Sakai, J. T.-W. Wang, S. Huettner, S. Buecheler, M. Fahlman, F. Gao and H. J. Snaith, Planar perovskite solar cells with long-term stability using ionic liquid additives, *Nature*, 2019, **571**, 245–250.

122 Z. Wang, *et al.*, Efficient ambient-air-stable solar cells with 2D–3D heterostructured butylammonium-caesium-formamidinium lead halide perovskites, *Nat. Energy*, 2017, **2**, 1–10.

123 T. Zhou, *et al.*, Crystal Growth Regulation of 2D/3D Perovskite Films for Solar Cells with Both High Efficiency and Stability, *Adv. Mater.*, 2022, **34**, 2200705, DOI: 10.1002/adma.202200705.
124 M. Salado, *et al.*, Towards Extending Solar Cell Lifetimes: Addition of a Fluorous Cation to Triple Cation-Based Perovskite Films, *ChemSusChem*, 2017, **10**, 3846–3853.
125 S. Wang, *et al.*, Water-soluble triazolium ionic-liquid-induced surface self-assembly to enhance the stability and efficiency of perovskite solar cells, *Adv. Funct. Mater.*, 2019, **29**, 1900417.
126 R. Xia, *et al.*, An efficient approach to fabricate air-stable perovskite solar cells *via* addition of a self-polymerizing ionic liquid, *Adv. Mater.*, 2020, **32**, 2003801.
127 J. Yang, *et al.*, Uncovering the Mechanism of Poly (ionic-liquid) s Multiple Inhibition of Ion Migration for Efficient and Stable Perovskite Solar Cells, *Adv. Energy Mater.*, 2022, **12**, 2103652.
128 X. Zhao, *et al.*, Accelerated aging of all-inorganic, interface-stabilized perovskite solar cells, *Science*, 2022, **377**, 307–310.
129 T. Zhang, *et al.*, Bication lead iodide 2D perovskite component to stabilize inorganic α-CsPbI(3) perovskite phase for high-efficiency solar cells, *Sci. Adv.*, 2017, **3**, e1700841, DOI: 10.1126/sciadv.1700841.
130 M. Khalid, *et al.*, Opportunities of copper addition in CH3NH3PbI3 perovskite and their photovoltaic performance evaluation, *J. Alloys Compd.*, 2022, **895**, 162626, DOI: 10.1016/j.jallcom.2021.162626.
131 J. Zhang, *et al.*, Uniform Permutation of Quasi-2D Perovskites by Vacuum Poling for Efficient, High-Fill-Factor Solar Cells, *Joule*, 2019, **3**, 3061–3071, DOI: 10.1016/j.joule.2019.09.020.
132 D. Bi, *et al.*, High-Performance Perovskite Solar Cells with Enhanced Environmental Stability Based on Amphiphile-Modified CH3 NH3 PbI3, *Adv. Mater.*, 2016, **28**, 2910–2915, DOI: 10.1002/adma.201505255.
133 Y. Liu, *et al.*, Ultrahydrophobic 3D/2D fluoroarene bilayer-based water-resistant perovskite solar cells with efficiencies exceeding 22%, *Sci. Adv.*, 2019, **5**, eaaw2543, DOI: 10.1126/sciadv.aaw2543.
134 Y. Zheng, *et al.*, High-performance CsPbIxBr3-x all-inorganic perovskite solar cells with efficiency over 18% *via* spontaneous interfacial manipulation, *Adv. Funct. Mater.*, 2020, **30**, 2000457.
135 M. Mangrulkar and K. J. Stevenson, The Progress of Additive Engineering for CH3NH3PbI3 Photo-Active Layer in the Context of Perovskite Solar Cells, *Crystals*, 2021, **11**, 814.
136 P. You, G. Tang and F. Yan, Two-dimensional materials in perovskite solar cells, *Mater. Today Energy*, 2019, **11**, 128–158, DOI: 10.1016/j.mtener.2018.11.006.
137 S. Bai, *et al.*, Planar perovskite solar cells with long-term stability using ionic liquid additives, *Nature*, 2019, **571**, 245–250, DOI: 10.1038/s41586-019-1357-2.
138 T.-H. Han, *et al.*, Interface and Defect Engineering for Metal Halide Perovskite Optoelectronic Devices, *Adv. Mater.*, 2019, **31**, 1803515.
139 B. Chen, *et al.*, Interface band structure engineering by ferroelectric polarization in perovskite solar cells, *Nano Energy*, 2015, **13**, 582–591, DOI: 10.1016/j.nanoen.2015.03.037.
140 A. Islam, S. Z. Haider, M. Wang, A. G. Ismail and H. Anwar, Interface engineering for improved performance of perovskite solar cells using CdTe buffer layer, *Results Eng.*, 2024, **23**, 102618, DOI: 10.1016/j.rineng.2024.102618.
141 H. Zhou, *et al.*, Interface engineering of highly efficient perovskite solar cells, *Science*, 2014, **345**, 542–546, DOI: 10.1126/science.1254050.
142 Q. Dong, *et al.*, Interpenetrating interfaces for efficient perovskite solar cells with high operational stability and mechanical robustness, *Nat. Commun.*, 2021, **12**, 973, DOI: 10.1038/s41467-021-21292-3.
143 G. Grancini, *et al.*, One-Year stable perovskite solar cells by 2D/3D interface engineering, *Nat. Commun.*, 2017, **8**, 15684, DOI: 10.1038/ncomms15684.
144 M. Kim, *et al.*, Moisture resistance in perovskite solar cells attributed to a water-splitting layer, *Commun. Mater.*, 2021, **2**, 6, DOI: 10.1038/s43246-020-00104-z.
145 X. Jian, J.-B. Liu, B.-X. Liu, J. Wang and B. Huang, Defect Engineering of Grain Boundaries in Lead-Free Halide Double Perovskites for Better Optoelectronic Performance, *Adv. Funct. Mater.*, 2019, 1805870.
146 H. Xiang, *et al.*, Towards highly stable and efficient planar perovskite solar cells: Materials development, defect control and interfacial engineering, *Chem. Eng. J.*, 2021, **420**, 127599, DOI: 10.1016/j.cej.2020.127599.
147 K. A. Bush, *et al.*, Compositional Engineering for Efficient Wide Band Gap Perovskites with Improved Stability to Photoinduced Phase Segregation, *ACS Energy Lett.*, 2018, **3**, 428–435, DOI: 10.1021/acsenergylett.7b01255.
148 Y. Zhang, Y. Liu and S. Liu, Composition Engineering of Perovskite Single Crystals for High-Performance Optoelectronics, *Adv. Funct. Mater.*, 2023, **33**, 2210335, DOI: 10.1002/adfm.202210335.
149 N. J. Jeon, J. H. Noh, W. S. Yang, Y. C. Kim, S. Ryu, J. Seo and S. I. Seok, Compositional engineering of perovskite materials for high-performance solar cells, *Nature*, 2015, **517**, 476–480, DOI: 10.1038/nature14133.
150 I. Kopacic, *et al.*, Enhanced Performance of Germanium Halide Perovskite Solar Cells through Compositional Engineering, *ACS Appl. Energy Mater.*, 2018, **1**, 343–347.
151 N. J. Jeon, *et al.*, Solvent engineering for high-performance inorganic–organic hybrid perovskite solar cells, *Nat. Mater.*, 2014, **13**, 897–903, DOI: 10.1038/nmat4014.
152 S. Zuo, *et al.*, Solvent coordination engineering for high-quality hybrid organic-inorganic perovskite films, *J. Mater. Sci.*, 2021, **56**, 9903–9913, DOI: 10.1007/s10853-021-05870-w.
153 Y. Liu, B. Cai, H. Yang, G. Boschloo and E. M. J. Johansson, Solvent Engineering of Perovskite Crystallization for High Band Gap FAPbBr3 Perovskite Solar Cells Prepared in Ambient Condition, *ACS Appl. Energy Mater.*, 2023, **6**, 7102–7108, DOI: 10.1021/acsaem.3c00791.
154 Z. Li, *et al.*, Solvent-Solute Coordination Engineering for Efficient Perovskite Luminescent Solar Concentrators, *Joule*, 2020, **4**, 631–643, DOI: 10.1016/j.joule.2020.01.003.

155 X. Guo and C. Burda, Coordination engineering toward high performance organic–inorganic hybrid perovskites, *Coord. Chem. Rev.*, 2016, **320–321**, 53–65, DOI: 10.1016/j.ccr.2016.03.013.

156 T. Rath, *et al.*, Solution-Processable Cu3BiS3 Thin Films: Growth Process Insights and Increased Charge Generation Properties by Interface Modification, *ACS Appl. Mater. Interfaces*, 2023, **15**, 41624–41633, DOI: 10.1021/acsami.3c10297.

157 J. Liu, *et al.*, Efficient and stable perovskite-silicon tandem solar cells through contact displacement by MgF_x, *Science*, 2022, **377**, 302–306, DOI: 10.1126/science.abn8910.

158 P. Wu, *et al.*, Efficient and Thermally Stable All-Perovskite Tandem Solar Cells Using All-FA Narrow-Bandgap Perovskite and Metal-oxide-based Tunnel Junction, *Adv. Energy Mater.*, 2022, **12**, 2202948.

159 A. Al-Ashouri, *et al.*, Monolithic perovskite/silicon tandem solar cell with 29% efficiency by enhanced hole extraction, *Science*, 2020, **370**, 1300–1309, DOI: 10.1126/science.abd4016.

160 M. Jošt, L. Kegelmann, L. Korte and S. Albrecht, Monolithic Perovskite Tandem Solar Cells: A Review of the Present Status and Advanced Characterization Methods Toward 30% Efficiency, *Adv. Energy Mater.*, 2020, **10**, 1904102, DOI: 10.1002/aenm.201904102.

161 R. Lin, *et al.*, All-Inorganic CsCu2I3 Single Crystal with High-PLQY (≈15.7%) Intrinsic White-Light Emission *via* Strongly Localized 1D Excitonic Recombination, *Adv. Mater.*, 2019, **31**, 1905079, DOI: 10.1002/adma.201905079.

162 H. Tan, A. J., O. Voznyy, X. Lan, F. P. de García Arquer, J. Z. Fan, R. Quintero-Bermudez, M. Yuan, B. Zhang, Y. Zhao, F. Fan, P. Li, L. N. Quan, Y. Zhao, Z.-H. Lu, Z. Yang, S. Hoogland and E. H. Sargent, Efficient and stable solution-processed planar perovskite solar cells *via* contact passivation, *Science*, 2017, **355**, 722.

163 C. Gong, *et al.*, Flexible Planar Heterojunction Perovskite Solar Cells Fabricated *via* Sequential Roll-to-Roll Microgravure Printing and Slot-Die Coating Deposition, *Sol. RRL*, 2020, **4**, 1900204, DOI: 10.1002/solr.201900204.

164 D. Luo, W. Y., Z. Wang, A. Sadhanala, Q. Hu, R. Su, R. Shivanna, G. F. Trindade, J. F. Watts, Z. Xu, T. Liu, K. Chen, F. Ye, P. Wu, L. Zhao, J. Wu, Y. Tu, Y. Zhang, X. Yang, W. Zhang, R. H. Friend, Q. Gong, H. J. Snaith and R. Zhu, Enhanced photovoltage for inverted planar heterojunction perovskite solar cells, *Science*, 2018, **360**, 1442.

165 S. Ašmontas, *et al.*, Photoelectric Properties of Planar and Mesoporous Structured Perovskite Solar Cells, *Materials*, 2022, **15**, 4300.

166 F. Khan, B. D. Rezgui, M. T. Khan and F. Al-Sulaiman, Perovskite-based tandem solar cells: Device architecture, stability, and economic perspectives, *Renewable Sustainable Energy Rev.*, 2022, **165**, 112553, DOI: 10.1016/j.rser.2022.112553.

167 S. Hasan, M. Zahid, S. Park and J. Yi, Stability Challenges for a Highly Efficient Perovskite/Silicon Tandem Solar Cell-A Review, *Sol. RRL*, 2024, **8**, 23009s67.

168 M. I. Asghar, J. Zhang, H. Wang and P. D. Lund, Device stability of perovskite solar cells– A review, *Renewable Sustainable Energy Rev.*, 2017, **77**, 131–146, DOI: 10.1016/j.rser.2017.04.003.

169 M. I. Elsmani, *et al.*, Recent Issues and Configuration Factors in Perovskite-Silicon Tandem Solar Cells towards Large Scaling Production, *Nanomaterials*, 2021, **11**, 3186.

170 Y. Wang, *et al.*, Encapsulation and Stability Testing of Perovskite Solar Cells for Real Life Applications, *ACS Mater. Au*, 2022, **2**, 215–236, DOI: 10.1021/acsmaterialsau.1c00045.

171 Q. Emery, *et al.*, Encapsulation and Outdoor Testing of Perovskite Solar Cells: Comparing Industrially Relevant Process with a Simplified Lab Procedure, *ACS Appl. Mater. Interfaces*, 2022, **14**, 5159–5167, DOI: 10.1021/acsami.1c14720.

172 D. Wang, M. Wright, N. K. Elumalai and A. Uddin, Stability of perovskite solar cells, *Sol. Energy Mater. Sol. Cells*, 2016, **147**, 255–275, DOI: 10.1016/j.solmat.2015.12.025.

173 Z. Liu, *et al.*, All-perovskite tandem solar cells achieving >29% efficiency with improved (100) orientation in wide-bandgap perovskites, *Nat. Mater.*, 2025, **24**, 252–259, DOI: 10.1038/s41563-024-02073-x.

174 J. A. Christians, S. N. Habisreutinger, J. J. Berry and J. M. Luther, Stability in Perovskite Photovoltaics: A Paradigm for Newfangled Technologies, *ACS Energy Lett.*, 2018, **3**, 2136–2143, DOI: 10.1021/acsenergylett.8b00914.

175 S. Wang, J. Sun, J. Xue and R. Wang, Protocol for fabricating long-lasting passivated perovskite solar cells, *STAR Protoc.*, 2024, **5**, 103265, DOI: 10.1016/j.xpro.2024.103265.

176 M. O. Reese, *et al.*, Consensus stability testing protocols for organic photovoltaic materials and devices, *Sol. Energy Mater. Sol. Cells*, 2011, **95**, 1253–1267, DOI: 10.1016/j.solmat.2011.01.036.

177 J. Panidi, D. G. Georgiadou, T. Schoetz and T. Prodromakis, Advances in organic and perovskite photovoltaics enabling a greener Internet of Things, *Adv. Funct. Mater.*, 2022, **32**, 2200694.

178 A. Machín and F. Marquez, *Advancements in Photovoltaic Cell Materials: Silicon, Organic, and Perovskite Solar Cells*, 2024.

179 X. Zhao, *et al.*, Accelerated aging of all-inorganic, interface-stabilized perovskite solar cells, *Science*, 2022, **377**, 307–310, DOI: 10.1126/science.abn5679.

180 M. V. Khenkin, *et al.*, Reconsidering figures of merit for performance and stability of perovskite photovoltaics, *Energy Environ. Sci.*, 2018, **11**, 739–743, DOI: 10.1039/C7EE02956J.

181 M. Saliba, M. Stolterfoht, C. M. Wolff, D. Neher and A. Abate, Measuring Aging Stability of Perovskite Solar Cells, *Joule*, 2018, **2**, 1019–1024, DOI: 10.1016/j.joule.2018.05.005.

182 R. Roesch, *et al.*, Procedures and Practices for Evaluating Thin-Film Solar Cell Stability, *Adv. Energy Mater.*, 2015, **5**, 1501407, DOI: 10.1002/aenm.201501407.

183 Y. Cheng and L. Ding, Pushing commercialization of perovskite solar cells by improving their intrinsic stability, *Energy Environ. Sci.*, 2021, **14**, 3233–3255, DOI: 10.1039/D1EE00493J.

184 C. Yang, *et al.*, Achievements, challenges, and future prospects for industrialization of perovskite solar cells, *Light:Sci. Appl.*, 2024, **13**, 227, DOI: 10.1038/s41377-024-01461-x.
185 C. Zhao, *et al.*, Stabilization of highly efficient perovskite solar cells with a tailored supramolecular interface, *Nat. Commun.*, 2024, **15**, 7139, DOI: 10.1038/s41467-024-51550-z.
186 M. Noman, A. H. H. Khan and S. T. Jan, Interface engineering and defect passivation for enhanced hole extraction, ion migration, and optimal charge dynamics in both lead-based and lead-free perovskite solar cells, *Sci. Rep.*, 2024, **14**, 5449, DOI: 10.1038/s41598-024-56246-4.
187 F. Izadi, A. Ghobadi, A. Gharaati, M. Minbashi and A. Hajjiah, Effect of interface defects on high efficient perovskite solar cells, *Optik*, 2021, **227**, 166061, DOI: 10.1016/j.ijleo.2020.166061.
188 A. Lele, *et al.*, in *2016 IEEE 43rd Photovoltaic Specialists Conference (PVSC)*, pp. 0790–0792.
189 Y. Li, Y. Wang, Z. Xu, B. Peng and X. Li, Key Roles of Interfaces in Inverted Metal-Halide Perovskite Solar Cells, *ACS Nano*, 2024, **18**, 10688–10725, DOI: 10.1021/acsnano.3c11642.
190 C. Das, *et al.*, Unraveling the Role of Perovskite in Buried Interface Passivation, *ACS Appl. Mater. Interfaces*, 2023, **15**, 56500–56510, DOI: 10.1021/acsami.3c13085.
191 S.-W. Lee, *et al.*, UV Degradation and Recovery of Perovskite Solar Cells, *Sci. Rep.*, 2016, **6**, 38150, DOI: 10.1038/srep38150.
192 B. P. Kore, M. Jamshidi and J. M. Gardner, The impact of moisture on the stability and degradation of perovskites in solar cells, *Mater. Adv.*, 2024, **5**, 2200–2217, DOI: 10.1039/D3MA00828B.
193 J. Hidalgo, *et al.*, Synergistic Role of Water and Oxygen Leads to Degradation in Formamidinium-Based Halide Perovskites, *J. Am. Chem. Soc.*, 2023, **145**, 24549–24557, DOI: 10.1021/jacs.3c05657.
194 C. Zhang, *et al.*, Metal Oxides Engineering: toward Sustainable Superhydrophobic Surfaces, *Adv. Funct. Mater.*, 2026, e12239, DOI: 10.1002/adfm.202512239.
195 S. Parvate, P. Dixit and S. Chattopadhyay, Superhydrophobic Surfaces: Insights from Theory and Experiment, *J. Phys. Chem. B*, 2020, **124**, 1323–1360, DOI: 10.1021/acs.jpcb.9b08567.
196 N. Wu, D. Walter, A. Fell, Y. Wu and K. Weber, The Impact of Mobile Ions on the Steady-State Performance of Perovskite Solar Cells, *J. Phys. Chem. C*, 2020, **124**, 219–229, DOI: 10.1021/acs.jpcc.9b10578.
197 M. C. Schmidt, E. Gutierrez-Partida, M. Stolterfoht and B. Ehrler, Impact of Mobile Ions on Transient Capacitance Measurements of Perovskite Solar Cells, *PRX Energy*, 2023, **2**, 043011, DOI: 10.1103/PRXEnergy.2.043011.
198 J. Thiesbrummel, *et al.*, Ion-induced field screening as a dominant factor in perovskite solar cell operational stability, *Nat. Energy*, 2024, **9**, 664–676, DOI: 10.1038/s41560-024-01487-w.
199 Y. Cheng, *et al.*, The detrimental effect of excess mobile ions in planar CH3NH3PbI3 perovskite solar cells, *J. Mater. Chem. A*, 2016, **4**, 12748–12755, DOI: 10.1039/C6TA05053K.
200 L. J. F. Hart, *et al.*, More is different: mobile ions improve the design tolerances of perovskite solar cells, *Energy Environ. Sci.*, 2024, **17**, 7107–7118, DOI: 10.1039/D4EE02669A.
201 A. Assi, W. Rashid Saleh and E. Mohajerani, Effect of Metals (Au, Ag, and Ni) as Cathode Electrode on Perovskite Solar Cells. IOP Conference Series Earth and Environmental, *Science*, 2021, **722**, 012019.
202 F. Behrouznejad, S. Shahbazi, N. Taghavinia, H.-P. Wu and E. Wei-Guang Diau, A study on utilizing different metals as the back contact of CH3NH3PbI3 perovskite solar cells, *J. Mater. Chem. A*, 2016, **4**, 13488–13498, DOI: 10.1039/C6TA05938D.
203 D. Yang, *et al.*, High efficiency planar-type perovskite solar cells with negligible hysteresis using EDTA-complexed SnO2, *Nat. Commun.*, 2018, **9**, 3239, DOI: 10.1038/s41467-018-05760-x.
204 I. Hussain, *et al.*, Functional materials, device architecture, and flexibility of perovskite solar cell, *Emergent Mater.*, 2018, **1**, 133–154, DOI: 10.1007/s42247-018-0013-1.
205 T. Baumeler, *et al.*, Champion Device Architectures for Low-Cost and Stable Single-Junction Perovskite Solar Cells, *ACS Mater. Lett.*, 2023, **5**, 2408–2421, DOI: 10.1021/acsmaterialslett.3c00337.
206 S.-H. Turren-Cruz, A. Hagfeldt and M. Saliba, Methylammonium-free, high-performance, and stable perovskite solar cells on a planar architecture, *Science*, 2018, **362**, 449–453, DOI: 10.1126/science.aat3583.
207 I. Mesquita, L. Andrade and A. Mendes, Temperature Impact on Perovskite Solar Cells Under Operation, *ChemSusChem*, 2019, **12**, 2186–2194, DOI: 10.1002/cssc.201802899.
208 A. Rizzo, *et al.*, Effects of thermal stress on hybrid perovskite solar cells with different encapsulation techniques, *2017 IEEE International Reliability Physics Symposium (IRPS)*, 2017, pp. PV-1.1–PV-1.6.
209 V. M. Le Corre, *et al.*, Charge Transport Layers Limiting the Efficiency of Perovskite Solar Cells: How To Optimize Conductivity, Doping, and Thickness, *ACS Appl. Energy Mater.*, 2019, **2**, 6280–6287, DOI: 10.1021/acsaem.9b00856.
210 N. E. Courtier, J. M. Cave, J. M. Foster, A. B. Walker and G. Richardson, How transport layer properties affect perovskite solar cell performance: insights from a coupled charge transport/ion migration model, *Energy Environ. Sci.*, 2019, **12**, 396–409, DOI: 10.1039/C8EE01576G.
211 K. Afridi, M. Noman and S. T. Jan, Evaluating the influence of novel charge transport materials on the photovoltaic properties of MASnI(3) solar cells through SCAPS-1D modelling, *R. Soc. Open Sci.*, 2024, **11**, 231202, DOI: 10.1098/rsos.231202.
212 E. K. Ashebir, B. T. Abay and T. A. Berhe, Sustainable A2BIBIIIX6 based lead free perovskite solar cells: The challenges and research roadmap for power conversion efficiency improvement, *AIMS Mater. Sci.*, 2024, **11**, 712–759, DOI: 10.3934/matersci.2024036.
213 H. Xu, *et al.*, Constructing robust heterointerfaces for carrier viaduct *via* interfacial molecular bridges enables efficient and stable inverted perovskite solar cells, *Energy*

Environ. Sci., 2023, **16**, 5792–5804, DOI: 10.1039/D3EE02591H.

214 D. Xu, *et al.*, Constructing molecular bridge for high-efficiency and stable perovskite solar cells based on P3HT, *Nat. Commun.*, 2022, **13**, 7020, DOI: 10.1038/s41467-022-34768-7.

215 X. Li, *et al.*, Multifunctional Interfacial Molecular Bridging Strategy Enables Efficient and Stable Inverted Perovskite Solar Cells, *Adv. Mater.*, 2025, 2508352, DOI: 10.1002/adma.202508352.

216 H. Wang, *et al.*, A Multi-functional Molecular Modifier Enabling Efficient Large-Area Perovskite Light-Emitting Diodes, *Joule*, 2020, **4**, 1977–1987, DOI: 10.1016/j.joule.2020.07.002.

217 Z. Li, *et al.*, Stabilized hole-selective layer for high-performance inverted p-i-n perovskite solar cells, *Science*, 2023, **382**, 284–289, DOI: 10.1126/science.ade9637.

218 S. Abicho, B. Hailegnaw, G. A. Workneh and T. Yohannes, Role of additives and surface passivation on the performance of perovskite solar cells, *Mater. Renewable Sustainable Energy*, 2022, **11**, 47–70, DOI: 10.1007/s40243-021-00206-9.

219 K. Wang, *et al.*, Multifunctional Additives to Enhanced Perovskite Solar Cell Performance, *Sol. RRL*, 2023, **7**, 2300137.

220 M.-J. Choi, *et al.*, Functional additives for high-performance inverted planar perovskite solar cells with exceeding 20% efficiency: Selective complexation of organic cations in precursors, *Nano Energy*, 2020, **71**, 104639, DOI: 10.1016/j.nanoen.2020.104639.

221 S. Liu, *et al.*, A review on additives for halide perovskite solar cells, *Adv. Energy Mater.*, 2020, **10**, 1902492.

222 J. Yang, *et al.*, A review on improving the quality of Perovskite Films in Perovskite Solar Cells *via* the weak forces induced by additives, *Appl. Sci.*, 2019, **9**, 4393.

223 J. Xie, *et al.*, Identifying the functional groups effect on passivating perovskite solar cells, *Sci. Bull.*, 2020, **65**, 1726–1734.

224 C. T. Triggs, *et al.*, Spacer Cation Design Motifs for Enhanced Air Stability in Lead-Free 2D Tin Halide Perovskites, *ACS Energy Lett.*, 2024, **9**, 1835–1843, DOI: 10.1021/acsenergylett.4c00615.

225 X. Li, J. M. Hoffman and M. G. Kanatzidis, The 2D Halide Perovskite Rulebook: How the Spacer Influences Everything from the Structure to Optoelectronic Device Efficiency, *Chem. Rev.*, 2021, **121**, 2230–2291, DOI: 10.1021/acs.chemrev.0c01006.

226 X. Zhang, *et al.*, Improved efficiency and stability of flexible perovskite solar cells by a new spacer cation additive, *RSC Adv.*, 2021, **11**, 33637–33645, DOI: 10.1039/D1RA05399J.

227 J. Hu, *et al.*, Synthetic control over orientational degeneracy of spacer cations enhances solar cell efficiency in two-dimensional perovskites, *Nat. Commun.*, 2019, **10**, 1276, DOI: 10.1038/s41467-019-08980-x.

228 Y. Chen, S. Yamaguchi, A. Sato, D. Xue and K. Marumoto, Operando spin observation elucidating performance-improvement mechanisms during operation of Ruddlesden–Popper Sn-based perovskite solar cells, *npj Flexible Electron.*, 2025, **9**, 1, DOI: 10.1038/s41528-024-00376-2.

229 D. Li, *et al.*, Selection of Functional Spacer Cations for Efficient 2D/3D Perovskite Solar Cells, *CCS Chem.*, 2023, **5**, 781–801, DOI: 10.31635/ccschem.023.202202409.

230 P. Liu, *et al.*, Molecular Structure Tailoring of Organic Spacers for High-Performance Ruddlesden–Popper Perovskite Solar Cells, *Nano-Micro Lett.*, 2024, **17**, 35, DOI: 10.1007/s40820-024-01500-7.

231 N. Zhou, *et al.*, The Spacer Cations Interplay for Efficient and Stable Layered 2D Perovskite Solar Cells, *Adv. Energy Mater.*, 2019, **10**, 1901566.

232 W. Feng, *et al.*, Small amines bring big benefits to perovskite-based solar cells and light-emitting diodes, *Chem*, 2022, **8**, 351–383, DOI: 10.1016/j.chempr.2021.11.010.

233 P. Długołęcki, J. Dąbrowska, K. Nijmeijer and M. Wessling, Ion conductive spacers for increased power generation in reverse electrodialysis, *J. Membr. Sci.*, 2010, **347**, 101–107, DOI: 10.1016/j.memsci.2009.10.011.

234 E. Mahal, S. C. Mandal and B. Pathak, Understanding the role of spacer cation in 2D layered halide perovskites to achieve stable perovskite solar cells, *Mater. Adv.*, 2022, **3**, 2464–2474, DOI: 10.1039/D1MA01135A.

235 E. Fransson, J. Wiktor and P. Erhart, Impact of Organic Spacers and Dimensionality on Templating of Halide Perovskites, *ACS Energy Lett.*, 2024, **9**, 3947–3954, DOI: 10.1021/acsenergylett.4c01283.

236 Y. Zhu, *et al.*, Beneficial use of rotatable-spacer side-chains in alkaline anion exchange membranes for fuel cells, *Energy Environ. Sci.*, 2018, **11**, 3472–3479, DOI: 10.1039/C8EE02071J.

237 T. Zhou, *et al.*, Energy Applications of Ionic Liquids: Recent Developments and Future Prospects, *Chem. Rev.*, 2023, **123**, 12170–12253, DOI: 10.1021/acs.chemrev.3c00391.

238 D. R. MacFarlane, *et al.*, Energy applications of ionic liquids, *Energy Environ. Sci.*, 2014, **7**, 232–250, DOI: 10.1039/C3EE42099J.

239 M. Watanabe, *et al.*, Application of Ionic Liquids to Energy Storage and Conversion Materials and Devices, *Chem. Rev.*, 2017, **117**, 7190–7239, DOI: 10.1021/acs.chemrev.6b00504.

240 K. Matuszek, *et al.*, Unexpected Energy Applications of Ionic Liquids, *Adv. Mater.*, 2024, **36**, 2313023, DOI: 10.1002/adma.202313023.

241 P. Sippel, P. Lunkenheimer, S. Krohns, E. Thoms and A. Loidl, Importance of liquid fragility for energy applications of ionic liquids, *Sci. Rep.*, 2015, **5**, 13922, DOI: 10.1038/srep13922.

242 X. Deng, *et al.*, Ionic liquids engineering for high-efficiency and stable perovskite solar cells, *Chem. Eng. J.*, 2020, **398**, 125594, DOI: 10.1016/j.cej.2020.125594.

243 S. Ghosh and T. Singh, Role of ionic liquids in organic-inorganic metal halide perovskite solar cells efficiency and stability, *Nano Energy*, 2019, **63**, 103828, DOI: 10.1016/j.nanoen.2019.06.024.

244 C. Chen, *et al.*, Two-Dimensional Hybrid Dion–Jacobson Germanium Halide Perovskites, *Chem. Mater.*, 2023, **35**, 3265–3275, DOI: 10.1021/acs.chemmater.3c00278.
245 F. Fan, *et al.*, Harnessing chemical functions of ionic liquids for perovskite solar cells, *J. Energy Chem.*, 2022, **68**, 797–810, DOI: 10.1016/j.jechem.2021.11.038.
246 K. Zhang, *et al.*, Role of Ionic Liquids in Perovskite Solar Cells, *Sol. RRL*, 2023, **7**, 2300115, DOI: 10.1002/solr.202300115.
247 L. Chao, T. Niu, Y. Xia, Y. Chen and W. Huang, Ionic Liquid for Perovskite Solar Cells: An Emerging Solvent Engineering Technology, *Acc. Mater. Res.*, 2021, **2**, 1059–1070, DOI: 10.1021/accountsmr.1c00154.
248 F. U. Shah, R. An and N. Muhammad, Editorial: Properties and Applications of Ionic Liquids in Energy and Environmental Science, *Front. Chem.*, 2020, **8**, 627213.
249 M. Shahiduzzaman, *et al.*, The benefits of ionic liquids for the fabrication of efficient and stable perovskite photovoltaics, *Chem. Eng. J.*, 2021, **411**, 128461, DOI: 10.1016/j.cej.2021.128461.
250 M. Salado, *et al.*, Surface passivation of perovskite layers using heterocyclic halides: Improved photovoltaic properties and intrinsic stability, *Nano Energy*, 2018, **50**, 220–228, DOI: 10.1016/j.nanoen.2018.05.035.
251 M. Shahiduzzaman, *et al.*, Viscosity effect of ionic liquid-assisted controlled growth of CH3NH3PbI3 nanoparticle-based planar perovskite solar cells, *Org. Electron.*, 2017, **48**, 147–153, DOI: 10.1016/j.orgel.2017.06.001.
252 M. I. Hossain, *et al.*, Near field control for enhanced photovoltaic performance and photostability in perovskite solar cells, *Nano Energy*, 2021, **89**, 106388, DOI: 10.1016/j.nanoen.2021.106388.
253 N. T. P. Hartono, *et al.*, How machine learning can help select capping layers to suppress perovskite degradation, *Nat. Commun.*, 2020, **11**, 4172, DOI: 10.1038/s41467-020-17945-4.
254 N. T. P. Hartono, *et al.*, in *2020 47th IEEE Photovoltaic Specialists Conference (PVSC)*, pp. 0693–0695.
255 D. Wang, L. Cheng, J. Chang, G. Wang and F. Meng, *In Situ* Forming of a 2D Inorganic Perovskite Capping Layer by Surface Reconstruction for Efficient and Stable CsPbI2Br Perovskite Solar Cells, *ACS Photonics*, 2024, **11**, 4682–4690, DOI: 10.1021/acsphotonics.4c01114.
256 N. Li, *et al.*, Multifunctional perovskite capping layers in hybrid solar cells, *J. Mater. Chem. A*, 2014, **2**, 14973–14978.
257 B. Li, *et al.*, Suppression of potential-induced degradation in monofacial PERC solar cells with gradient-designed capping layer, *Sol. Energy*, 2021, **225**, 634–642, DOI: 10.1016/j.solener.2021.07.067.
258 M. A. Uddin, R. L. Calabro, D.-Y. Kim and K. R. Graham, Halide exchange and surface modification of metal halide perovskite nanocrystals with alkyltrichlorosilanes, *Nanoscale*, 2018, **10**, 16919–16927, DOI: 10.1039/C8NR04763D.
259 Y. Jiang and Z. Li, The effect of additives on the morphology of organic solar cells: A brief review, *Synth. Met.*, 2023, **299**, 117480, DOI: 10.1016/j.synthmet.2023.117480.
260 F. U. Kosasih, E. Erdenebileg, N. Mathews, S. G. Mhaisalkar and A. Bruno, Thermal evaporation and hybrid deposition of perovskite solar cells and mini-modules, *Joule*, 2022, **6**, 2692–2734, DOI: 10.1016/j.joule.2022.11.004.
261 H. Guan, *et al.*, Solid Additive Enables Organic Solar Cells with Efficiency up to 18.6%, *ACS Appl. Mater. Interfaces*, 2023, **15**, 25774–25782, DOI: 10.1021/acsami.3c02787.
262 D.-K. Lee and N.-G. Park, Additive engineering for highly efficient and stable perovskite solar cells, *Appl. Phys. Rev.*, 2023, **10**, 011308.
263 R. Yu, *et al.*, Design and application of volatilizable solid additives in non-fullerene organic solar cells, *Nat. Commun.*, 2018, **9**, 4645, DOI: 10.1038/s41467-018-07017-z.
264 A. D. Halala, K. Siraj and D. Shitaw, Optimal extraction, phytochemical and electrochemical potential assessment of pigments from Persicaria Lapathifolia for dye-sensitized solar cell application, *Discov. electrochem.*, 2024, **1**, 4, DOI: 10.1007/s44373-024-00004-8.
265 Y.-F. Ma, Y. Zhang and H.-L. Zhang, Solid additives in organic solar cells: progress and perspectives, *J. Mater. Chem. C*, 2022, **10**, 2364–2374, DOI: 10.1039/D1TC04224F.
266 Q. Liang, *et al.*, Recent Advances of Solid Additives Used in Organic Solar Cells: Toward Efficient and Stable Solar Cells, *ACS Appl. Energy Mater.*, 2023, **6**, 31–50, DOI: 10.1021/acsaem.2c03180.
267 C. Li, *et al.*, Achieving Record-Efficiency Organic Solar Cells upon Tuning the Conformation of Solid Additives, *J. Am. Chem. Soc.*, 2022, **144**, 14731–14739, DOI: 10.1021/jacs.2c05303.
268 N. Chepngetich, *et al.*, Recent trends on the application of phytochemical-based compounds as additives in the fabrication of perovskite solar cells, *Energy Adv.*, 2024, **3**, 741–764, DOI: 10.1039/D4YA00025K.
269 N. Kumar and J. Jose, Current developments in the nanomediated delivery of photoprotective phytochemicals, *Environ. Sci. Pollut. Res.*, 2020, **27**, 38446–38471, DOI: 10.1007/s11356-020-10100-y.
270 F. Nalimu, J. Oloro, I. Kahwa and P. E. Ogwang, Review on the phytochemistry and toxicological profiles of Aloe vera and Aloe ferox, *Futur. J. Pharm. Sci.*, 2021, **7**, 145, DOI: 10.1186/s43094-021-00296-2.
271 M. Shahinuzzaman, *et al.*, Synthesis of tungsten-doped zinc oxide nanoparticles using Aloe vera extracts for perovskite solar cells, *Optik*, 2024, **313**, 172006, DOI: 10.1016/j.ijleo.2024.172006.
272 W. Ghann, *et al.*, Fabrication, Optimization and Characterization of Natural Dye Sensitized Solar Cell, *Sci. Rep.*, 2017, **7**, 41470, DOI: 10.1038/srep41470.
273 T. Li, *et al.*, Multiple functional groups synergistically improve the performance of inverted planar perovskite solar cells, *Nano Energy*, 2021, **82**, 105742, DOI: 10.1016/j.nanoen.2021.105742.
274 C. U. Udeze, A. O. Nwokoye, J. C. Ejeka, I. L. Ikhioya and O. O. Anyanor, Investigating the influence of natural dye extracts from Ocimum gratissimum, Solanum melongena, Piper guineese, and their blend in the fabrication of perovskite solar cells, *Hybrid Adv.*, 2024, **6**, 100198, DOI: 10.1016/j.hybadv.2024.100198.

275 C. U. Udeze, A. O. Nwokoye, J. C. Ejeka, I. L. Ikhioya and O. O. Anyanor, Investigating the influence of natural dye extracts from Ocimum gratissimum, Solanum melongena, Piper guineese, and their blend in the fabrication of perovskite solar cells, *Hybrid Adv.*, 2024, **6**, 100198.
276 L.-C. Chen and Q. Zhao, Enhanced Performance of Perovskite Solar Cells Through the Application of Pure Natural Centella asiatica Extract Additives, *Progr. Photovolt.: Res. Appl.*, 2025, **33**, 644–651, DOI: 10.1002/pip.3907.
277 A. J. Rout, P. K. Jena, U. K. Patrida and B. K. Bindhani, Green Synthesis of Silver Nanoparticles Using Leaves Extract of Centella Asiatica L, for Studies against Human Pathogens, *Int. J. Pharma Bio Sci.*, 2013, **4**, 661–674.
278 I. S. Mohamad, *et al.*, Enhancement of Power Conversion Efficiency with Zinc Oxide as Photoanode and Cyanococcus, Punica granatum L., and Vitis vinifera as Natural Fruit Dyes for Dye-Sensitized Solar Cells, *Coatings*, 2022, **12**, 1781.
279 Y. Liu, *et al.*, Enhancement of CsPbBr3 Hole-Free Perovskite Solar Cells through Natural Dye Modifications, *Sol. RRL*, 2023, **7**, 2300454, DOI: 10.1002/solr.202300454.
280 N. K. J. Jose, Current developments in the nanomediated delivery of photoprotective phytochemicals, *Environ. Sci. Pollut. Res.*, 2020, **27**, 38446–38471.
281 A. M. H. Al-Rajhi, *et al.*, Molecular Interaction Studies and Phytochemical Characterization of Mentha pulegium L. Constituents with Multiple Biological Utilities as Antioxidant, Antimicrobial, Anticancer and Anti-Hemolytic Agents, *Molecules*, 2022, **27**, 4824.
282 M. Pradeep, D. Kruszka, P. Kachlicki, D. Mondal and G. Franklin, Uncovering the Phytochemical Basis and the Mechanism of Plant Extract-Mediated Eco-Friendly Synthesis of Silver Nanoparticles Using Ultra-Performance Liquid Chromatography Coupled with a Photodiode Array and High-Resolution Mass Spectrometry, *ACS Sustainable Chem. Eng.*, 2022, **10**, 562–571, DOI: 10.1021/acssuschemeng.1c06960.
283 T. Du, *et al.*, Molecular-level regulating intersystem crossing of polyphenols: Engineering high-efficiency phytochemical photosensitizer for MRSA elimination, *Nano Today*, 2024, **58**, 102456, DOI: 10.1016/j.nantod.2024.102456.
284 A. Venkateasan, R. Prabakaran and V. Sujatha, Phytoextract-mediated synthesis of zinc oxide nanoparticles using aqueous leaves extract of Ipomoea pes-caprae (L).R.br revealing its biological properties and photocatalytic activity. Nanotechnology for, *Environ. Eng.*, 2017, **2**, 8, DOI: 10.1007/s41204-017-0018-7.
285 A. E. Magdalin, *et al.*, Development of lead-free perovskite solar cells: Opportunities, challenges, and future technologies, *Results Eng.*, 2023, **20**, 101438, DOI: 10.1016/j.rineng.2023.101438.
286 D. Skarupova, J. Vostalova and A. Rajnochova Svobodova, Ultraviolet A protective potential of plant extracts and phytochemicals, *Biomed. pap. Med. Fac. Univ. Palacky, Olomouc Czechoslov.*, 2020, **164**, 1–22, DOI: 10.5507/bp.2020.010.
287 V. M. Adhami, D. N. Syed, N. Khan and F. Afaq, Phytochemicals for Prevention of Solar Ultraviolet Radiation-induced Damages, *Photochem. Photobiol.*, 2008, **84**, 489–500, DOI: 10.1111/j.1751-1097.2007.00293.x.
288 M. Pimpilova, A brief review on methods and materials for electrode modification: electroanalytical applications towards biologically relevant compounds, *Discov. electrochem.*, 2024, **1**, 12, DOI: 10.1007/s44373-024-00012-8.
289 S. Savitha, S. Surendhiran, K. S. Balu and A. Karthik, *In vitro* and bio-electrochemical characteristics of phytochemical enriched CoO nanoparticles loaded biomimetic scaffold for preclinical analysis, *Polym. Adv. Technol.*, 2024, **35**, e6215, DOI: 10.1002/pat.6215.
290 N. Samadi, M. R. Naghavi, N. Moratalla-López, G. L. Alonso and M. Shokrpour, Morphological, molecular and phytochemical variations induced by colchicine and EMS chemical mutagens in Crocus sativus L, *Food Chem.: Mol. Sci.*, 2022, **4**, 100086, DOI: 10.1016/j.fochms.2022.100086.
291 A. Gulzar, M. B. Siddiqui and S. Bi, Phenolic acid allelochemicals induced morphological, ultrastructural, and cytological modification on Cassia sophera L. and Allium cepa L, *Protoplasma*, 2016, **253**, 1211–1221, DOI: 10.1007/s00709-015-0862-x.
292 A. Dinkova-Kostova, Phytochemicals as Protectors Against Ultraviolet Radiation: Versatility of Effects and Mechanisms, *Planta Med.*, 2008, **74**, 1548–1559, DOI: 10.1055/s-2008-1081296.
293 D. McClements, Requirements for Food Ingredient and Nutraceutical Delivery Systems, in *Encapsulation Technologies and Delivery Systems for Food Ingredients and Nutraceuticals*, Elsevier, 2012, pp. 3–18.
294 D. S. Sultana, L. Fitriani, M. Taher and E. Zaini, Crystal Engineering Approach in Physicochemical Properties Modifications of Phytochemicals, *Sci. Technol. Indones.*, 2022, **7**, 353–371.
295 S. Kumar, Pharmaceutical Cocrystals: an Overview, *Indian J. Pharm. Sci.*, 2018, **79**(6), 858–871.
296 K. Hadi, *PhD thesis*, Uppsala University, 2015.
297 W. Chung, Commentary on Crystallization Vital Role in the Purification of Organic Compounds, *Org. Chem.:Curr. Res.*, 2023, **12**, 312.
298 I. B. Yael Tsarfati, E. Wiedenbeck, L. Houben, H. Cölfen and B. Rybtchinski, Continuum Crystallization Model Derived from Pharmaceutical Crystallization Mechanisms, *ACS Cent. Sci.*, 2021, **7**, 900–908.
299 H. Amrollahi Bioki, A. Moshaii and M. Borhani Zarandi, Improved morphology, structure and optical properties of CH3NH3PbI3 film *via* HQ additive in PbI2 precursor solution for efficient and stable mesoporous perovskite solar cells, *Synth. Met.*, 2022, **283**, 116965, DOI: 10.1016/j.synthmet.2021.116965.
300 E. Hosseinzadeh, A. Foroumadi and L. Firoozpour, What is the role of phytochemical compounds as capping agents for the inhibition of aggregation in the green synthesis of metal oxide nanoparticles? A DFT molecular level response, *Inorg. Chem. Commun.*, 2023, **147**, 110243, DOI: 10.1016/j.inoche.2022.110243.
301 J. Hu, *et al.*, Overcoming photovoltage deficit *via* natural amino acid passivation for efficient perovskite solar cells and modules, *J. Mater. Chem. A*, 2021, **9**, 5857–5865, DOI: 10.1039/D0TA12342K.

302 S. Bakrim, *et al.*, Phytochemical Compounds and Nanoparticles as Phytochemical Delivery Systems for Alzheimer's Disease Management, *Molecules*, 2022, **27**, 9043.
303 K. Debnath, S. Shekhar, V. Kumar, N. R. Jana and N. R. Jana, Efficient Inhibition of Protein Aggregation, Disintegration of Aggregates, and Lowering of Cytotoxicity by Green Tea Polyphenol-Based Self-Assembled Polymer Nanoparticles, *ACS Appl. Mater. Interfaces*, 2016, **8**, 20309–20318, DOI: 10.1021/acsami.6b06853.
304 N. A. Ali, K. K. Dash, V. K. Pandey, A. Tripathi, S. A. Mukarram, E. Harsányi and B. Kovács, Extraction and Encapsulation of Phytocompounds of Poniol Fruit *via* Co-Crystallization: Physicochemical Properties and Characterization, *Molecules*, 2023, **28**, 4764.
305 Y. Wang, I. Ahmad, T. Leung, J. Lin, W. Chen, F. Liu, A. M. C. Ng, Y. Zhang and A. B. Djurišić, Encapsulation and Stability Testing of Perovskite Solar Cells for Real Life Applications, *ACS Mater. Au*, 2022, **2**, 215–236.
306 J. E. P. Chibeom Park and H. C. Choi, Crystallization-Induced Properties from Morphology-Controlled Organic Crystals, *Acc. Chem. Res.*, 2014, **47**, 2353–2364.
307 T. S. Hinoue, Y. Shigenoi, M. Sugino, Y. Mizobe, I. Hisaki, M. Miyata and N. Tohnai, Regulation of π-stacked anthracene arrangement for fluorescence modulation of organic solid from monomer to excited oligomer emission, *Chem.– Eur. J.*, 2012, **18**, 4634–4643.
308 L. Huang, Q. Liao, Q. Shi, H. Fu, J. Ma and J. Yao, Rubrene micro-crystals from solution routes: their crystallography, morphology and optical properties, *J. Mater. Chem.*, 2010, **20**, 159–166.
309 X. Wang, *et al.*, Regulating phase homogeneity by self-assembled molecules for enhanced efficiency and stability of inverted perovskite solar cells, *Nat. Photonics*, 2024, **18**, 1269–1275, DOI: 10.1038/s41566-024-01531-x.
310 G. Qu, *et al.*, Self-assembled materials with an ordered hydrophilic bilayer for high performance inverted Perovskite solar cells, *Nat. Commun.*, 2025, **16**, 86, DOI: 10.1038/s41467-024-55523-0.
311 C. Xu, *et al.*, Molecular ferroelectric self-assembled interlayer for efficient perovskite solar cells, *Nat. Commun.*, 2025, **16**, 835, DOI: 10.1038/s41467-025-56182-5.
312 D. Gaoss, *et al.*, High-efficiency perovskite solar cells enabled by suppressing intermolecular aggregation in hole-selective contacts, *Nat. Photonics*, 2025, **19**, 1070–1077, DOI: 10.1038/s41566-025-01725-x.
313 L. Luo, *et al.*, Stabilization of 3D/2D perovskite heterostructures *via* inhibition of ion diffusion by cross-linked polymers for solar cells with improved performance, *Nat. Energy*, 2023, **8**, 294–303, DOI: 10.1038/s41560-023-01205-y.
314 X. Tang, *et al.*, Enhancing the efficiency and stability of perovskite solar cells *via* a polymer heterointerface bridge, *Nat. Photonics*, 2025, **19**, 701–708, DOI: 10.1038/s41566-025-01676-3.
315 Z. Zhu, *et al.*, Highly Efficient and Stable Perovskite Solar Cells Enabled by All-Crosslinked Charge-Transporting Layers, *Joule*, 2018, **2**, 168–183, DOI: 10.1016/j.joule.2017.11.006.
316 Z. Li, *et al.*, Hyperbranched polymer functionalized flexible perovskite solar cells with mechanical robustness and reduced lead leakage, *Nat. Commun.*, 2023, **14**, 6451, DOI: 10.1038/s41467-023-41931-1.
317 D.-H. Kim, *et al.*, Mixed Self-Assembled Hole-Transport Monolayer Enables Simultaneous Improvement of Efficiency and Stability of Perovskite Solar Cells, *Sol. RRL*, 2024, **8**, 2400067, DOI: 10.1002/solr.202400067.
318 M.-H. Yu, *et al.*, Impact of self-assembled monolayer structural design on perovskite phase regulation, hole-selective contact, and energy loss in inverted perovskite solar cells, *Nano Energy*, 2024, **132**, 110405, DOI: 10.1016/j.nanoen.2024.110405.
319 H.-W. Yu, *et al.*, Co-Assembly with Donor-Acceptor Self-Assembled Monolayers to Enhance Interfacial Hole Extraction, Wettability, and Crystallization in Inverted Perovskite Solar Cells, *Small*, 2026, e14211, DOI: 10.1002/smll.202514211.
320 Y. Chang, *et al.*, Highly Oriented and Ordered Co-Assembly Monolayers for Inverted Perovskite Solar Cells, *Angew. Chem., Int. Ed.*, 2025, **64**, e202418883, DOI: 10.1002/anie.202418883.
321 R. Yin, *et al.*, Coassembled Self-Assembled Monolayers Enable Efficient and Stable Inverted Perovskite Solar Cells, *ACS Nano*, 2025, **19**, 40345–40353, DOI: 10.1021/acsnano.5c07208.
322 W. Wu, *et al.*, Stable and uniform self-assembled organic diradical molecules for perovskite photovoltaics, *Science*, 2025, **389**, 195–199, DOI: 10.1126/science.adv4551.
323 J. Suo, B. Yang, D. Bogachuk, G. Boschloo and A. Hagfeldt, The Dual Use of SAM Molecules for Efficient and Stable Perovskite Solar Cells, *Adv. Energy Mater.*, 2025, **15**, 2400205, DOI: 10.1002/aenm.202400205.
324 D. Li, *et al.*, Co-adsorbed self-assembled monolayer enables high-performance perovskite and organic solar cells, *Nat. Commun.*, 2024, **15**, 7605, DOI: 10.1038/s41467-024-51760-5.
325 B. Dong, *et al.*, Self-assembled bilayer for perovskite solar cells with improved tolerance against thermal stresses, *Nat. Energy*, 2025, **10**, 342–353, DOI: 10.1038/s41560-024-01689-2.
326 C. Vericat, M. E. Vela, G. Benitez, P. Carro and R. C. Salvarezza, Self-assembled monolayers of thiols and dithiols on gold: new challenges for a well-known system, *Chem. Soc. Rev.*, 2010, **39**, 1805–1834, DOI: 10.1039/B907301A.
327 A. Kulkarni, *et al.*, A Universal Strategy of Perovskite Ink - Substrate Interaction to Overcome the Poor Wettability of a Self-Assembled Monolayer for Reproducible Perovskite Solar Cells, *Adv. Funct. Mater.*, 2023, **33**, 2305812, DOI: 10.1002/adfm.202305812.
328 C. Yao, *et al.*, Trifluoromethyl Group-Modified Non-Fullerene Acceptor toward Improved Power Conversion Efficiency over 13% in Polymer Solar Cells, *ACS Appl. Mater. Interfaces*, 2020, **12**, 11543–11550, DOI: 10.1021/acsami.9b20544.
329 R. Xu, *et al.*, Buried Interface Engineering: a Key to Unlocking the Potential of Self-Assembled Monolayer (SAM)-Based Inverted Perovskite Solar Cells, *Small*, 2025, **21**, 2503114.

330 T. Yang, *et al.*, One-stone-for-two-birds strategy to attain beyond 25% perovskite solar cells, *Nat. Commun.*, 2023, **14**, 839, DOI: 10.1038/s41467-023-36229-1.
331 Y. Luo, *et al.*, Inductive effects in molecular contacts enable wide-bandgap perovskite cells for efficient perovskite/TOPCon tandems, *Nat. Commun.*, 2025, **16**, 4516, DOI: 10.1038/s41467-025-59896-8.
332 Z. Deng, *et al.*, A resonance spacer cation-based heterostructure enables efficient and stable perovskite solar cells, *J. Mater. Chem. A*, 2024, **12**, 10965–10973, DOI: 10.1039/D4TA00394B.
333 B. Liu, *et al.*, Vitamin Natural Molecule Enabled Highly Efficient and Stable Planar n–p Homojunction Perovskite Solar Cells with Efficiency Exceeding 24.2%, *Adv. Energy Mater.*, 2023, **13**, 2203352, DOI: 10.1002/aenm.202203352.
334 M. Liu, *et al.*, Perovskite Homojunction Solar Cells by Buried Interface Engineering, *Angew. Chem., Int. Ed.*, 2025, **64**, e202502994, DOI: 10.1002/anie.202502994.
335 X. Lu, S. Tang, Y. Zhang and X. Lin, Separating σ-inductive and π-resonance effects of substituents on modulating resonance-assisted hydrogen bonds, *Phys. Chem. Chem. Phys.*, 2025, **27**, 11986–11992, DOI: 10.1039/D5CP00884K.
336 R. Nasrollahi, L. Martín-Gomis, F. Fernández-Lázaro, S. Zakavi and Á. Sastre-Santos, Effect of the Number of Anchoring and Electron-Donating Groups on the Efficiency of Free-Base- and Zn-Porphyrin-Sensitized Solar Cells, *Materials*, 2019, **12**, 650.
337 L. Zhang, *et al.*, Electronic Effect of Self-Assembled Molecules on Buried Interface Recombination in n-i-p Perovskite Solar Cells, *ACS Appl. Mater. Interfaces*, 2025, **17**, 41342–41349.
338 J. Rochford, D. Chu, A. Hagfeldt and E. Galoppini, Tetrachelate Porphyrin Chromophores for Metal Oxide Semiconductor Sensitization: Effect of the Spacer Length and Anchoring Group Position, *J. Am. Chem. Soc.*, 2007, **129**, 4655–4665, DOI: 10.1021/ja068218u.
339 T. M. Krygowski and B. T. Stępień, Sigma- and Pi-Electron Delocalization: Focus on Substituent Effects, *Chem. Rev.*, 2005, **105**, 3482–3512, DOI: 10.1021/cr030081s.
340 J. Mao, *et al.*, Benzotriazole-Bridged Sensitizers Containing a Furan Moiety for Dye-Sensitized Solar Cells with High Open-Circuit Voltage Performance, *Chem.– Asian J.*, 2012, **7**, 982–991, DOI: 10.1002/asia.201100967.
341 A. Siddiqui, Suman and S. P. Singh, An indacenodithiophene core moiety for organic solar cells, *Mater. Chem. Front.*, 2021, **5**, 7724–7736, DOI: 10.1039/D1QM01100F.
342 M. Balcı, *Reaction Mechanisms in Organic Chemistry*, WILEY-VCH GmbH, Weinheim, 2022.
343 O. A. Stasyuk, H. Szatylowicz, T. M. Krygowski and C. Fonseca Guerra, How amino and nitro substituents direct electrophilic aromatic substitution in benzene: an explanation with Kohn–Sham molecular orbital theory and Voronoi deformation density analysis, *Phys. Chem. Chem. Phys.*, 2016, **18**, 11624–11633, DOI: 10.1039/C5CP07483E.
344 J. E. Anthony, A. Facchetti, M. Heeney, S. R. Marder and X. Zhan, n-Type Organic Semiconductors in Organic Electronics, *Adv. Mater.*, 2010, **22**, 3876–3892, DOI: 10.1002/adma.200903628.
345 Y. Zhang, W. Zhang, Z. Chen, L. Wang and G. Yu, Recent developments in polymer semiconductors with excellent electron transport performances, *Chem. Soc. Rev.*, 2025, **54**, 2483–2519, DOI: 10.1039/D4CS00504J.
346 J. Munárriz, M. Gallegos, J. Contreras-García and Á. Martín Pendás, Energetics of Electron Pairs in Electrophilic Aromatic Substitutions, *Molecules*, 2021, **26**, 513.
347 S. N. Afraj, *et al.*, Recent progress in molecularly tailored organic hole transporting materials for highly efficient perovskite solar cells, *J. Mater. Chem. C*, 2025, **13**, 15234–15289, DOI: 10.1039/D5TC01870F.
348 B. Jothi, A. D. S. Arputharaj, K. Selvaraju, S. L. Priyadharshini and A. G. Al-Sehemi, A Theoretical Investigation on the Properties of Charge Transport of Hexaazatrinaphthylene Derivatives, *ChemistrySelect*, 2024, **9**, e202304156, DOI: 10.1002/slct.202304156.
349 J. Ashenhurst, *Reactions of Aromatic Molecules*, Master Organic chemistry-Activating and Deactivating Groups In Electrophilic Aromatic Substitution, 2025.
350 L. Venkataraman, *et al.*, Electronics and Chemistry: Varying Single-Molecule Junction Conductance Using Chemical Substituents, *Nano Lett.*, 2007, **7**, 502–506, DOI: 10.1021/nl062923j.
351 R. G. Pearson, Hard and soft acids and bases, HSAB, part 1: Fundamental principles, *J. Chem. Educ.*, 1968, **45**, 581, DOI: 10.1021/ed045p581.
352 Z. Iqbal, *et al.*, Interface Modification for Energy Level Alignment and Charge Extraction in CsPbI3 Perovskite Solar Cells, *ACS Energy Lett.*, 2023, **8**, 4304–4314, DOI: 10.1021/acsenergylett.3c01522.
353 X. Shi, *et al.*, Strategies for Enhancing Energy-Level Matching in Perovskite Solar Cells: An Energy Flow Perspective, *Nano-Micro Lett.*, 2025, **17**, 313, DOI: 10.1007/s40820-025-01815-z.
354 L. Nakka, Y. Cheng, A. G. Aberle and F. Lin, Analytical Review of Spiro-OMeTAD Hole Transport Materials: Paths Toward Stable and Efficient Perovskite Solar Cells, *Adv. Energy Sustainability Res.*, 2022, **3**, 2200045, DOI: 10.1002/aesr.202200045.
355 A. Shimizu, *et al.*, HOMO–LUMO Energy-Gap Tuning of π-Conjugated Zwitterions Composed of Electron-Donating Anion and Electron-Accepting Cation, *J. Org. Chem.*, 2021, **86**, 770–781, DOI: 10.1021/acs.joc.0c02343.
356 S. Zhang, *et al.*, Minimizing buried interfacial defects for efficient inverted perovskite solar cells, *Science*, 2023, **380**, 404–409, DOI: 10.1126/science.adg3755.
357 H. Zhu, *et al.*, Tin perovskite transistors and complementary circuits based on A-site cation engineering, *Nat. Electron.*, 2023, **6**, 650–657, DOI: 10.1038/s41928-023-01019-6.
358 D.-J. Xue, *et al.*, Regulating strain in perovskite thin films through charge-transport layers, *Nat. Commun.*, 2020, **11**, 1514, DOI: 10.1038/s41467-020-15338-1.
359 J. Wu, *et al.*, Inhibiting Interfacial Nonradiative Recombination in Inverted Perovskite Solar Cells with a

Multifunctional Molecule, *Adv. Mater.*, 2024, **36**, 2407433, DOI: 10.1002/adma.202407433.
360 C. Zhang, *et al.*, Work function tuning of a weak adhesion homojunction for stable perovskite solar cells, *Joule*, 2024, **8**, 1394–1411, DOI: 10.1016/j.joule.2024.02.015.
361 J. Dou, *et al.*, Improved interfacial adhesion for stable flexible inverted perovskite solar cells, *J. Energy Chem.*, 2023, **76**, 288–294, DOI: 10.1016/j.jechem.2022.09.044.
362 G. Yan, Y. Yuan, M. Kaba and T. Kirchartz, Visualizing Performances Losses of Perovskite Solar Cells and Modules: From Laboratory to Industrial Scales, *Adv. Energy Mater.*, 2025, **15**, 2403706, DOI: 10.1002/aenm.202403706.
363 R. Breugelmans, *et al.*, Investigation of Potential-Induced Degradation in Perovskite Solar Cells under Inert Conditions, *Sol. RRL*, 2025, **9**, 2400923, DOI: 10.1002/solr.202400923.
364 T. Zhang, *et al.*, Surface Lattice Engineering Enables Efficient Inverted Perovskite Solar Cells, *Adv. Energy Mater.*, 2025, **15**, 2403554, DOI: 10.1002/aenm.202403554.
365 S. S. Sangale, D. S. Mann, H.-J. Lee, S.-N. Kwon and S.-I. Na, Influence of interfacial roughness on slot-die coatings for scaling-up high-performance perovskite solar cells, *Commun. Mater.*, 2024, **5**, 201, DOI: 10.1038/s43246-024-00645-7.
366 S. Yu, *et al.*, Homogenized NiOx nanoparticles for improved hole transport in inverted perovskite solar cells, *Science*, 2023, **382**, 1399–1404, DOI: 10.1126/science.adj8858.
367 M. Du, *et al.*, Surface redox engineering of vacuum-deposited NiOx for top-performance perovskite solar cells and modules, *Joule*, 2022, **6**, 1931–1943, DOI: 10.1016/j.joule.2022.06.026.
368 T. Guo, *et al.*, Self-assembled interlayer aiming at the stability of NiOx based perovskite solar cells, *J. Energy Chem.*, 2022, **69**, 211–220, DOI: 10.1016/j.jechem.2022.01.049.
369 Z. Yu and L. Sun, Inorganic Hole-Transporting Materials for Perovskite Solar Cells, *Small Methods*, 2018, **2**, 1700280, DOI: 10.1002/smtd.201700280.
370 X. Yin, Y. Guo, H. Xie, W. Que and L. B. Kong, Nickel Oxide as Efficient Hole Transport Materials for Perovskite Solar Cells, *Sol. RRL*, 2019, **3**, 1900001, DOI: 10.1002/solr.201900001.
371 N. Singh and Y.-T. Tao, Effect of surface modification of nickel oxide hole-transport layer *via* self-assembled monolayers in perovskite solar cells, *Sol. RRL*, 2021, **2**, 2390–2399, DOI: 10.1002/nano.202100004.
372 K. Wang, *et al.*, Defect Passivation in Perovskite Solar Cells by Cyano-Based π-Conjugated Molecules for Improved Performance and Stability, *Adv. Funct. Mater.*, 2020, **30**, 2002861, DOI: 10.1002/adfm.202002861.
373 P. Chen, *et al.*, The Promise and Challenges of Inverted Perovskite Solar Cells, *Chem. Rev.*, 2024, **124**, 10623–10700, DOI: 10.1021/acs.chemrev.4c00073.
374 X. Luo, *et al.*, Recent Advances of Inverted Perovskite Solar Cells, *ACS Energy Lett.*, 2024, **9**, 1487–1506, DOI: 10.1021/acsenergylett.4c00140.
375 M. Li, M. Liu, F. Qi, F. R. Lin and A. K. Y. Jen, Self-Assembled Monolayers for Interfacial Engineering in Solution-Processed Thin-Film Electronic Devices: Design, Fabrication, and Applications, *Chem. Rev.*, 2024, **124**, 2138–2204, DOI: 10.1021/acs.chemrev.3c00396.
376 H. Zhang, *et al.*, Pinhole-Free and Surface-Nanostructured NiOx Film by Room-Temperature Solution Process for High-Performance Flexible Perovskite Solar Cells with Good Stability and Reproducibility, *ACS Nano*, 2016, **10**, 1503–1511, DOI: 10.1021/acsnano.5b07043.
377 W. Liu, *et al.*, Buried Interface Engineering for Scalable Processing of High-Performance Inverted Perovskite Solar Modules, *Adv. Energy Mater.*, 2025, **15**, 2404374, DOI: 10.1002/aenm.202404374.
378 W. Gao, *et al.*, Interface Matters: Boosting Efficient Pb-Sn Perovskite Solar Cells for All-Perovskite Tandem Photovoltaics, *Adv. Mater.*, 2026, **38**, e21789, DOI: 10.1002/adma.202521789.
379 S. Liu, *et al.*, Buried interface molecular hybrid for inverted perovskite solar cells, *Nature*, 2024, **632**, 536–542, DOI: 10.1038/s41586-024-07723-3.
380 C. Luo, *et al.*, Engineering bonding sites enables uniform and robust self-assembled monolayer for stable perovskite solar cells, *Nat. Mater.*, 2025, **24**, 1265–1272, DOI: 10.1038/s41563-025-02275-x.
381 H. G. Schmidt, Safe Piranhas: A Review of Methods and Protocols, *ACS Chem. Health Saf.*, 2022, **29**, 54–61, DOI: 10.1021/acs.chas.1c00094.
382 H. Zhang, *et al.*, A Self-Assembling Composite Structural Design for the Conversion of Hydroxyl-Anchored Bonds Obtains High Efficient and Stable Perovskite Solar Cells, *Adv. Mater.*, 2025, **37**, 2420155, DOI: 10.1002/adma.202420155.
383 B. Li, *et al.*, Highly Efficient and Scalable p-i-n Perovskite Solar Cells Enabled by Poly-metallocene Interfaces, *J. Am. Chem. Soc.*, 2024, **146**, 13391–13398, DOI: 10.1021/jacs.4c02220.
384 G. Li, *et al.*, Highly efficient p-i-n perovskite solar cells that endure temperature variations, *Science*, 2023, **379**, 399–403, DOI: 10.1126/science.add7331.
385 S. You, *et al.*, C60 based ionic salt electron shuttle for high-performance inverted perovskite solar modules, *Science*, 2025, **388**, 964–968, DOI: 10.1126/science.adv4701.
386 T. Xue, *et al.*, Self-healing ion-conducting elastomer towards record efficient flexible perovskite solar cells with excellent recoverable mechanical stability, *Energy Environ. Sci.*, 2024, **17**, 2621–2630, DOI: 10.1039/D4EE00462K.
387 W. Jiang, *et al.*, Toughened self-assembled monolayers for durable perovskite solar cells, *Nature*, 2025, **646**, 95–101.
388 M. Li, *et al.*, A molecularly engineered electron-selective self-assembled monolayer enhances quasi-Fermi level splitting in inverted perovskite solar cells, *Nat. Energy*, 2026, DOI: 10.1038/s41560-026-02025-6.
389 H. Li, *et al.*, 2D/3D heterojunction engineering at the buried interface towards high-performance inverted methylammonium-free perovskite solar cells, *Nat. Energy*, 2023, **8**, 946–955, DOI: 10.1038/s41560-023-01295-8.

390 R. Azmi, *et al.*, Double-side 2D/3D heterojunctions for inverted perovskite solar cells, *Nature*, 2024, **628**, 93–98, DOI: 10.1038/s41586-024-07189-3.
391 T. Duan, *et al.*, Chiral-structured heterointerfaces enable durable perovskite solar cells, *Science*, 2024, **384**, 878–884.
392 Y. Tian, *et al.*, High-entropy hybrid perovskites with disordered organic moieties for perovskite solar cells, *Nat. Photonics*, 2024, **18**, 960–966, DOI: 10.1038/s41566-024-01468-1.
393 S. Zhang, *et al.*, Minimizing buried interfacial defects for efficient inverted perovskite solar cells, *Science*, 2023, **380**, 404–409.
394 R. Azmi, *et al.*, Damp heat–stable perovskite solar cells with tailored-dimensionality 2D/3D heterojunctions, *Science*, 2022, **376**, 73–77.
395 C. Liu, *et al.*, Two-dimensional perovskitoids enhance stability in perovskite solar cells, *Nature*, 2024, **633**, 359–364.
396 C. Liu, *et al.*, Bimolecularly passivated interface enables efficient and stable inverted perovskite solar cells, *Science*, 2023, **382**, 810–815.
397 S. M. Park, *et al.*, Engineering ligand reactivity enables high-temperature operation of stable perovskite solar cells, *Science*, 2023, **381**, 209–215.
398 J. Xue, *et al.*, Reconfiguring the band-edge states of photovoltaic perovskites by conjugated organic cations, *Science*, 2021, **371**, 636–640.
399 C. Liu, *et al.*, Tuning structural isomers of phenylenediammonium to afford efficient and stable perovskite solar cells and modules, *Nat. Commun.*, 2021, **12**, 6394.
400 S. Teale, M. Degani, B. Chen, E. H. Sargent and G. Grancini, Molecular cation and low-dimensional perovskite surface passivation in perovskite solar cells, *Nat. Energy*, 2024, **9**, 779–792.
401 S. Ye, *et al.*, Expanding the low-dimensional interface engineering toolbox for efficient perovskite solar cells, *Nat. Energy*, 2023, **8**, 284–293.
402 H. Rao, *et al.*, Selective templating growth of chemically inert low-dimensional interfaces for perovskite solar cells, *Nat. Energy*, 2025, **10**, 991–1000, DOI: 10.1038/s41560-025-01815-8.
403 Inert low-dimensional interfaces for perovskite solar cells, *Nat. Energy*, 2025, **10**, 932–933, DOI: 10.1038/s41560-025-01818-5.
404 J. Chen, *et al.*, Highly efficient and stable perovskite solar cells enabled by low-dimensional perovskitoids, *Sci. Adv.*, 2022, **8**, eabk2722, DOI: 10.1126/sciadv.abk2722.
405 X. Wang, *et al.*, Achieving Buried Interface/Bulk Synergistic Passivation *via* Chlorophyll Derivative for Efficient Inverted Perovskite Solar Cells, *Angew. Chem., Int. Ed.*, 2025, **64**, e202504304, DOI: 10.1002/anie.202504304.
406 Z. Song, *et al.*, Buried and bulk synergistic engineering enables high-performance inverted 2D/3D perovskite solar cells, *Energy Environ. Sci.*, 2025, **18**, 3740–3749, DOI: 10.1039/D5EE00156K.
407 L. Li, *et al.*, Synergistic Buried and Bulk Engineering by Pre-Crystallized 2D Seeds Enables High Performance Inverted Perovskite Solar Cells, *Small Methods*, 2026, **10**, e02245, DOI: 10.1002/smtd.202502245.
408 Y. Hua, *et al.*, Synergistic engineering of buried interfaces for high-efficiency and stable perovskite solar cells, *J. Mater. Chem. A*, 2025, **13**, 26320–26326, DOI: 10.1039/D5TA03804A.
409 C. Zhang, *et al.*, Simultaneous passivation of bulk and interface defects through synergistic effect of anion and cation toward efficient and stable planar perovskite solar cells, *J. Energy Chem.*, 2021, **63**, 452–460, DOI: 10.1016/j.jechem.2021.07.011.
410 J. Deng, *et al.*, Synergistic Passivation *via* Spatial Configuration Engineering of Ammonium Salts for High-Efficiency Tandem Perovskite Solar Cells, *Adv. Funct. Mater.*, 2026, e29984, DOI: 10.1002/adfm.202529984.
411 W. Li, *et al.*, Steric-Complementary Synergistic Strategy for High-Efficiency Monolithic Perovskite/Silicon Tandem Solar Cells, *Adv. Funct. Mater.*, 2025, e21431, DOI: 10.1002/adfm.202521431.
412 J. Yang, *et al.*, Uncovering the Mechanism of Poly(ionic-liquid)s Multiple Inhibition of Ion Migration for Efficient and Stable Perovskite Solar Cells, *Adv. Energy Mater.*, 2022, **12**, 2103652, DOI: 10.1002/aenm.202103652.
413 R. Zhao, *et al.*, Synergistic A-site engineering and B-site anchoring in photovoltaic perovskites renders efficient and stable solar cells, *Chem. Eng. J.*, 2025, **523**, 168452, DOI: 10.1016/j.cej.2025.168452.
414 D. Wang, *et al.*, Tailoring Interfacial Dipole Molecules to Mitigate Carrier and Energy Losses in Perovskite Solar Cells, *Adv. Funct. Mater.*, 2025, **35**, 2412068, DOI: 10.1002/adfm.202412068.
415 X. Huang, *et al.*, Enhancing inverted perovskite solar cells *via* dipole-moment-tuned self-assembled monolayers with efficiency of 25.75%, *Chem. Eng. J.*, 2025, **511**, 161967, DOI: 10.1016/j.cej.2025.161967.
416 Y. Yang, *et al.*, Improving Photovoltaic Performance and Stability of Perovskite Solar Cells *via* Molecular Bridge Strategy, *Adv. Opt. Mater.*, 2023, **11**, 2300684, DOI: 10.1002/adom.202300684.
417 Y. Ji, *et al.*, Synergistic molecular bridge passivation strategy enables highly efficient perovskite/silicon tandem solar cells, *Chem. Eng. J.*, 2025, **524**, 169117, DOI: 10.1016/j.cej.2025.169117.
418 X. Li, *et al.*, Multifunctional Interfacial Molecular Bridging Strategy Enables Efficient and Stable Inverted Perovskite Solar Cells, *Adv. Mater.*, 2025, **37**, 2508352, DOI: 10.1002/adma.202508352.
419 Z. Nie, *et al.*, Molecular Hybrid Bridging for Efficient and Stable Inverted Perovskite Solar Cells without a Pre-Deposited Hole Transporting Layer, *Adv. Mater.*, 2025, **37**, e10685, DOI: 10.1002/adma.202510685.
420 K. Wang, *et al.*, Chiral Molecular Engineering for Synergistic Defect Passivation and Phase Stabilization Enables 22.19%-Efficient Inorganic Perovskite Solar Cells,

Adv. Energy Mater., 2026, **16**, e06140, DOI: 10.1002/aenm.202506140.

421 A. Khorasani, F. Mohamadkhani, M. Marandi, H. Luo and M. Abdi-Jalebi, Opportunities, Challenges, and Strategies for Scalable Deposition of Metal Halide Perovskite Solar Cells and Modules, *Adv. Energy Sustainability Res.*, 2024, **5**, 2300275, DOI: 10.1002/aesr.202300275.

422 N. K. Rana, *et al.*, Interface engineering for stabilization of efficient perovskite mini-modules with over 1300 h operational stability, *Sol. Energy Mater. Sol. Cells*, 2026, **302**, 114333, DOI: 10.1016/j.solmat.2026.114333.

423 Y. Tian, *et al.*, *In Situ* Interfacial Engineering in Perovskite Solar Cells: The Importance of Additives, *ACS Energy Lett.*, 2025, **10**, 4102–4130, DOI: 10.1021/acsenergylett.5c02002.

424 C. Zhao, H. Zhang, A. Krishna, J. Xu and J. Yao, Interface Engineering for Highly Efficient and Stable Perovskite Solar Cells, *Adv. Opt. Mater.*, 2024, **12**, 2301949, DOI: 10.1002/adom.202301949.

425 H.-C. Hsu, S.-H. Wu and C.-F. Shih, Enhanced photovoltaic performance and longevity of perovskite modules *via* interface engineering of transport layer, *Jpn. J. Appl. Phys.*, 2024, **63**, 12SP20, DOI: 10.35848/1347-4065/ad9931.

426 L. Cao, *et al.*, Engineering light absorption in semiconductor nanowire devices, *Nat. Mater.*, 2009, **8**, 643–647, DOI: 10.1038/nmat2477.

427 M. E. Nasr and A. E. Abouelregal, Light absorption process in a semiconductor infinite body with a cylindrical cavity *via* a novel photo-thermoelastic MGT model, *Arch. Appl. Mech.*, 2022, **92**, 1529–1549, DOI: 10.1007/s00419-022-02128-y.

428 F. Todescato, *et al.*, Engineering of Semiconductor Nanocrystals for Light Emitting Applications, *Materials*, 2016, **9**, 672.

429 L. Protesescu, *et al.*, Nanocrystals of Cesium Lead Halide Perovskites (CsPbX3, X = Cl, Br, and I): Novel Optoelectronic Materials Showing Bright Emission with Wide Color Gamut, *Nano Lett.*, 2015, **15**, 3692–3696, DOI: 10.1021/nl5048779.

430 K. Ahmad and S. M. Mobin, Organic–Inorganic Copper (II)-Based Perovskites: A Benign Approach toward Low-Toxicity and Water-Stable Light Absorbers for Photovoltaic Applications, *Energy Technol.*, 2020, **8**, 1901185, DOI: 10.1002/ente.201901185.

431 S. S. Kumar and K. Balakrishna, A novel optimal identification of various solar PV cell parameters by using MRDT controller, *Sci. Rep.*, 2024, **14**, 10467, DOI: 10.1038/s41598-024-61359-x.

432 N. Gomidze, *et al.*, Toward sustainable solar energy: Analyzing key parameters in photovoltaic systems, *AIP Adv.*, 2024, **14**, 110701.

433 S. Baghel, R. Jha and N. Jindal, Material Selection for Dye Sensitized Solar Cells Using Multiple Attribute Decision Making Approach, *J. Renewable Energy*, 2014, **2014**, 506216, DOI: 10.1155/2014/506216.

434 J. Wen, *et al.*, Copper-based perovskites and perovskite-like halides: A review from the perspective of molecular level, *Nano Energy*, 2024, **128**, 109802, DOI: 10.1016/j.nanoen.2024.109802.

435 B. Vargas, E. Ramos, E. Pérez-Gutiérrez, J. C. Alonso and D. Solis-Ibarra, A Direct Bandgap Copper–Antimony Halide Perovskite, *J. Am. Chem. Soc.*, 2017, **139**, 9116–9119, DOI: 10.1021/jacs.7b04119.

436 T. Cai, *et al.*, Lead-Free Cs4CuSb2Cl12 Layered Double Perovskite Nanocrystals, *J. Am. Chem. Soc.*, 2020, **142**, 11927–11936, DOI: 10.1021/jacs.0c04919.

437 R. Okumura, T. Oku and A. Suzuki, Electronic structures of ABX3 perovskite crystals with a monovalent copper ion as the A-site cation, *Chem. Phys. Impact*, 2024, **8**, 100534, DOI: 10.1016/j.chphi.2024.100534.

438 L.-Y. Bi, *et al.*, Template effects in Cu(i)–Bi(iii) iodide double perovskites: a study of crystal structure, film orientation, band gap and photocurrent response, *J. Mater. Chem. A*, 2020, **8**, 7288–7296, DOI: 10.1039/D0TA00949K.

439 R. A. Nath, A. Raj, J. A. Salam, A. M. Anand and R. Jayakrishnan, Is the replacement of "Pb" by "Cu" in methylammonium lead bromide possible?, *Opt. Mater.*, 2023, **135**, 113373, DOI: 10.1016/j.optmat.2022.113373.

440 A. Elattar, *et al.*, Single crystal of two-dimensional mixed-halide copper-based perovskites with reversible thermochromism, *J. Mater. Chem. C*, 2021, **9**, 3264–3270, DOI: 10.1039/D0TC04307A.

441 J. P. Banerjee and S. Banerjee, *Physics of Semiconductors and Nanostructures*, CRC Press, 2019, DOI: 10.1201/9781315156804.

442 T. Liu, *et al.*, Dopant compensation in p-type doped MAPb1−xCuxI3 alloyed perovskite crystals, *Appl. Phys. Lett.*, 2022, **121**, 012102.

443 A. M. Elseman, *et al.*, Copper-Substituted Lead Perovskite Materials Constructed with Different Halides for Working (CH3NH3)2CuX4-Based Perovskite Solar Cells from Experimental and Theoretical View, *ACS Appl. Mater. Interfaces*, 2018, **10**, 11699–11707, DOI: 10.1021/acsami.8b00495.

444 S. Naseem, *et al.*, DFT based study of copper calcium halide perovskite nanomaterials for optoelectronic and energy applications, *Results Phys.*, 2024, **58**, 107485, DOI: 10.1016/j.rinp.2024.107485.

445 J. I. Gómez-Peralta and X. Bokhimi, Ternary halide perovskites for possible optoelectronic applications revealed by Artificial Intelligence and DFT calculations, *Mater. Chem. Phys.*, 2021, **267**, 124710, DOI: 10.1016/j.matchemphys.2021.124710.

446 W. Su, Y. Jiang, X. Zuo, C. Li and H. Wang, Engineering nucleation/crystallization to intensify the enzymatic reactions and fermentation: A review, *Chem. Eng. J.*, 2022, **431**, 134186, DOI: 10.1016/j.cej.2021.134186.

447 N. Liu, M. Liu, J. Dai, X. Cheng and Z. Chen, Nucleation Engineering to Strengthen Interface Contacts in Single-Crystal Perovskite Photovoltaics, *Angew. Chem., Int. Ed.*, 2026, e202500947, DOI: 10.1002/anie.202500947.

448 C. H. L. Goodman, The prediction of semiconducting properties in inorganic compounds, *J. Phys. Chem. Solids*, 1958, **6**, 305–314, DOI: 10.1016/0022-3697(58)90050-7.

449 H. Yuan, H. Wang and Y. Cui, Two-Dimensional Layered Chalcogenides: From Rational Synthesis to Property

Control *via* Orbital Occupation and Electron Filling, *Acc. Chem. Res.*, 2015, **48**, 81–90.

450 M. Daub, D. Natalukha and H. Hillebrecht, Crystal Structures of the Perovskite-Related System A/Rb/Cu(II)/Br (A=BA, Gu, PEA, 5-AVA, H2en) with Winners, Losers and Compromises– Versatility from 0D to 3D on Different Levels, *Eur. J. Inorg. Chem.*, 2022, **2022**, e202200136, DOI: 10.1002/ejic.202200136.

451 T. Zhou, *et al.*, Syntheses, Structures, and Photoluminescence of Copper-Based Halides. lnorg, *Chem*, 2023, **62**, 7376–7384, DOI: 10.1021/acs.inorgchem.3c00580.

452 B. A. Connor, *et al.*, Alloying a single and a double perovskite: a Cu+/2+ mixed-valence layered halide perovskite with strong optical absorption, *Chem. Sci.*, 2021, **12**, 8689–8697, DOI: 10.1039/D1SC01159F.

453 X.-G. Zhao, *et al.*, Cu–In Halide Perovskite Solar Absorbers, *J. Am. Chem. Soc.*, 2017, **139**, 6718–6725, DOI: 10.1021/jacs.7b02120.

454 M. T. Dylla, S. D. Kang and G. J. r. Snyder, Effect of two-dimensional crystal orbitals on Fermi surfaces and electron transport in three-dimensional perovskite oxides, *Angew. Chem., Int. Ed.*, 2019, **58**, 5503.

455 Y. Zhang, L. Xi, Y. Wanga, J. Zhang, P. Zhang and W. Zhang, Electronic properties of energy harvesting Cu-chalcogenides: p–d hybridization and d-electron localization, *Comput. Mater. Sci.*, 2015, **108**, 239–249.

456 Y. Liu, *et al.*, Two-Inch-Sized Perovskite CH3NH3PbX3 (X = Cl, Br, I) Crystals: Growth and Characterization, *Adv. Mater.*, 2015, **27**, 5176–5183, DOI: 10.1002/adma.201502597.

457 B.-L. Chen, K.-F. Mok and S.-C. Ng, Synthesis, crystal structures and dynamic NMR studies of novel trinuclear copper(I) halide complexes with 2,5-bis[(diphenylphosphino) methyl]thiophene, *J. Chem. Soc., Dalton Trans.*, 1998, 2861–2866, DOI: 10.1039/A803440K.

458 S. Bai, *et al.*, Planar perovskite solar cells with long-term stability using ionic liquid additives, *Nature*, 2019, **571**, 245–250, DOI: 10.1038/s41586-019-1357-2.

459 H. Tan, *et al.*, Efficient and stable solution-processed planar perovskite solar cells *via* contact passivation, *Science*, 2017, **355**, 722–726, DOI: 10.1126/science.aai9081.

460 H. Chen, *et al.*, Improved charge extraction in inverted perovskite solar cells with dual-site-binding ligands, *Science*, 2024, **384**, 189–193, DOI: 10.1126/science.adm9474.

461 C. Liu, *et al.*, Bimolecularly passivated interface enables efficient and stable inverted perovskite solar cells, *Science*, 2023, **382**, 810–815, DOI: 10.1126/science.adk1633.

462 R. Naeem, *et al.*, Photoelectrochemical water splitting over mesoporous CuPbI3 films prepared by electrophoretic technique, *Monatsh. fur Chem.*, 2017, **148**, 981–989, DOI: 10.1007/s00706-016-1880-x.

463 R. Siavash Moakhar, *et al.*, Photoelectrochemical Water-Splitting Using CuO-Based Electrodes for Hydrogen Production: A Review, *Adv. Mater.*, 2021, **33**, 2007285, DOI: 10.1002/adma.202007285.

464 M. G. Walter, *et al.*, Solar Water Splitting Cells, *Chem. Rev.*, 2010, **110**, 6446–6473, DOI: 10.1021/cr1002326.

465 P. Pitriana, T. D. K. Wungu, H. Herman and R. Hidayat, Electronic Structure Calculations of Alkali Lead Iodide APbI3 (A=Li, Na, K, Rb or Cs) using Density Functional Theory (DFT) Method, *J. Phys.: Conf. Ser.*, 2019, **1204**, 012107, DOI: 10.1088/1742-6596/1204/1/012107.

466 M. U. Ghani, M. Sagir, M. B. Tahir and S. Ullah, Evaluation of structural, electronic, optical, mechanical, and thermodynamic properties of LiXCl3 (X = Sn, Pb) for solar cell applications: first-principles approach, *Opt. Quantum Electron.*, 2024, **56**, 1292, DOI: 10.1007/s11082-024-07212-x.

467 M. Awais Rehman, J. ur Rehman and M. Bilal Tahir, A DFT study of structural, electronic, optical, mechanical, thermoelectric, and magnetic properties of Pb-halide perovskites LiPbX3 (X = Cl, Br, and I) for photovoltaic applications, *Comput. Theor. Chem.*, 2023, **1223**, 114085, DOI: 10.1016/j.comptc.2023.114085.

468 S. Aldawood, *et al.*, Study and characterization of γ-ray doses dependent properties of CuPbI3 perovskite thin films, *J. Mater. Res. Technol.*, 2021, **14**, 108–120, DOI: 10.1016/j.jmrt.2021.06.034.

469 M. I. Ustinova, *et al.*, Towards Better Perovskite Absorber Materials: Cu+ Doping Improves Photostability and Radiation Hardness of Complex Lead Halides, *EcoMat*, 2025, **7**, e12512, DOI: 10.1002/eom2.12512.

470 R. Okumura, *et al.*, First-principles calculation analysis and photovoltaic properties of Cu compound-added perovskite solar cells, *Jpn. J. Appl. Phys.*, 2023, **62**, SK1029, DOI: 10.35848/1347-4065/accaef.

471 T. A. Kuku and A. M. Salau, Electrical conductivity of CuSnI3, CuPbI3 and KPbI3, *Solid State Ionics*, 1987, **25**, 1–7, DOI: 10.1016/0167-2738(87)90171-8.

472 J. Huang, *et al.*, First-principles calculations to investigate structural, electronic and optical properties of ternary copper halides AlCumXn (A = K, Rb, Cs; X = Cl, Br, I), *Chem. Phys.*, 2023, **571**, 111915, DOI: 10.1016/j.chemphys.2023.111915.

473 I. Chung, *et al.*, CsSnI3: Semiconductor or Metal? High Electrical Conductivity and Strong Near-Infrared Photoluminescence from a Single Material. High Hole Mobility and Phase-Transitions, *J. Am. Chem. Soc.*, 2012, **134**, 8579–8587, DOI: 10.1021/ja301539s.

474 T. A. Kuku, Structure and ionic conductivity of CuCdCl3, *Solid State Ionics*, 1987, **25**, 105–108, DOI: 10.1016/0167-2738(87)90109-3.

475 A. Jain, S. L. Pal, Y. Jaiswal and S. Srivastava, XRD and TG-DTG Probes for Thermal Stability and Durability of CuPbI3: Eu+2/Eu+3 and CuPbI3 Perovskite as Catalysts, *J. Inst. Eng. (India): Ser. E*, 2022, **103**, 73–77, DOI: 10.1007/s40034-020-00187-w.

476 W. Bannoob, S. M. Ali and S. Aldawood, Influence of gamma rays on the electrical properties of CuPbI3 perovskite thin films, *Radiat. Phys. Chem.*, 2023, **202**, 110538, DOI: 10.1016/j.radphyschem.2022.110538.

477 S. Aldawood, W. M. Bannoob and S. M. Ali, Impact of gamma rays on the structural, optical, and current-voltage characteristics of CuPbI3/p-Si heterojunctions, *Mater. Chem. Phys.*, 2023, **309**, 128420, DOI: 10.1016/j.matchemphys.2023.128420.

478 T. A. Kuku, Ionic transport and galvanic cell discharge characteristics of CuPbI3 thin films, *Thin Solid Films*, 1998, **325**, 246–250, DOI: 10.1016/S0040-6090(98)00430-1.
479 C. Eames, *et al.*, Ionic transport in hybrid lead iodide perovskite solar cells, *Nat. Commun.*, 2015, **6**, 7497, DOI: 10.1038/ncomms8497.
480 Z. Tan, *et al.*, Thinning ferroelectric films for high-efficiency photovoltaics based on the Schottky barrier effect, *NPG Asia Mater.*, 2019, **11**, 20, DOI: 10.1038/s41427-019-0120-3.
481 J. Zhang, *et al.*, Advancing perovskite photovoltaic technology through machine learning-driven automation, *InfoMat*, 2025, **7**, e70005, DOI: 10.1002/inf2.70005.
482 W.-Y. Gao, *et al.*, Machine learning guided efficiency improvement for Sn-based perovskite solar cells with efficiency exceeding 20%, *Rare Met.*, 2024, **43**, 5720–5733, DOI: 10.1007/s12598-024-02775-w.
483 Y. Liu, *et al.*, Machine Learning for Perovskite Solar Cells and Component Materials: Key Technologies and Prospects, *Adv. Funct. Mater.*, 2023, **33**, 2214271, DOI: 10.1002/adfm.202214271.